Image segmentation of Leaf Spot Diseases on Maize using multi-stage Cauchy-enabled grey wolf algorithm

Article *in* Engineering Applications of Artificial Intelligence · March 2022

DOI: 10.1016/j.engappai.2021.104653

Image Segmentation of Leaf Spot Diseases on Maize using Multi-Stage Cauchy-enabled Grey Wolf Algorithm

Helong Yu[1], Jiuman Song[1], Chengcheng Chen[2], Ali Asghar Heidari[3], Jiawen Liu[1], Huiling Chen[3]*, Atef Zaguia[4], Majdi Mafarja[5]

[1] College of Information Technology, Jilin Agricultural University, Changchun 130118, China

yuhelong@aliyun.com, songjiuman@mails.jlau.edu.cn, liu_jia_wen_ljw@163.com

[2] College of Computer Science and Technology, Jilin University, Changchun 130012, China

chencc18@mails.jlu.edu.cn

[3] Department of Computer Science and Artificial Intelligence, Wenzhou University, Wenzhou 325035, China

chenhuiling.jlu@gmail.com, aliasghar68@gmail.com

[4] Department of computer science, College of Computers and Information Technology, Taif University, P.O. BOX 11099, Taif 21944, Saudi Arabia

zaguia.atef@tu.edu.sa

[5] Department of Computer Science, Birzeit University, POBox 14, West Bank, Palestine

mmafarja@birzeit.edu

* Corresponding Author: Huiling Chen

E-mail: chenhuiling.jlu@gmail.com (Huiling Chen)

Abstract:

Grey wolf optimizer (GWO) is a widespread metaphor-based algorithm based on the enhanced variants of velocity-free particle swarm optimizer with proven defects and shortcomings in performance. Regardless of the proven defect and lack of novelty in this algorithm, the GWO has a simple algorithm and it may face considerable unbalanced exploration and exploitation trends. However, GWO is easy to be utilized, and it has a low capacity to deal with multi-modal functions, and it quickly falls into the optima trap or fails to find the global optimal solution. To improve the shortcomings of the basic GWO, this paper proposes an improved GWO called multi-stage grey wolf optimizer (MGWO). By dividing the search process into three stages and using different population updating strategies at each stage, the MGWO's optimization ability is improved while maintaining a certain convergence speed. The MGWO cannot easily fall into premature convergence and has a better ability to get rid of the local optima trap than GWO. Meanwhile, the MGWO achieves a better balance of exploration and exploitation and has a rough balance curve. Hence, the proposed MGWO can obtain a higher-quality solution. Based on verification on the thirty benchmark functions of IEEE CEC2017 as the objective functions, the simulation experiments in which MGWO compared with some swarm-based optimization algorithms and the balance and diversity analysis were conducted. The results verify the effectiveness and superiority of MGWO. Finally, the MGWO was applied to the multi-threshold image segmentation of Leaf Spot Diseases on Maize at four different threshold levels. The segmentation results were analyzed by comparing each comparative algorithm's PSNR, SSIM, and FSIM.

The results proved that the MGWO has noticeable competitiveness, and it can be used as an effective optimizer for multi-threshold image segmentation.

Keywords: Grey wolf optimizer; Salp swarm algorithm; Global optimization; Multi-threshold image segmentation; Kapur's entropy; Leaf Spot Diseases on Maize

1. Introduction

1.1 Motivation

Optimization problems have three critical components that are decision, objective, and constraint (Ba et al., 2020; Gupta et al., 2019; Liang et al., 2020; Zhang et al., 2020a). The constraint is optional, and optimization problems can have one or more constraints. According to the number of objectives, optimization problems can be divided into single-objective optimization and multi-objective optimization. Moreover, according to the types of independent variables of the objective function, optimization problems can be divided into continuous optimization and discrete optimization. Solving optimization problems is to obtain the actual optimal solution or its approximate solution by achieving one or several maximizations or minimization goals under certain constraints. Recently, the optimization algorithms have applied many fields, including wind speed prediction (Chen et al., 2019c), detection of foreign fiber in cotton (Zhao et al., 2015; Zhao et al., 2014), medical data classification (Hu et al., 2017; Huang et al., 2019; Li et al., 2018; Zhao et al., 2019b), fault diagnosis of rolling bearings (Deng et al., 2020a; Zhao et al., 2020d), gate resource allocation (Deng et al., 2020c; Deng et al., 2020e), and the hard maximum satisfiability problem (Zeng et al., 2011a).

Gradient Descent, Newton's method, Quasi-Newton method, and Conjugate Gradient can solve simple optimization problems in real life and production. The Lagrange multiplier method can be used when the objective is a constrained optimization problem. However, as the complexity, dimensions, or objectives of optimization problems increases, it becomes impractical to use precise methods. The solution is to use bio-inspired methods or heuristic algorithms or meta-heuristic algorithms (MAs) (Pang et al., 2018; Zhou et al., 2018), which can help us to find the optimum or approximate optimum value (Wang et al., 2020c). MAs are widely concerned and applied because of their simplicity of implementation and openness to various improvements (Hu et al., 2021b; Li et al., 2017a; Liu et al., 2015; Zhang et al., 2020b; Zhang et al., 2020d). MAs do not seek the answer with specific steps but explore and exploit the search space with an empirical rule to approach the optimal solution as much as possible (Zhao et al., 2020b; Zhao et al., 2020c). MAs overcome the shortcomings of the traditional methods, such as slow convergence speed and low precision (Pang et al., 2018; Zhou et al., 2018). After appropriate improvement, improved MAs can solve the multi-objective optimization problems and constrained optimization problems. At present, there are many MAs, including particle swarm optimizer (PSO) (Kennedy and Eberhart, 1995), artificial bee colony algorithm (ABC) (Karaboga and Basturk, 2007), ant colony optimization (ACO) (Dorigo and Blum, 2005), firefly algorithm (FA) (Yang, 2010), bacterial foraging optimization (BFO) (Fan et al., 2018), fruit fly optimization (FOA) (Shen et al., 2016), and Bat-inspired Algorithm (BA). MAs that have been proposed in the past three years include slime mould algorithm (SMA) (Li et al., 2020b), hunger games search (HGS) (Yang et al., 2021a), Runge Kutta optimizer (RUN)[1] (Ahmadianfar et al., 2021), and Harris hawks optimization (HHO)[2] (A et al., 2019). Slime mould algorithm[3] (SMA) was proposed based upon the oscillation mode and the cooperative behavior of slime mould in nature. HHO was inspired by the chasing style of Harris' hawks in nature called surprise pounce. Hunger games search[4] (HGS) was developed based on the hunger-driven activities of animals for searching for food. Moreover, RUN was developed based on the concepts of Runge Kutta methods in mathematics. However, performance aspects of HGS and RUN still need further verifications for different problems in the future. In addition, these MAs has found there application in many fields such as the hard maximum satisfiability problem (Zeng et al., 2011b; Zeng et al., 2012), bankruptcy prediction (Cai et al., 2019; Yu et al., 2021; Zhang et al., 2020c), parameter optimization (Heidari et al., 2019a; Shen et al., 2016; Wang and Chen, 2020; Wang et al., 2017b), PID optimization control (Zeng et al., 2015; Zeng et al., 2014; Zeng et al., 2019), gate resource allocation (Deng et al., 2020d; W et al., 2020), fault diagnosis of rolling bearings (Deng et al., 2020b; Zhao et al., 2019a), cloud workflow scheduling (Chen et al., 2018; Wang et al., 2019c), energy vehicle dispatch (Liang et al., 2019), and design of power electronic circuit (Liu et al., 2021; Zhan et al., 2016).

GWO is an optimization method centered around three optimal individuals. GWO controls the algorithm's exploration and exploitation processes through the unexpected change of variable C and the linear change of parameter a. Compared with other swarm intelligence optimization algorithms, GWO has apparent advantages when dealing with unimodal functions, with a fair balance between exploration and exploitation. When the objective function is multimodal, GWO pays more attention to the exploration process. The algorithm's convergence rate is not considerable, and it quickly falls into the local optima trap or obtains the solution with low precision. Each swarm intelligence optimization algorithm has two processes of exploration and exploitation when solving optimization problems. The algorithm tries to discover the problem search space areas that are more likely to contain the optimal solution in the exploration process. In the exploitation process, the primary goal is to gain better solutions by searching the neighborhood of each solution obtained in the exploration process. Enhancing the algorithm's exploration ability is bound to sacrifice the convergence rate, and enhancing the algorithm's exploitation ability will increase the algorithm's risk of falling into the local optima trap. Therefore, exploration and exploitation are two conflicting processes in an algorithm's optimization for a given problem. Balancing the exploration and exploitation in the search process is the main challenge of the swarm intelligence algorithms. Given the shortcomings of primary GWO, we hope to improve its performance on multimodal functions, achieve a fairer balance between exploration and exploitation and improve the obtained solution's accuracy.

1.2 Literature review

Complex feature spaces often bring many possibilities and variables into the loop. Decision-makers always need to have a set of optimal choices to make their operation cost-efficient. This cost can be subject to constraints and the project's target, but choosing and finding the best set of solutions is a global requirement. These real-world problems are from different classes, such as data-to-text

[1] https://aliasgharheidari.com/RUN.html

[2] https://aliasgharheidari.com/HHO.html

[3] https://aliasgharheidari.com/SMA.html

[4] https://aliasgharheidari.com/HGS.html

generation (Jiang et al., 2020a), crowdsensing (Jiang et al., 2020c), service function chains (Cai et al., 2021; Luo et al., 2020a), airline crew rostering problem (Zhou et al., 2020), design of power electronic circuit (Liu et al., 2021; Zhan et al., 2016), and scene alignment (Zhong et al., 2022). One of the possible methods for dealing with such feature spaces and complex cases is a branch of solver called metaheuristic. GWO is a metaphor-based algorithm that is technically a variant of PSO (Villalón et al., 2020). Regardless of its novelty and defects, we pay attention on its performance procedures. GWO divides the whole process into three main steps. Limited by the population updating mechanism, GWO has a certain convergence speed in the early iterations, which is not excellent in the later iterations. Niu et al. (Niu et al., 2019b) found that for optimization problems with an optimal solution of 0, GWO has a good performance. Still, the farther the optimal solution of the function is from 0, the worse its performance will be. GWO has a low capacity to deal with the objective with a multi-modal search landscape, as it seems that all three alpha, beta, and gamma agents have a tendency to converge to the same point. In such a case, GWO quickly falls into the optima trap or fails to find the global optimal solution. Faris et al. (Faris et al., 2018) have proposed that adding more random components to mutate the solutions during optimization will increase finding the global optimum.

Many researchers have proposed different improved GWO algorithms because of the GWO's shortcomings. There are many approaches to enhance the performance of the primary GWO. Introduce effective mechanisms into GWO to improve the global exploration and local exploitation capacities, the algorithm's convergence rate, and the solution's quality (Amirsadri et al., 2018; Fan et al., 2020; Gupta and Deep, 2019; Ibrahim et al., 2018; Saxena et al., 2018; Zhang et al., 2018; Zhao et al., 2019b). Lu et al. (Lu et al., 2020) investigated three chaotic strategies with eleven various chaotic map functions and incorporated the most suitable one into GWO to enhance the algorithm's performance. Many improved GWOs use different chaos strategies to initialize a population or change individuals' positions during iterations(Saxena et al., 2019; Teng et al., 2019). Li et al. (Wang et al., 2020a) utilized Kent chaotic algorithm to initialize the population, proposed an adaptive adjustment strategy of a control parameter, and introduced the individual speed and position updates of PSO into the primary GWO. These strategies enhance the population's diversity, balance exploration, and exploitation, and accelerate the convergence speed, respectively. Gupta et al. (Gupta and Deep, 2020) proposed the memory-based GWO. The wolves' search mechanism is modified based on the personal best history of each individual wolves, crossover, and greedy selection. Experiments showed that this algorithm has better search efficiency, solution accuracy, and convergence speed. Wang et al. (Wang et al., 2019a) introduced the Gaussian estimation of distribution (GED) strategy into GWO. Gauss probability model is used to estimate the distribution of the selected superior individuals and shifts the weighted mean to adjust the search directions to enhance the local search ability.

The performance of GWO can be improved by changing the leadership hierarchy of grey wolves. Cai et al. (Cai et al., 2019) proposed an improved GWO (IGWO) with a new mechanism in which random local search around the optimal grey wolf was introduced in beta grey wolves. A random global search was introduced in omega grey wolves, improving the grey wolves' stochastic behavior and exploration capability. The reconfiguration of the position updating formula of wolves is also a method to improve the GWO. After introducing the fitness-based self-adaptive weight coefficients to simulate the grey wolf hierarchy, Miao et al. (Miao et al., 2020) proposed an improved position-updating equation to improve the advanced leadership wolves, thus strengthening the GWO's global exploration ability. Other optimization algorithms can be combined with GWO to make up for the shortcomings of the primary GWO. Tang et al. (Tang et al., 2020b) introduced FA and opposition-based learning into the

GWO and took advantage of them to mitigate the immature convergence of GWO. Zhang et al. (Li et al., 2020a) adjusted the exploration rate of basic GWO based on reinforcement learning principles, improved neural network algorithm (NNA) by discarding transfer operator, introducing random modification factors, and combining them with dynamic population mechanisms. The proposed grey wolf optimization with a neural network algorithm (GNNA) makes full use of the NAA's good global search ability and the GWO's fast convergence. Qu et al. (Qu et al., 2020) used GWO to modify the commensalism phase of the symbiotic organisms search (SOS) algorithm, proposed HSGWO-MSOS, which combines the simplified grey wolf optimizer (SGWO) and the modified SOS. Long et al. (Long et al., 2020b) proposed a hybrid algorithm based on GWO and cuckoo search (CS). A new opposition learning strategy for the decision layer individuals was added to enhance the population's diversity and enable the algorithm to balance exploration and exploitation. Al-Betar et al. (Al-Betar et al., 2020) integrated the beta-hill climbing optimizer (beta HC) into GWO, where GWO is mainly used for exploration. In contrast, beta HC is used primarily for exploitation to better balance exploration and development in a single optimization framework.

With appropriate improvements, GWO can be adapted to solve multi-objective optimization problems. A novel multi-objective GWO called MMOGWO (Liu et al., 2020) based on adaptive chaotic mutation strategy, boundary mutation strategy, and elitism strategy was proposed by Liu et al. Lu et al. (Lu et al., 2019) proposed a novel multi-objective cellular GWO (MOCGWO) that integrates the merits of cellular automata (CA) for diversification and variable neighborhood search (VNS) for intensification, to balance exploration and exploitation. For optimization problems with a high dimension, Dong et al. (Dong and Dong, 2020) proposed a surrogate-assisted GWO (SAGWO) algorithm in which radial basis function (RBF) is employed as the surrogate model. The knowledge gained from the RBF model assists the generation of new wolf leaders in each iteration. Moreover, some researchers have improved GWO to variants suitable for binary problems. Luo et al. (Luo and Zhao, 2019) proposed binary GWO to tackle the multidimensional knapsack problems. The new algorithm contains an initial elite population generator, a pseudo-utility-based quick repair operator, and a differentiated position updating strategy.

Due to the significant advantages of GWO, it has been widely used in various applications from crucial domains, and there have been many improved GWO for specific applications. These domains include machine learning, engineering applications, wireless sensor network (WSN), medical diagnosis, and image processing. There are some overlapping and combinative cases among the above domains.

The significant applications of GWO and variants in machine learning are feature selection, neural network training, and support vector machine (SVM) optimization. Pathak et al. (Pathak et al., 2019) proposed a novel levy flight-based GWO and used it to select the steganalysis algorithm's prominent features from a set of original features. To tackle the Arabic text classification problem, Chantar et al. (Chantar et al., 2020a) proposed an enhanced binary GWO within a wrapper FS approach, where binary GWO played the role of a wrapper-based feature selection technique. Li et al. (Li et al., 2017b) proposed an improved GWO, a feature selection approach used to find the optimal feature subset for medical data. Then, the kernel extreme learning machine (KELM) was integrated into the improved GWO and formed a new predictive framework for medical diagnosis. Wei et al. (Wei et al., 2017) combined SVM with an improved GWO to develop a new and effective prediction system, in which the improved GWO was used to identify the most discriminative features for significant prediction. Path planning is an engineering application that can use GWO and variants to realization. Dewangan et al. (Dewangan et al., 2019) utilized GWO to solve three Dimensional multi-Unmanned Aerial Vehicle (UAV). And it is proved by experiments that GWO outperforms the other deterministic algorithms in path planning for 3D multi-UAV. Lipare et al. (Lipare et al., 2019) proposed two novel fitness functions for clustering and routing problems and applied the GWO approach for energy-efficient clustering and routing in WSN. To handle the zero-day security attacks in open WSN, Davahli et al. (Davahli et al., 2020) presented a lightweight machine learning-based intrusion detection technique with high performance based on the hybridization of genetic algorithm (GA) and GWO. Sundaramurthy et al. (Sundaramurthy and Jayavel, 2020) enhanced the capability of C4.5 by using the hybridization of GWO and PSO to develop an effective Rheumatoid Arthritis prediction system. Ma et al. (Ma et al., 2019) introduced GWO into the fractional grey model to find the optimal value of fractional order and improve forecasting methods. To deal with the least square representation problem more effectively to obtain optimal reconstruction weights, Rajput et al. (Rajput et al., 2019) proposed a GWO based face image super-resolution algorithm. Dappuri et al. (Dappuri et al., 2020) proposed an enhanced GWO. They used it to optimize the proposed algorithm called singular value decomposition in translation-invariant wavelet (SVD-TIW), a non-blind color image watermarking approach.

Aiming at the development and improvement of MAs, part of the related work of the team is as follows: SMA (Li et al., 2020b) and HGS (Yang et al., 2021b) have been developed, and the IGWO (Cai et al., 2019) briefly described above has been proposed. Wang et al. (Wang et al., 2017a) proposed a new KELM parameter tuning strategy using GWO for bankruptcy prediction. Heidari et al. (Heidari et al., 2019b) took advantage of several exploratory and exploitative mechanisms, including random leaders, opposition-based learning, Lévy flight, random spiral-form motions to boost the convergence rate and the performance of the GWO, then called the improved algorithm OBLGWO. Hu et al. (Hu et al., 2021b) used the advantages of covariance matrix adaptation evolution strategy, Lévy flight, and orthogonal learning strategy to enhance the GWO's performance for dealing with complex optimization problems. To boost the BA's stability and convergence speed, Yu et al. (Yu et al., 2020) proposed a chaos-enhanced BA, which uses a threshold to control the steps of chaotic mapping as well as uses a velocity inertia weight to synchronize agents' velocity. Chen et al. (Chen et al., 2019a) drew Lévy flight and chaotic local search into the original WOA to guide the swarm and boost the whole algorithm's exploratory capacity. Huang (Huang et al., 2020) presented an improved SCA called CLSCA, utilizing two strategies which are Lévy flight and chaotic local search mechanism, to boost the algorithm's exploratory and exploitative abilities respectively for dealing with optimization problems with different dimensions. To relieve the original GOA's disadvantages, including premature convergence and slow convergence rate, Luo et al. (Luo et al., 2018) combined three strategies which are Gaussian mutation, Lévy flight, and opposition-based learning into GOA, then proposed an effective kernel extreme learning machine model based on the improved GOA for financial stress prediction.

Image segmentation is the process of dividing an image into several groups of uniform and mutually exclusive pixels, and it is the preprocessing step of many advanced image processing and target recognition. Image segmentation can be performed by recursively segmenting the entire image or merging a number of small regions until the predetermined conditions are met. At present, the widely used image segmentation is thresholding segmentation, region growing, region splitting and merging, segmentation based on neural network, segmentation based on clustering analysis, and so on. Thresholding segmentation is one of the essential techniques in the image segmentation field. The traditional threshold segmentation method using the histogram to segment the foreground and background of an image has the advantages of simplicity, good robustness, short convergence time, and high accuracy. However, with the increase of thresholds level and limited by the inherent fuzziness of natural images, the exhaustive search method becomes lower in efficiency and accuracy. Therefore, many evolutionary algorithms and swarm intelligence algorithms are applied to search for the optimal thresholds. After reasonable improvement, the traditional threshold segmentation method also can be applied to color image segmentation (Rahkar Farshi et al., 2018).

Bhandari (Bhandari, 2020) proposed a new beta differential evolution (BDE)-based fast color image multi-threshold scheme. Ahmed et al. (Ahmed et al., 2018) proposed an alternative hybrid swarm algorithm that combined the WOA and the PSO for multi-threshold image segmentation. Gao et al. [56] proposed a segmentation method based on a new ABC algorithm for doing more fine-tuning searches and further enhancing image segmentation achievements. Chakraborty et al. (Chakraborty et al., 2019) presented a novel improved PSO (IPSO)-based multi-threshold algorithm to search the near-optimal minimum cross-entropy thresholding thresholds. Xu et al. (Xu et al., 2019a) presented a memetic algorithm of dragonfly algorithm (DA) and DE for color image segmentation.

The Otsu algorithm can be used to evaluate the optimal thresholds. Moreover, other adaptive methods that are used to evaluate the optimal thresholds can also be encapsulated as the objective functions of swarm intelligence optimization algorithms, such as Rényi entropy (Mittal and Saraswat, 2018), Shannon entropy (Naidu et al., 2018), Fuzzy entropy (Bhandari and Rahul, 2019), Kapur's entropy (Upadhyay and Chhabra, 2020), Tsallis entropy (Wang et al., 2019b) and Masi entropy (Khairuzzaman and Chaudhury, 2019). Habba et al. (Habba et al., 2018) presented a novel evaluation criterion based on the Gini index and the entropy calculation. Pare et al. (Pare et al., 2018) presented a modified fuzzy entropy (MFE) function to perform the multi-threshold segmentation of color images. Oliva et al. (Oliva et al., 2019) proposed using evolutionary computation algorithms combined with the Type II Fuzzy entropy as the objective function. The quality of image segmentation essentially affects the performance of automatic image analysis systems. Therefore, how to evaluate the quality of image segmentation is also a crux. The assessment indexes widely used in present researches are as follows: feature similarity (FSIM), peak signal-to-noise ratio (PSNR), structural similarity (SSIM) and mean structural similarity (MSSIM) (Boubechal et al., 2019). There are many multi-threshold image segmentation applications, such as breast cancer thermography image segmentation, magnetic resonance image (MRI) segmentation in the medical field, color satellite image segmentation, weather radar image segmentation, and so on.

1.3 Contribution and paper organization

This paper's contributions are as follows: 1) The iterative search process of the original algorithm is divided into three stages. At the first stage, the MGWO takes full advantage of the primary GWO's strong exploration capability. SSA has a reasonable convergence rate and is not easily fall into the local optima trap. Therefore, at the second stage, part of the position update formula of the SSA algorithm is used to change the individual grey wolf's position to alleviate the shortcomings of the primary GWO. Thus, the proposed algorithm's convergence rate and the ability to jump out of the local optima trap are improved. At the last stage, the algorithm is dedicated to exploiting promising areas. A more accurate solution can be obtained by performing Cauchy mutation on each dimension of the current optimal solution. Based on the above innovations, a new, improved multi-stage GWO (MGWO) is proposed. Besides, by comparing with other competitors, the superiority of MGWO is proved. 2) The proposed MGWO was applied to the multi-threshold image segmentation of Leaf Spot Diseases on Maize, and experiments prove that MGWO has apparent competitiveness over other comparative algorithms at four threshold levels.

The remainder of the paper is organized as follows. Section 2 describes the original GWO and SSA. The details of the proposed MGWO are described in Section 3. Section 4 shows and discusses the experimental results. Section 5 contains the summary and prospect of this research.

2. Overview

In this section, the details of the GWO, SSA, and Kapur's entropy are described.

2.1 Grey wolf optimizer

GWO is a popular variant of PSO with a metaphor language first appeared in 2014 (Mirjalili et al., 2014; Niu et al., 2019a; Villalón et al., 2020). The algorithm is not so pure in its novelty, but a popular method, as its novelty is denied by researchers in (Villalón et al., 2020). It simulates the grey wolf population's hierarchy and the behavior of hunting prey in the natural environment (Mirjalili et al., 2020).Search agents of this method follow alpha, beta, and delta to encircle and attack prey, which is the global optimal solution of the optimization problem (Aljarah et al., 2019; Chantar et al., 2020b; Hu et al., 2021b; Tang et al., 2020a).

Based on the mathematical modeling of the hunting behavior of grey wolves, the position update formula of grey wolves is obtained as follows:

$$X_{t+1} = X_t - A \cdot D \tag{1}$$

where t is the current iteration, X_t is the wolf's current position and X_{t+1} is the next position. A is a coefficient matrix, and D is a coefficient vector. They are essential parameters to control the connection and transformation of exploration and exploitation. D is determined by the position of the prey and can be calculated according to the following formula:

$$D = |C \cdot X_P - X_t| \tag{2}$$

$$C = 2r_2 \tag{3}$$

where r_2 is a randomly generated vector from the interval [0,1].

$$A = 2a \cdot r_1 - a \tag{4}$$

$$a = 2 - FEs \cdot \left(\frac{2}{Max\_FEs}\right) \tag{5}$$

where Max_FEs is the maximum evaluations and FEs is the current number of evaluations. a decreases linearly from 2 to 0 with the increase of evaluation numbers. r_1 is a randomly generated vector from the interval [0,1], so that numerical values in matrix A is are limited in an interval $[-2a, 2a]$. Other wolves have to update their positions, and the calculation formula is as follows:

$$X_{new} = \frac{X_1 + X_2 + X_3}{3} \tag{6}$$

where X_1, X_2 and X_3 are calculated as follows:

$$\begin{aligned} X_1 &= X_{Alpha} - A_1 \cdot D_1 , \\ X_2 &= X_{Beta} - A_2 \cdot D_2 , \\ X_3 &= X_{Delta} - A_3 \cdot D_3 \end{aligned} \tag{7}$$

$$\begin{aligned} D_1 &= |C_1 \cdot X_{Alpha} - X_{old}| , \\ D_2 &= |C_2 \cdot X_{Beta} - X_{old}| , \\ D_3 &= |C_3 \cdot X_{Delta} - X_{old}| \end{aligned} \tag{8}$$

The pseudo-code of the GWO algorithm is presented in **Algorithm 1**.

Algorithm 1 Pseudo code of the GWO algorithm

Objective function $f(X), X = (x_1, \ldots, x_d)^T$
Parameters initialization: *N* is the population size, *Max_FEs* is maximum function evaluations. Set current evaluation number *FEs=0*.
Initialize the grey wolf population $X_i (i = 1,2, \ldots, n)$
while (FEs ≤ Max_FEs)
    Calculate each wolf's fitness
    $X_{Alpha} =$ the current best solution,
    $X_{Beta} =$ the current second-best solution,
    $X_{Delta} =$ the current third-best solution.
    Update the number of *FEs*
    Update parameters: a by Eq. (5)
    for each individual wolf
        Update the current wolf's position by Eq. (4) and (6) – (8)
    end for
end while
Postprocess results and visualization

2.2 Kapur's entropy in multi-threshold image segmentation

This section detailed the nonlocal mean filtering, two-dimensional (2D) histogram, and Kapur's entropy.

Among many multi-threshold image segmentation methods, Kapur's entropy is widely used by related researchers and workers in the field of image segmentation due to its efficient performance and easy implementation. Kapur's entropy was firstly proposed by Kapur et al. (Kapur et al., 1985) in 1985 to segment the gray scale image by maximizing the entropy of the histogram. The method of calculating Kapur's entropy using a one-dimensional histogram is as follows: assuming that the image with a grey value range $[0, L-1]$ and size $M \times N$ is divided into *K* regions, and the number of the thresholds is $K-1$. Let $f_0, f_1, f_2, \ldots, f_i, \ldots, f_{L-1}$ be the grey-level frequencies and let h_a $(a = 1,2, \ldots, K-1)$ is the image thresholds.

$$P_i = \frac{f_i}{M \times N}, \quad i = 1,2, \ldots, L-1 \tag{9}$$

$$P_1 = \sum\nolimits_{i=0}^{h_1} P_i, P_2 = \sum\nolimits_{i=h_1+1}^{h_2} P_i, \ldots, P_K = \sum\nolimits_{i=h_{K-1}+1}^{L-1} P_i \tag{10}$$

$$\begin{gathered} H_1(h) = \sum\nolimits_{i=0}^{h_1} \frac{P_i}{P_1} \cdot ln \frac{P_i}{P_1}, \\ H_2(h) = \sum\nolimits_{i=h_1+1}^{h_2} \frac{P_i}{P_2} \cdot ln \frac{P_i}{P_2}, \\ \vdots \\ H_K(h) = \sum\nolimits_{i=h_{K-1}+1}^{L-1} \frac{P_i}{P_K} \cdot ln \frac{P_i}{P_K} \end{gathered} \tag{11}$$

Then, the Kapur's entropy is calculated by:

$$H(h) = \sum_{i=1}^{K} H_i \tag{12}$$

In the multi-threshold image segmentation experiments in Section 4.5, a 2D histogram will be used to calculate Kapur's entropy. The following will detail the calculation methods of non-local mean filtering, 2D histogram, and Kapur's entropy-based on the 2D histogram.

Non-local mean filtering is an image denoising algorithm proposed by Buades et al. (Buades et al., 2005). Its idea is to set a fixed size neighborhood block around a point to be filtered as the current block and set a reference block of the same size as the current block, then traverse the whole image pixel by pixel (this point is the center pixel of the reference block), and calculate the Euclidean distance between the reference block and the current block. In image *I*, $I(i)$ and $I(j)$ are the grey values of pixel *i* and *j*, respectively. $L(i)$ and $L(j)$ are square areas of length *m* centered on pixels *i* and j, respectively. Firstly, the local mean values of two center pixels are calculated as follows:

$$u(i) = \frac{1}{m \times m} \sum_{i \in L(i)} I(i) \tag{13}$$

$$u(j) = \frac{1}{m \times m} \sum_{j \in L(j)} I(j) \tag{14}$$

Then the weight $\omega(i,j)$ between two blocks is calculated as follows:

$$\omega(i,j) = e^{-\frac{|u(i)-u(j)|^2}{\sigma^2}} \tag{15}$$

where *e* is the base of the natural logarithm. Finally, the non-local mean filtering value of pixel *i* is obtained as follows:

$$NL(i) = \frac{\sum_{i \in I} I(i) \cdot \omega(i,j)}{\sum_{i \in I} \omega(i,j)} \tag{16}$$

The corresponding 2D histogram is generated by the combination of non-local mean image and grey image. The grey image $G(i,j)$ of an image $I(i,j)$ with size $M \times N$ and the non-local mean image $NL(i,j)$ generated by this grey image are both $M \times N$ in size, and the grey value range is $[0, L-1]$. The grey value $G(i,j)$ in the grey image and corresponding grey value $NL(i,j)$ in the non-local mean image of a specific pixel constitutes a point (x,y) in the xOy plane of the 2D histogram, and $h(i,j)$ is the total number of occurrences of (x,y). The final 2D histogram is obtained by normalizing the statistical times according to the following equation:

$$P_{ij} = \frac{h(i,j)}{M \times N} \tag{17}$$

Assuming that the image is divided into *K* regions, the number of the thresholds is $K-1$. In the 2D histogram, $t_a\,(a = 1,2,\dots,K-1)$ represent the thresholds of the grey image and $s_a\,(a = 1,2,\dots,K-1)$ represent the thresholds of the non-local mean image.

The Kapur's entropy of the image is calculated for K subregions on the main diagonal of the 2D histogram, and the calculation formulas are as follows:

$$\begin{aligned} H(s,t) = &-\sum_{j=0}^{s_1} \sum_{i=0}^{t_1} \frac{P_{ij}}{P_1} \cdot ln \frac{P_{ij}}{P_1} - \sum_{j=t_1+1}^{s_2} \sum_{i=t_1+1}^{t_2} \frac{P_{ij}}{P_2} \cdot ln \frac{P_{ij}}{P_2} - \\ &\dots \sum_{j=t_{K-1}+1}^{L-1} \sum_{i=t_{K-1}+1}^{L-1} \frac{P_{ij}}{P_K} \cdot ln \frac{P_{ij}}{P_K} \end{aligned} \tag{18}$$

$$P_1 = \sum_{j=0}^{s_1} \sum_{i=0}^{t_1} P_{ij}\ , P_2 = \sum_{j=t_1+1}^{s_2} \sum_{i=t_1+1}^{t_2} P_{ij}\ , P_K = \sum_{j=t_{K-1}+1}^{L-1} \sum_{i=t_{K-1}+1}^{L-1} P_{ij} \tag{19}$$

Taking $H(s,t)$ as the optimization algorithms' objective function, the optimal thresholds are obtained by the following formula:

$$T^* = argmax(H) \tag{20}$$

In this optimization problem, the independent variables of the objective function are all thresholds $t_a\ (a = 1,2,\dots,K-1)$, and the dependent variable is the Kapur's entropy $H(s,t)$ of 2D histogram. The objective function is a single objective bound constraint function. There are no other constraints except boundary constraints. When the number of thresholds is specified, this optimization problem aims to gain a combination of thresholds that maximizes Kapur's entropy.

3. Proposed MGWO

3.1 Mechanism of multi-stage search

The whole algorithm's iterative process of searching for the optimal value is divided into several different stages. Different effective search strategies at each stage are an effective way to interfere with the connection and transformation of exploration and exploitation. This method can be used to achieve a better balance between exploration and exploitation. According to the objective function's characteristics, we can emphasize one of the two exploration and exploitation processes to get a solution with higher quality. For example, when the search domain of the objective function is wide, but the optimal value neighborhood is relatively smooth, the algorithm's exploration process can be emphasized. Suppose the search domain of the objective function is small, but the optimal value neighborhood is steep. In that case, the algorithm's exploitation process can be emphasized to gain a high precision solution. Pelusi et al. (Oliva et al., 2019) divided the search process into three segments, the first for exploration, the last for exploitation, and the middle is the transition stage of exploration and exploitation. However, this method has the consequences of reducing the convergence speed and increasing the algorithm's time complexity due to the forced segmentation of the whole optimization process according to the number of iterations or evaluation times.

In the proposed MGWO algorithm, we divide the whole search process into three stages to better balance exploration and exploitation, especially in dealing with problems with a multi-modal function. At the first stage, the primary GWO algorithm with a strong ability to explore the search domain with an extensive range is used to explore the candidate solutions. The strategy used at the second stage makes the algorithm not easily converge prematurely and improves the convergence rate. At the last stage, the exploitation in the neighborhood of candidate solutions is emphasized to obtain a solution with higher precision and accuracy. The evaluation number is divided into the intervals I_1, I_2 and I_3, which are defined:

$$\begin{aligned} I_1 &= [1, \lambda * Max\_FEs] \cap \mathbb{N}, \\ I_2 &= [\lambda * Max\_FEs, \mu * Max\_FEs] \cap \mathbb{N}, \\ I_3 &= [\mu * Max\_FEs, Max\_FEs] \cap \mathbb{N} \end{aligned} \tag{21}$$

where $\mathbb{N}$ is the set of natural numbers. λ and μ are two parameters that control the intervals of the whole evaluation process. Note that these two parameters need to satisfy the condition $0 < \lambda < \mu < 1$. And their values are 0.4 and 0.7 respectively in MGWO, which are proved by the following comparative experimental results. In the comparative experiment, the population size is 30, the dimension of the objective function is 30, the maximum number of evaluations is 300000, and the number of parallel random runs is 30. **Table 1** displays the test results obtained by algorithms with different values of λ and μ on 30 benchmark functions of IEEE CEC 2017. *Avg* is the average of the ranks obtained on 30 benchmark functions by algorithms with different values of λ and μ, and *Rank* is the final rank that can visually observe the performance of the algorithms. According to the *Avg* and *Rank*, setting the λ and μ to 0.4 and 0.7 respectively is the best choice.

Table 2 displays the standard deviations (*STD*) obtained by the MGWO with different values of λ and μ on 30 benchmark functions with 30 parallel random runs. The value of standard deviation reflects the influence of hyper-parameters on the stability of the algorithm. Therefore, the minimum one among the standard deviations obtained by MGWO with different parameter values is marked in bold on each benchmark function. It can be seen that the stability of MGWO is better on unimodal functions and simple multimodal functions. On the hybrid functions, MGWO7 has the best stability, and MGWO is second only to it. MGWO4 has better stability on the composition functions, but when the comparison algorithms are ranked using the average of the results obtained in 30 parallel random runs, MGWO still ranks first.

Figure 1 reveals the box plots of MGWO with different values of λ and μ on 30 benchmark functions with 30 times of parallel random runs. The tick labels of the x-axis respectively represent MGWO~MGWO7 in **Table 1**. Box plot is composed of the minimum observation value (*min*), the maximum observation value (*max*), the lower quartile (*Q1*), the median, the upper quartile (*Q3*), and outliers. Set the length of the box *IQR=Q3-Q1*, then the *min=Q1-1.5*IQR*, and the *max=Q3+1.5*IQR*. The red line located inside the box represents the median of the dataset. There is an extension line called whisker between *Q3* and *max*. If a point whose value is larger than the maximum observation value, the point is called an outlier and is plotted with "+".

Similarly, there is a whisker between *Q1* and *min*, and outliers whose values are smaller than the minimum observation value are plotted with "+". Box plots can visually identify the abnormal values in the data and judge the data's degree of dispersion and bias. It can be seen from **Figure 1** that when the parameters λ and μ are set to 0.4 and 0.7, on most benchmark functions, the boxes obtained by MGWO are closer to the x-axis and shorter in length than other competitors, the median is also significantly lower, and the number of outliers is significantly reduced. This shows that MGWO can obtain more accurate optimization results and has stronger stability than other competitors. Box plots further prove that setting λ and μ to 0.4 and 0.7 is a correct choice.

Table 1. Comparative experimental results of MGWO with different values of λ and μ

		MGWO	MGWO2	MGWO3	MGWO4	MGWO5	MGWO6	MGWO7
Value	$\boldsymbol{\lambda}$	0.4	0.1	0.2	0.3	0.4	0.4	0.4
	$\boldsymbol{\mu}$	0.7	0.7	0.7	0.7	0.6	0.8	0.9
Avg		3.23	4.60	3.50	3.73	3.83	4.13	4.97
Rank		1	6	2	3	4	5	7

Table 2. The STD obtained by the MGWO with different values of λ and μ

	F1	F2	F3	F4	F5
MGWO	3.8959E+04	**1.0809E-03**	**1.5039E-01**	**2.2784E+01**	1.4418E+01
MGWO2	**2.5451E+04**	1.6215E-03	2.0303E-01	2.3586E+01	1.5983E+01
MGWO3	2.9891E+04	1.3524E-03	2.2546E-01	2.5328E+01	1.4206E+01
MGWO4	3.3942E+04	1.4565E-03	1.7151E-01	2.6625E+01	**1.3942E+01**
MGWO5	6.4580E+05	1.4702E+01	2.7567E+00	2.4792E+01	1.5410E+01

MGWO6	6.0441E+04	1.4792E-03	1.5715E-01	2.6603E+01	1.4876E+01
MGWO7	6.9686E+04	1.8872E-03	1.9434E-01	2.7909E+01	1.4953E+01
	F6	**F7**	**F8**	**F9**	**F10**
MGWO	**3.7576E-01**	2.2075E+01	**9.7239E+00**	**2.8198E+02**	4.4804E+02
MGWO2	5.7130E-01	2.6873E+01	1.6123E+01	6.5763E+02	6.1719E+02
MGWO3	5.9772E-01	**1.8129E+01**	1.5568E+01	4.6786E+02	5.2624E+02
MGWO4	4.0422E-01	2.6992E+01	1.4287E+01	4.5942E+02	5.0736E+02
MGWO5	1.5404E+00	2.7267E+01	1.1964E+01	5.5681E+02	**3.9606E+02**
MGWO6	1.2914E+00	2.9103E+01	1.5940E+01	4.1485E+02	5.5302E+02
MGWO7	2.8906E+00	2.4485E+01	1.2990E+01	3.5609E+02	5.0194E+02
	F11	**F12**	**F13**	**F14**	**F15**
MGWO	2.1898E+01	8.4563E+04	2.3287E+04	**1.9965E+03**	1.1787E+04
MGWO2	4.0161E+01	1.1255E+05	2.3629E+04	4.4003E+03	**7.3246E+03**
MGWO3	3.7057E+01	7.0153E+04	2.3964E+04	4.4514E+03	1.3356E+04
MGWO4	3.0167E+01	**6.5588E+04**	2.4050E+04	2.6136E+03	1.3864E+04
MGWO5	3.0530E+01	6.9350E+04	2.1637E+04	4.4544E+03	9.5169E+03
MGWO6	2.4081E+01	1.2883E+05	2.3498E+04	3.8510E+03	1.0734E+04
MGWO7	**2.1561E+01**	3.1761E+05	**2.0474E+04**	5.4585E+03	9.3046E+03
	F16	**F17**	**F18**	**F19**	**F20**
MGWO	2.1844E+02	**1.0037E+02**	**7.5519E+04**	1.6109E+04	1.0906E+02
MGWO2	2.6681E+02	1.2148E+02	9.7769E+04	1.6764E+04	1.1415E+02
MGWO3	**1.7529E+02**	1.0976E+02	9.5808E+04	1.8938E+04	9.8350E+01
MGWO4	2.5958E+02	1.5091E+02	8.4834E+04	1.6853E+04	1.2438E+02
MGWO5	2.2915E+02	1.2852E+02	8.1772E+04	1.7855E+04	1.1424E+02
MGWO6	2.4662E+02	1.3050E+02	1.1675E+05	1.6013E+04	1.1888E+02
MGWO7	2.7184E+02	1.3669E+02	9.5998E+04	**1.0724E+0**4	**1.0644E+02**
	F21	**F22**	**F23**	**F24**	**F25**
MGWO	1.3381E+01	**1.0834E+03**	2.2294E+01	2.7106E+01	1.4900E+00
MGWO2	1.5627E+01	1.3781E+03	2.3438E+01	1.9541E+01	1.1946E+01
MGWO3	1.2780E+01	1.4263E+03	2.2366E+01	1.8538E+01	5.4755E+00
MGWO4	**1.0790E+01**	1.1329E+03	**1.9299E+01**	**1.7746E+01**	1.2693E+00
MGWO5	1.6827E+01	1.2759E+03	2.2249E+01	2.0316E+01	1.6512E+00
MGWO6	1.3176E+01	1.2202E+03	2.6731E+01	2.0735E+01	1.2888E+00
MGWO7	1.2383E+01	1.4685E+03	2.3861E+01	2.1943E+01	**1.2497E+00**
	F26	**F27**	**F28**	**F29**	**F30**
MGWO	2.9693E+02	1.5957E+01	5.2642E+01	1.1683E+02	2.8793E+03
MGWO2	3.4988E+02	1.5294E+01	6.0607E+01	1.1176E+02	2.8976E+03
MGWO3	2.7278E+02	1.9715E+01	5.5688E+01	**9.7085E+01**	**2.1942E+03**
MGWO4	**2.4359E+02**	1.5284E+01	6.0997E+01	1.5083E+02	2.8727E+03
MGWO5	3.5335E+02	**1.1486E+01**	5.2514E+01	1.4553E+02	2.5470E+03

MGWO6	2.7056E+02	1.6602E+01	**4.9552E+01**	1.2110E+02	2.7242E+03
MGWO7	3.5525E+02	1.6122E+01	5.4402E+01	1.1526E+02	2.8976E+03

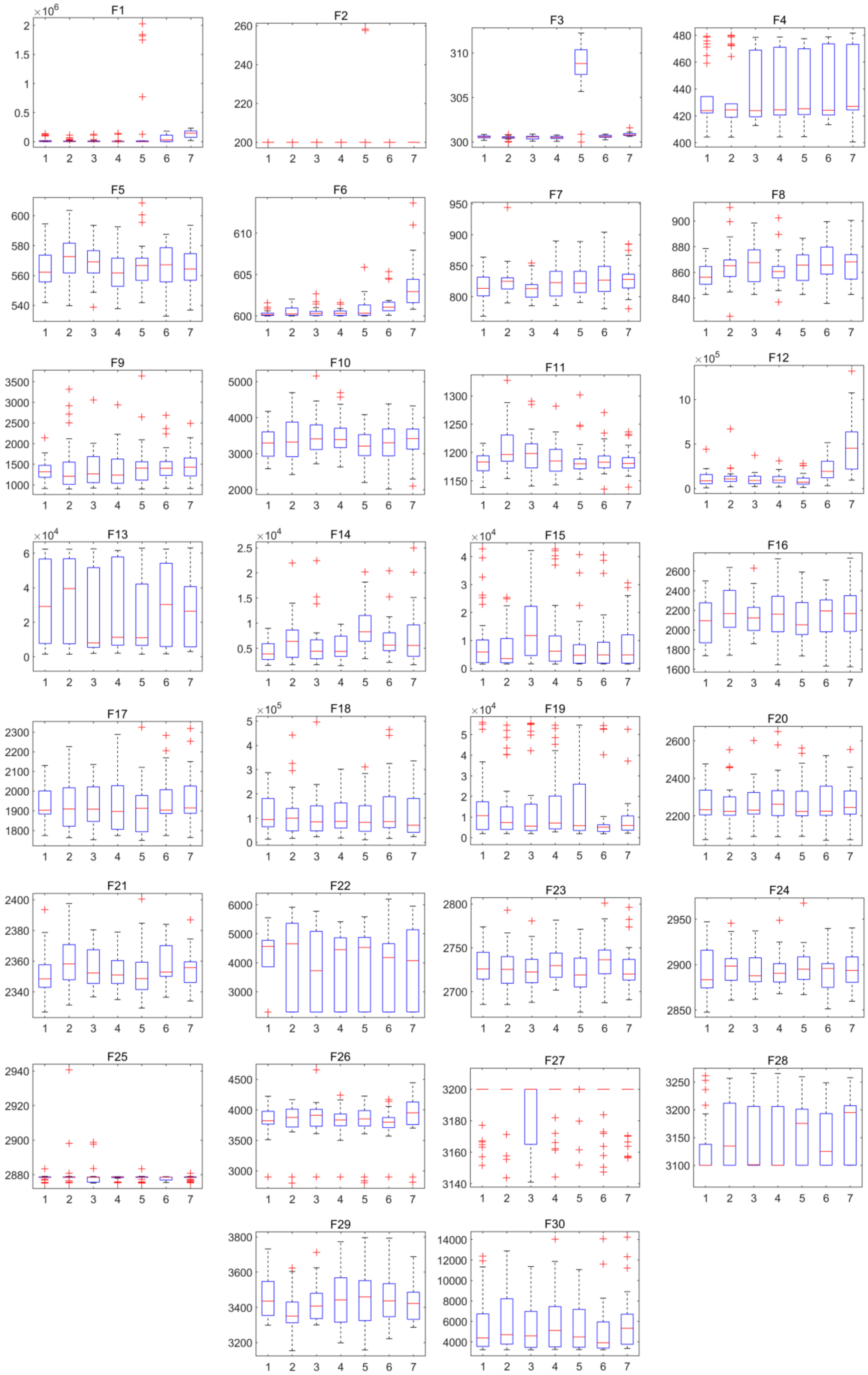

Fig. 1 The box plots of MGWO with different values of λ and μ on 30 benchmark functions

3.2 The position update formula of leader salp in SSA

Salp is a kind of marine organism, and the swarming behavior called the salp chain's swarming behavior helps salps move and forage. SSA is a swarm intelligence optimization algorithm first proposed by Mirjalili et al. in 2007, inspired by the foraging salp chain pattern. According to the positions of individuals in the slap chain, slaps are divided into leaders and followers. Followers must update their positions under the guidance of a leader. In the MGWO algorithm proposed in this paper, the position update formula of leader salp in the original SSA will be used.

The position update formula is as follows:

$$(X_{i,j}^{new})^T = \begin{cases} y_j + c_1 \times \left(c_2 \times \left(ub_j - lb_j\right) + lb_j\right), & c_3 < 0.5 \\ y_j - c_1 \times \left(c_2 \times \left(ub_j - lb_j\right) + lb_j\right), & c_3 \geq 0.5 \end{cases} \tag{22}$$

$$c_1 = 2e^{-\left(\frac{4FEs}{Max\_FEs}\right)^2} \tag{23}$$

where c_2 and c_3 are random numbers between the interval $[0,1]$. Max_FEs is the maximum evaluations, and FEs is the current number of evaluations. y_j presents the *j*th dimension value of the position that the current optimal individual locates. lb_j and ub_j represent the lower bound and the upper bound of the *j*th dimension, respectively. $(X_{i,j}^{new})^T$ is the transposed value of the new position that the *i*th salp obtained on the *j*th dimension.

Let $r = \left\|\mathrm{X}_i - \mathrm{X}_{Alpha}\right\|$ is the Cartesian distance of the *i*th individual and the current optimal individual. At the second stage, when the r is greater than 0.5, the MGWO algorithm performs the above position update operation on the *i*th grey wolf. When r is less than 0.5, it can be considered that the *i*-th individual is already very near the current optimal individual. To ensure the diversity of the population at the second stage, no movement operation will be performed on the current individual. The purpose of setting the distance threshold is to keep the distance between individuals and prevent the grey wolf population from entering the convergence ahead of time and falling into the local optima trap. Using this strategy at the second stage will enable the algorithm to achieve a faster convergence rate than the original GWO, and the algorithm will not quickly converge prematurely. Although after this stage, the algorithm can obtain a solution with much higher accuracy than the original GWO, there is still a risk of falling into the local optima trap to a great extent.

3.3 Position mutation by Cauchy distribution

The Cauchy mutation was embedded in optimization algorithms as an update strategy by many researchers. It has been proved to be an effective technique for improving optimization algorithms (Ali and Pant, 2011). By adjusting the Cauchy mutation parameters, an algorithm's exploration ability or the exploitation ability can be enhanced. When the step size of the Cauchy mutation is large, it can be regarded as a random walk method so that the algorithm is guided to explore the entire search domain. When the step size of the Cauchy mutation is small enough, the algorithm is guided to exploit the candidate solutions' neighborhood to obtain higher quality solutions. Wang et al. (Wang et al., 2020d) used Cauchy mutation as the adaptive learning strategy of agents and used a specific time to limit the adaptive learning. Then the better solutions generated by the Cauchy mutation replaced the original candidate solutions. Although Cauchy mutation is an effective strategy to improve the performance of the algorithm, too many times of Cauchy mutation in each iteration will increase the time complexity of the algorithm.

The theoretical basis of Cauchy mutation is the Cauchy probability density function，which is as follows:

$$f(x)=\frac{1}{\pi}*\left[\frac{\gamma}{(x-x_0)^2+\gamma^2}\right] \tag{24}$$

where x_0 is the location parameter defining the peak position of the distribution, and γ is the scale parameter of half-width at half of the maximum value. Let X obeys Cauchy distribution as $X{\sim}C(x_0,\gamma)$. The smaller γ is, the more likely the value obtained by the Cauchy probability density function falls into the neighborhood of x_0 is. The Cauchy mutation used in the MGWO algorithm obeys $X{\sim}C(0,0.5)$. Controlled by the current optimal solution, a new position Y is randomly generated according to the upper and lower bounds of the objective function. And then perform the following mutation strategy on each dimension of Y:

$$Y^j=X_{Alpha}^j+cauchy*\left(X_{r1}^j-X_{r2}^j\right) \tag{25}$$

where *cauchy* is a random number generated by the Cauchy distribution, which obeys $X{\sim}C(0,0.5)$. X_{Alpha}^j is the *j*th dimensional position of the optimal solution obtained so far. X_{r1}^j and X_{r2}^j are the *j*th dimensional positions of two wolves randomly selected from the wolf population. Noted that these two wolves are not equal to the current optimal wolf. The addition of a multiplier $X_{r1}^j-X_{r2}^j$ is to increase the population's diversity and control the Cauchy mutation's scope within the search domain limit. When this term is small enough, the algorithm exploits the current optimal solution neighborhood, and when the term is large, the algorithm will explore the entire search domain. This term's value is random, but at the last stage of the entire search process, the population tends to converge and this value is not extremely large. Thus, the population's situation will not be excessively chaotic.

When the mutation strategy progressed to the *j*th dimension if the fitness of Y is worse than that of X_{Alpha}, continue to update Y in the next dimension. Once the fitness of Y is better than that of X_{Alpha}, let $X_{new}=Y$ and $X_{Alpha}=Y$, and then continue to update Y in the next dimension. The mutation near the optimal solution can make the algorithm gain a more vital exploitation ability at the last stage and enhance the algorithm's ability to get rid of the local optimal trap.

γ is a fixed parameter with a value of 0.5, which is proved by the following comparative experimental results. In the comparative experiment, the population size is 30, the dimension of the objective function is 30, the maximum number of evaluations is 300000, and the number of parallel random runs is 30. **Table 3** displays the test results obtained by algorithms with different values of γ on 30 benchmark functions of IEEE CEC 2017. *Avg* is the average of the ranks obtained on 30 benchmark functions by algorithms with different values of γ and *Rank* is the final rank that can visually observe the performance of the algorithms. According to the *Avg* and *Rank*, setting the γ parameter to 0.5 is the best choice.

Table 4 displays the standard deviations (*STD*) obtained by the MGWO with different values of γ on 30 benchmark functions with 30 times of parallel random runs. The minimum one among the standard deviations obtained by MGWO with different parameter values is marked in bold on each benchmark function. MGWO, whose value of γ is setting to 0.5, has the best stability on unimodal functions, simple multimodal functions, and hybrid functions, but its stability on composition functions has declined. However, when the comparison algorithms are ranked using the average of the results obtained in 30 parallel random runs, the ranking of the MGWO with parameter γ value of 0.5 is still the first.

Figure 2 reveals the box plots of MGWO with different values of γ on 30 benchmark functions with 30 times of parallel random runs. The tick labels of the x-axis respectively represent MGWO~MGWOIV in **Table 3**. It can be seen that when the parameter γ is set to 0.5, on most benchmark functions, MGWO can get smaller *min* and median than other competitors. The number of outliers in the dataset obtained by MGWO with different parameter values is not much different. These show that MGWO can obtain more accurate optimization results than other competitors without taking stability as the cost. Box plots further prove that setting γ to 0.5 is a correct choice.

Table 3. Comparative experimental results of MGWO with different values of γ

	MGWO	**MGWOII**	**MGWOIII**	**MGWOIV**
Value	0.5	1.0	1.5	2.0
Avg	1.57	2.47	2.77	3.20
Rank	1	2	3	4

Table 4. The STD obtained by the MGWO with different values of γ

	F1	**F2**	**F3**	**F4**	**F5**
MGWO	**3.5481E+04**	**1.1370E-03**	**2.0183E-01**	2.7817E+01	**1.3526E+01**
MGWOII	5.9830E+04	2.7306E+00	2.9523E-01	**2.3239E+01**	1.6987E+01
MGWOIII	6.4173E+04	3.3066E+00	3.6419E-01	2.4874E+01	1.8387E+01
MGWOIV	6.0368E+04	1.7255E-01	3.9819E-01	2.3469E+01	1.6090E+01
	F6	**F7**	**F8**	**F9**	**F10**
MGWO	**5.5100E-01**	2.4199E+01	1.2295E+01	**3.8305E+02**	5.0894E+02
MGWOII	2.5260E+00	**1.8066E+01**	1.5135E+01	4.7029E+02	4.5979E+02
MGWOIII	2.7302E+00	2.7782E+01	**8.4836E+00**	5.6674E+02	5.7411E+02
MGWOIV	2.6953E+00	2.3765E+01	1.3889E+01	6.2428E+02	**4.3243E+02**
	F11	**F12**	**F13**	**F14**	**F15**
MGWO	**2.5535E+01**	**5.0986E+04**	**2.1944E+04**	7.2940E+03	**8.3263E+03**
MGWOII	3.5192E+01	6.7870E+05	2.3046E+04	5.2692E+03	9.9754E+03
MGWOIII	3.8956E+01	8.7334E+05	2.6382E+04	**4.7801E+03**	1.5184E+04
MGWOIV	3.2161E+01	9.9835E+05	3.0480E+04	4.9225E+03	1.2388E+04
	F16	**F17**	**F18**	**F19**	**F20**
MGWO	**2.1325E+02**	1.3668E+02	**6.8155E+04**	1.9973E+04	1.3123E+02
MGWOII	2.4677E+02	1.3283E+02	1.0930E+05	1.9461E+04	1.2524E+02
MGWOIII	2.7728E+02	**1.1166E+02**	1.2037E+05	**1.1561E+04**	**1.1517E+02**
MGWOIV	2.4208E+02	1.3001E+02	7.8510E+04	1.5625E+04	1.2475E+02
	F21	**F22**	**F23**	**F24**	**F25**
MGWO	1.7558E+01	1.4263E+03	2.0614E+01	2.3874E+01	3.7100E+00
MGWOII	1.1650E+01	1.3241E+03	2.0349E+01	**2.0826E+01**	**3.5539E+00**
MGWOIII	**1.0974E+01**	1.3135E+03	**1.7952E+01**	2.2727E+01	1.8441E+01
MGWOIV	1.2447E+01	**1.3115E+03**	2.3708E+01	2.3856E+01	7.5744E-01
	F26	**F27**	**F28**	**F29**	**F30**
MGWO	2.7377E+02	1.9399E+01	5.2041E+01	1.3180E+02	3.1842E+03

MGWOII	2.6871E+02	1.3567E+01	**5.1143E+01**	1.5275E+02	2.9212E+03
MGWOIII	**1.9449E+02**	1.2088E+01	5.6786E+01	**1.1785E+02**	**2.1785E+03**
MGWOIV	3.1305E+02	**9.6027E+00**	5.6405E+01	1.4112E+02	5.4840E+03

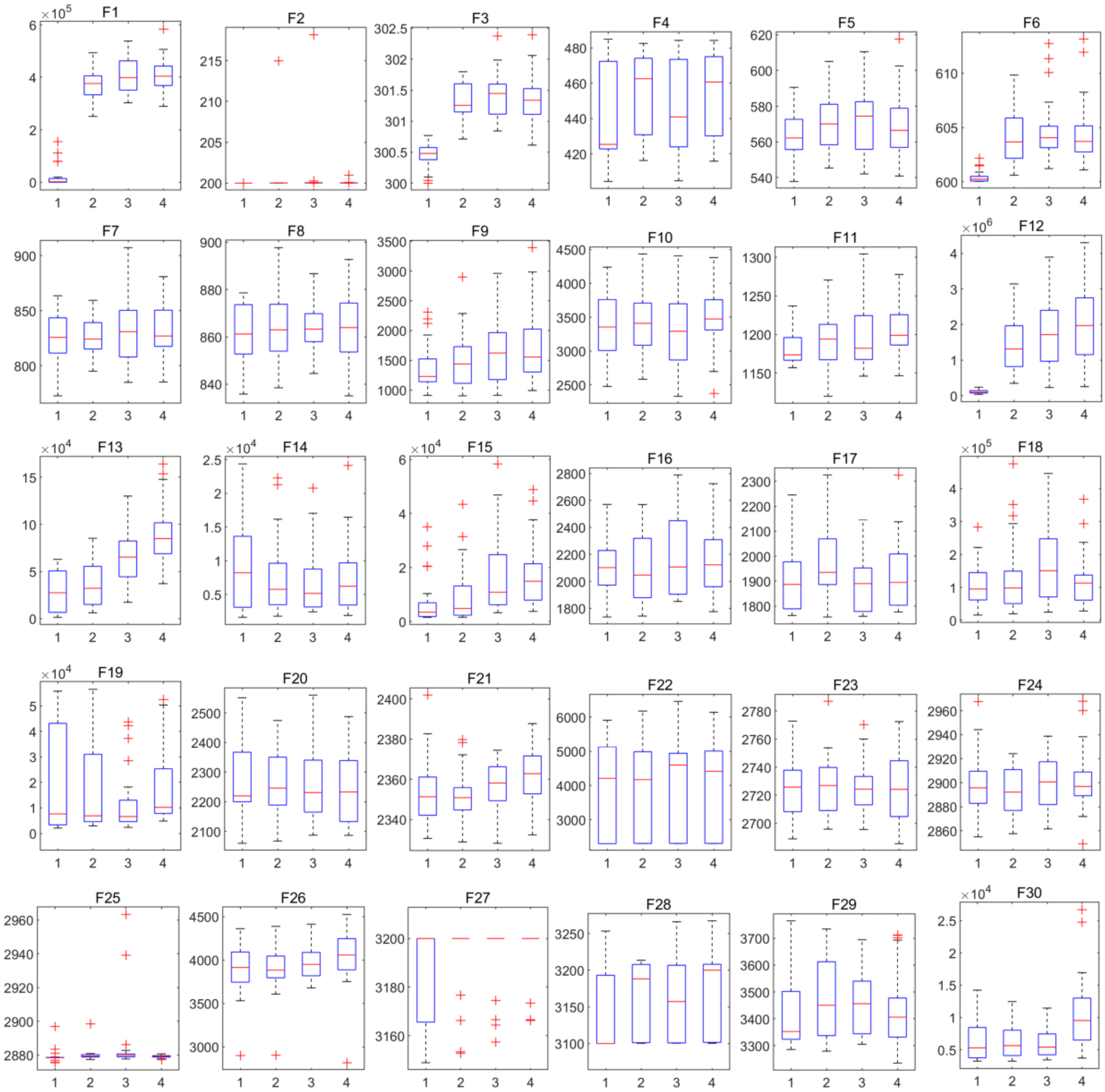

Fig. 2 The box plots of MGWO with different values of γ on 30 benchmark functions

3.4 The ensemble process of MGWO

In the proposed MGWO, the whole search process is divided into three stages, where the parameters' values of λ and μ are 0.4 and 0.7, respectively. The complete MGWO algorithm is obtained by performing different operations to update the agents' positions at different stages. First, the parameters and variables are initialized, and then the iterative process begins. At the first stage, the MGWO algorithm uses the original GWO algorithm's position update strategy. At the second stage, when the Cartesian distance between the individual wolf and the current optimal solution is greater than 0.5, the MGWO algorithm will perform the position update operation described in Section 3.2 on the current grey wolf. The mutation strategy described in Section 3.3 is performed for each dimension of the current individual wolf at the last stage. When the new position's fitness value obtained by Cauchy mutation is less than the fitness value of the current optimal solution, the new position is used to replace the current grey wolf's position. When the current evaluation times reach the preset maximum evaluation times, the program stops running and returns the current optimal solution as the final global optimal solution. **Algorithm 2** shows the pseudo-code of the MGWO algorithm.

Algorithm 2 Pseudo code of the MGWO algorithm

Objective function $f(X), X = (x_1, \dots, x_d)^T$

Parameters initialization: *N* is the population size, *Max_FEs* is maximum function evaluations. Set current evaluation number *FEs=0*.

Initialize the grey wolf population $X_i (i = 1,2, \dots, n)$

$\varphi_1 = \lambda * Max\_FEs\,; \varphi_2 = \mu * Max\_FEs$

while (FEs ≤ Max_FEs)

  Calculate each wolf's fitness

  $X_{Alpha} =$ the current best solution,

  $X_{Beta} =$ the current second-best solution,

  $X_{Delta} =$ the current third-best solution.

  Update the number of *FEs*

  Update parameters: a by Eq. (5)

  for each individual wolf

    if $(FEs < \varphi_1)$

      Update the current wolf's position by Eq. (4) and (6) – (8)

    else if $(FEs \geq \varphi_1$ and $FEs < \varphi_2)$

      Calculate the Cartesian distance r between the current wolf and X_{Alpha}

      if $(r > 0.5)$

        Update the current wolf's position by Eq. (22) – (23)

      end if

    else

      Generate a new agent Y by upper and lower bounds of objective function.

      for each dimension

        Calculate the new position of Y by Eq. (25)

        if $(f(Y) < f(X_{Alpha}))$

          Accept Y as the current grey wolf

          Accept Y as X_{Alpha}

        end if

      end for

    end if

  end for

end while

Postprocess results and visualization

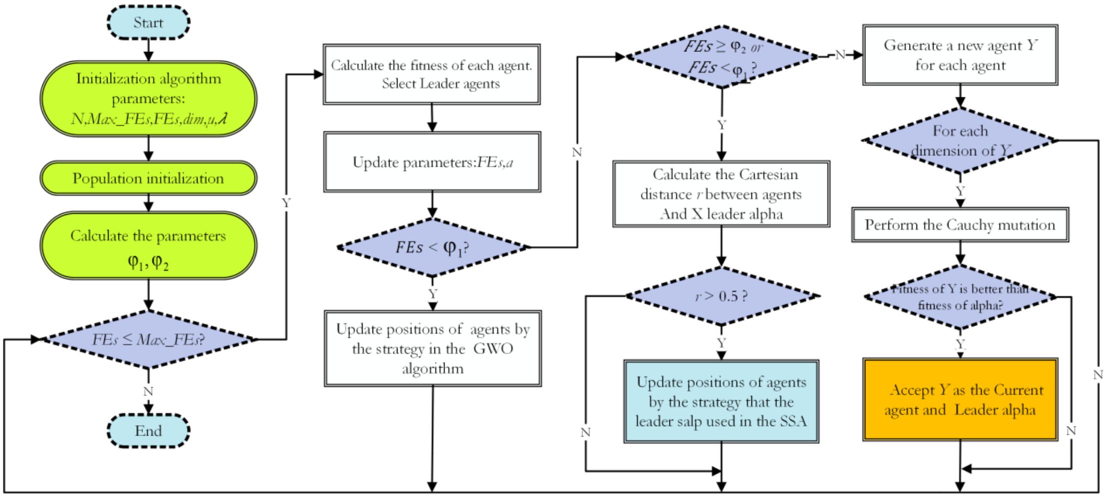

Fig. 3 The flowchart of MGWO

Figure 3 shows the MGWO algorithm's main process. The time complexity of the MGWO algorithm is determined by the number of individuals (*N*), the dimension of the objective function (*dim*), and the maximum number of evaluations (*Max_FEs*). The number of iterations (*T*) is obtained by $(Max\_FEs)/N$. The total time complexity is *O*(MGWO)=*O*(initialization)+*T***O*(calculation of the fitness and selection of the top three agents)+*T***O*(update parameter *a*) +$T*\lambda*O$(perform the GWO algorithm's position update formula)+$T*\lambda*O$(calculation of the distance *r*)+$T*(\mu-\lambda)*O$(perform the position update formula of leader salp in the SSA)+$T*(\mu-\lambda)*O$(generate new agents)+$T*(1-\mu)*O$(perform the Cauchy mutation and calculate the new fitness)+$T*(1-\mu)*O$(update the best solution and the current agent). After calculation, $O(\text{MGWO}) = O(N*dim)+O((N+1)*dim)+T*O(1)+T*\lambda*O(N*dim)+T*\lambda*O(N)+T*(\mu-\lambda)*O(N*dim)+T*(\mu-\lambda)*O(N*dim)+T*(1-\mu)*O(N*dim)+T*(1-\mu)*O(N*dim)=(2T-T*\lambda+2)*O(N*dim)+T*\lambda*O(N)$.

4. Experimental results and discussions

To verify the MGWO algorithm's superiority in dealing with optimization problems, a series of comparative experiments are carried out on 30 benchmark functions of IEEE CEC2017 with other competitive optimization algorithms. Section 4.1 introduces the classifications and search domains of benchmark functions used in the experiments. In Section 4.2, the MGWO algorithm is compared with several traditional meta-heuristic optimization algorithms: whale optimization algorithm (WOA) (Mirjalili et al., 2019), moth-flame optimization (MFO) (Mirjalili et al., 2019), salp swarm algorithm (SSA) (Mirjalili et al., 2019), GWO, DE (Storn and Price, 1997), PSO, FA, and BA. and. In Section 4.3, the MGWO algorithm is compared with several improved GWO algorithms which are HGWO (Zhu et al., 2015), OBLGWO (Heidari et al., 2019b), IGWO (Cai et al., 2019), CAGWO (Lu et al., 2018), and other improved swarm intelligence optimization algorithms which are ALCPSO (Chen et al., 2013), IWOA (Tubishat et al., 2019), BWOA (Chen et al., 2019a), CLSCA (Huang et al., 2020), MSCA (Qu et al., 2018), CMFO (Li et al., 2019), and LGCMFO (Xu et al., 2019c). The feasibility and diversity analysis of the MGWO algorithm and the primary GWO algorithm is carried out in Section 4.4. The comparative experiments on the multi-threshold image segmentation of Leaf Spot Diseases on Maize are in Section 4.5. To ensure the experiments' fairness (Chen et al., 2019b; He et al., 2020; Sun et al., 2020; Wang et al., 2020e; Weng et al., 2021; Zhou et al., 2021), the environments of all experiments are kept in the same condition. All experiments were performed on a 2.10GHz Intel Xeon Gold 5218R processor and 64GB RAM computer, and the MATLAB 2018a was used to write the programs and perform the simulation experiments. **Table 5** lists the parameters that need to be consistent in the simulation experiments. *N* is the number of agents, *dim* is the objective function's dimension, *Max_FEs* represents the maximum number of evaluations, and *Flod* is the number of parallel random runs. Experiments on multi-threshold image segmentation are carried out in Section 4.5, where the number of agents is 20.

Table 5. The relevant parameters involved in the experiments

N	*dim*	*Max_FEs*	*Flod*
30	30	dim*10000	30

Other related parameters and the corresponding values of MGWO, the original GWO, and all other comparison optimization algorithms are shown in **Table 6**, which are derived from their respective papers.

Table 6. The parameters setting of MGWO and the original GWO

Algorithm	Related parameters setting
MGWO	$\lambda = 0.4, \mu = 0.7; \gamma = 0.5;$ $r_1 \in [0,1];\ r_2 \in [0,1]; c_2 \in [0,1];\ c_3 \in [0,1]$
GWO	$r_1 \in [0,1];\ r_2 \in [0,1]$
SSA	$c_2 \in [0,1];\ c_3 \in [0,1]$
DE	$F \in [0.2, 0.8]; CR = 0.2$
PSO	$v_{max} = 6;\ C_1 = 2; C_2 = 2;\ \omega = 1;\ r_1 \in [0,1];\ r_2 \in [0,1]$
WOA	$b = 1;\ r_1 \in [0,1];\ r_2 \in [0,1]; p \in [0,1]; l \in [-1,1]$
FA	$\beta_0 = 1;\ \gamma = 1;\ \alpha \in [0,1]$
BA	$\alpha = \gamma = 0.9; f_{min} = 0, f_{max} = 2;\ A_0 \in [1,2];\ r_0 \in [0,1]$
MFO	$b = 1;\ t \in [-2,1]$
ALCPSO	$\omega = 0.4;\ c_1 = 2;\ c_2 = 2; lifespan = 60; T = 2;$ $r_1 \in [0,1];\ r_2 \in [0,1]$
HGWO	$F \in [0.2, 0.8]; CR = 0.2;\ r_1 \in [0,1];\ r_2 \in [0,1]$
OBLGWO	$b = 1;\ r_1 \in [0,1];\ r_2 \in [0,1]; p \in [0,1];\ \beta \in [2,0]$
IGWO	$beta_{num} = 10; omega_{num} = 15;\ r_1 \in [0,1];\ r_2 \in [0,1]$
CAGWO	$ColumnNum = 5;\ r_1 \in [0,1];\ r_2 \in [0,1]$
IWOA	$b = 1;\ r_1 \in [0,1];\ r_2 \in [0,1]; p \in [0,1]; l \in [-1,1];$ $F \in [0,1]; CR = 0.1$
BWOA	$b = 1; m = 2500;\ \beta = 1.5;\ r_1 \in [0,1];\ r_2 \in [0,1];$ $p \in [0,1]; l \in [-1,1]; x \in [0,1]$
CLSCA	$a = 2;\ \beta = 1.5; d = 1;$ $r_2 \in [0,2\pi];\ r_3 \in [0,2]; r_4 \in [0,1]; x \in [0,1]$
MSCA	$a = 2;\ \beta = 1.5;\ \varepsilon = 30;\ \lambda = 0.01;\ \omega_{min} = 0.4;\ \omega_{max} = 0.9;$ $\sigma_v = 1;\ r_2 \in [0,2\pi];\ r_3 \in [0,2]; r_4 \in [0,1];$
CMFO	$b = 1;\ cc_0(Singer\ maps) = 0.7$
LGCMFO	$b = 1;\ t \in [-2,1];\ \beta = 1.5; \mu = 0; \sigma^2 = 1; g = 1$

4.1Benchmark function validation

The related contents of the 30 benchmark functions derived from IEEE CEC2017 are shown in **Table 7**, where *Range* is the range of the search space on each dimension, and *F(min)* represents the optimal solution. These benchmark functions are all single objective boundary constraint functions. There are no other constraints except boundary constraints. F1~F3 are unimodal functions. F4~F10 are simple multimodal functions with many local optima. F11~F20 are hybrid functions. F21~F30 are composition functions. Therefore, these 30 benchmark functions can be used to test the optimization algorithms' performances more comprehensively. Thus, the experimental results can show which types of optimization problems the MGWO algorithm can solve better by the MGWO algorithm.

Table 7. Benchmark functions of IEEE CEC2017

ID	Function	Range	F(min)
F1	Shifted and Rotated Bent Cigar Function	[-100,100]	100
F2	Shifted and Rotated Sum of Different Power Function	[-100,100]	200
F3	Shifted and Rotated Zakharov Function	[-100,100]	300
F4	Shifted and Rotated Rosenbrock's Function	[-100,100]	400
F5	Shifted and Rotated Rastrigin's Function	[-100,100]	500
F6	Shifted and Rotated Expanded Scaffer's F6 Function	[-100,100]	600
F7	Shifted and Rotated Lunacek Bi_Rastrigin Function	[-100,100]	700
F8	Shifted and Rotated Non-Continuous Rastrigin's Function	[-100,100]	800
F9	Shifted and Rotated Levy Function	[-100,100]	900
F10	Shifted and Rotated Schwefel's Function	[-100,100]	1000
F11	Hybrid Function 1 (*N=3*)	[-100,100]	1100
F12	Hybrid Function 2 (*N=3*)	[-100,100]	1200
F13	Hybrid Function 3 (*N=3*)	[-100,100]	1300
F14	Hybrid Function 4 (*N=4*)	[-100,100]	1400
F15	Hybrid Function 5 (*N=4*)	[-100,100]	1500
F16	Hybrid Function 6 (*N=4*)	[-100,100]	1600
F17	Hybrid Function 7 (*N=5*)	[-100,100]	1700
F18	Hybrid Function 8 (*N=5*)	[-100,100]	1800
F19	Hybrid Function 9 (*N=5*)	[-100,100]	1900
F20	Hybrid Function 10 (*N=6*)	[-100,100]	2000
F21	Composition Function 1 (*N=3*)	[-100,100]	2100
F22	Composition Function 2 (*N=3*)	[-100,100]	2200
F23	Composition Function 3 (*N=4*)	[-100,100]	2300
F24	Composition Function 4 (*N=4*)	[-100,100]	2400
F25	Composition Function 5 (*N=5*)	[-100,100]	2500
F26	Composition Function 6 (*N=5*)	[-100,100]	2600
F27	Composition Function 7 (*N=6*)	[-100,100]	2700
F28	Composition Function 8 (*N=6*)	[-100,100]	2800
F29	Composition Function 9 (*N=3*)	[-100,100]	2900
F30	Composition Function 10 (*N=3*)	[-100,100]	3000

4.2 Comparison with traditional MAs

This section compares the proposed MGWO algorithm with several common MAs: GWO, SSA, DE, PSO, WOA, FA, BA, and MFO on benchmark functions described above. **Table 8** shows the experimental results of the MGWO algorithm and competitors on each benchmark function. Where Avg and Std represent the average value and the standard deviation of the optimal values obtained by each algorithm running independently for 30 times on each benchmark function, respectively. Avg is used to measure the quality of the global optimal solution obtained, and Std is used to measure the algorithms' stability. The symbols $''+''$, $''$-$''$ and $''=''$ indicate the number of the benchmark functions on which performance of the MGWO algorithm is superior or inferior to other algorithms, or there is no apparent difference between the two competitive algorithms. At the end of the table, the average rank (*Avg*) of the results and the final rank (*Rank*) counted by the Friedman test (Derrac et al., 2011) are shown. Apparently, the Wilcoxon signed-rank test result indicates that MGWO ranks first among the nine optimization algorithms, and the *Avg* is 1.53.

Because the optimization algorithms are to search the global minima of all benchmark functions, the smallest the value of *Avg* is, the better the quality of algorithms obtained by algorithms. The smallest *Std* is, the more stable the algorithm is. Therefore, the smallest *Avg* and the smallest *Std* are marked in bold. Among the 30 benchmark functions, the globally optimal solutions of 28 functions obtained by the MGWO algorithm were statistically superior to those obtained by the GWO algorithm. Moreover, there was no significant performance difference between the two algorithms on the remaining two benchmark functions. It is proved that the MGWO algorithm improves the performance of the original GWO algorithm because the former can obtain approximate values closer to the real global optimal values than the latter. Compared with the competitive algorithm DE, the MGWO algorithm also has apparent advantages on 19 benchmark functions. There was no significant performance difference between the two algorithms on the other five benchmark functions. Compared with the other six traditional MAs, the advantages of the MGWO algorithm are more prominent.

Table 8. Comparison of the MGWO algorithm with traditional MAs

	F1		**F2**	
	Avg	Std	Avg	Std
MGWO	2.4194E+04	4.0913E+04	**2.0000E+02**	1.1530E-03
GWO	2.0300E+09	1.4800E+09	1.1800E+31	3.6100E+31
SSA	6.8894E+03	6.9353E+03	2.0276E+02	8.4467E+00
DE	**9.4041E+02**	**1.4075E+03**	2.8700E+21	8.5600E+21
PSO	1.3300E+08	1.6600E+07	1.1300E+27	4.3000E+27
WOA	3.4311E+06	3.0024E+06	1.7400E+21	5.3900E+21
FA	1.3900E+10	1.6500E+09	1.9800E+34	5.6400E+34
BA	6.0789E+05	3.8505E+05	**2.0000E+02**	**7.8800E-05**
MFO	9.0100E+09	7.0200E+09	1.0500E+37	4.9400E+37
	F3		**F4**	
	Avg	Std	Avg	Std

MGWO	3.0053E+02	1.4260E-01	**4.3366E+02**	2.6162E+01
GWO	3.3699E+04	1.3719E+04	5.8283E+02	6.4499E+01
SSA	**3.0000E+02**	**8.4100E-09**	4.9057E+02	**1.8798E+01**
DE	2.0027E+04	4.2468E+03	4.9265E+02	1.1017E+01
PSO	6.4572E+02	4.6359E+01	5.1777E+02	2.3996E+01
WOA	1.6230E+05	5.9307E+04	5.2832E+02	2.9742E+01
FA	5.9473E+04	8.6754E+03	1.4014E+03	1.3584E+02
BA	3.0014E+02	1.4270E-01	4.7014E+02	3.6213E+01
MFO	9.7972E+04	8.9262E+04	1.2927E+03	8.6214E+02
	F5		**F6**	
	Avg	Std	Avg	Std
MGWO	**5.6328E+02**	1.6718E+01	6.0040E+02	7.0649E-01
GWO	5.9779E+02	3.1201E+01	6.0728E+02	3.7124E+00
SSA	6.1587E+02	2.9841E+01	6.3061E+02	9.4540E+00
DE	6.0960E+02	8.2401E+00	**6.0000E+02**	**0.0000E+00**
PSO	7.4058E+02	3.3489E+01	6.4913E+02	1.5729E+01
WOA	7.7491E+02	6.0319E+01	6.7433E+02	1.1000E+01
FA	7.5696E+02	**1.0412E+01**	6.4391E+02	2.7444E+00
BA	8.3760E+02	6.4574E+01	6.7134E+02	1.0097E+01
MFO	7.0022E+02	4.5105E+01	6.3657E+02	9.7714E+00
	F7		**F8**	
	Avg	Std	Avg	Std
MGWO	**8.2146E+02**	2.3771E+01	**8.6696E+02**	1.7649E+01
GWO	8.6084E+02	3.7516E+01	8.9272E+02	2.9468E+01
SSA	8.6522E+02	3.2550E+01	9.1031E+02	3.2472E+01
DE	8.4104E+02	**8.0786E+00**	9.0900E+02	8.7635E+00
PSO	9.1992E+02	1.7930E+01	9.9174E+02	2.4140E+01
WOA	1.2157E+03	8.7575E+01	1.0052E+03	5.9909E+01
FA	1.3747E+03	3.9619E+01	1.0491E+03	**1.1026E+01**
BA	1.6328E+03	1.9465E+02	1.0621E+03	8.0426E+01
MFO	1.1089E+03	2.4868E+02	1.0080E+03	4.5646E+01
	F9		**F10**	
	Avg	Std	Avg	Std
MGWO	1.3645E+03	3.8822E+02	**3.3999E+03**	5.5125E+02
GWO	1.7317E+03	5.3961E+02	3.8978E+03	6.3232E+02
SSA	3.0950E+03	1.2880E+03	4.9105E+03	7.6037E+02
DE	**9.0000E+02**	**9.6743E-14**	5.9171E+03	2.9090E+02
PSO	5.2904E+03	2.1348E+03	6.2501E+03	5.3422E+02
WOA	8.0920E+03	2.6791E+03	6.1643E+03	7.7617E+02
FA	5.3628E+03	5.2487E+02	7.9610E+03	**2.3948E+02**
BA	1.3828E+04	5.4927E+03	5.6293E+03	5.9239E+02

MFO	6.2666E+03	1.7145E+03	5.3614E+03	7.0395E+02
	F11		**F12**	
	Avg	Std	Avg	Std
MGWO	1.1757E+03	**1.9279E+01**	**1.5297E+05**	**1.4689E+05**
GWO	2.1107E+03	9.7803E+02	4.7268E+07	7.2172E+07
SSA	1.2566E+03	4.7190E+01	1.6137E+06	1.2617E+06
DE	**1.1555E+03**	2.5041E+01	1.6345E+06	7.6583E+05
PSO	1.2891E+03	3.9330E+01	2.6520E+07	1.0586E+07
WOA	1.5224E+03	1.8900E+02	4.0232E+07	3.4064E+07
FA	3.5287E+03	4.4247E+02	1.4975E+09	2.7120E+08
BA	1.3296E+03	7.7239E+01	2.3166E+06	2.0014E+06
MFO	5.9585E+03	5.6447E+03	3.6092E+08	8.4887E+08
	F13		**F14**	
	Avg	Std	Avg	Std
MGWO	**2.5774E+04**	2.0935E+04	7.7290E+03	5.9384E+03
GWO	1.6035E+07	6.5705E+07	2.2769E+05	3.2979E+05
SSA	9.5942E+04	5.8882E+04	**4.0867E+03**	**2.1834E+03**
DE	3.1134E+04	**1.8650E+04**	3.8371E+04	2.8748E+04
PSO	6.9569E+06	1.2946E+07	1.2549E+04	2.2571E+04
WOA	1.7338E+05	1.0463E+05	7.9914E+05	8.8314E+05
FA	5.9296E+08	1.8809E+08	2.1299E+05	7.9892E+04
BA	2.8724E+05	1.0480E+05	7.4888E+03	4.9374E+03
MFO	2.0179E+08	6.0685E+08	3.2763E+05	1.1869E+06
	F15		**F16**	
	Avg	Std	Avg	Std
MGWO	1.0049E+04	1.3060E+04	2.1576E+03	2.4090E+02
GWO	1.5224E+05	4.4815E+05	2.4001E+03	2.4235E+02
SSA	4.8333E+04	2.7033E+04	2.4271E+03	2.7542E+02
DE	**7.1219E+03**	**3.3429E+03**	**2.0600E+03**	**1.2773E+02**
PSO	4.1611E+05	1.7336E+05	2.8118E+03	2.3697E+02
WOA	7.9413E+04	6.4775E+04	3.4044E+03	4.3608E+02
FA	7.1584E+07	2.0832E+07	3.4268E+03	1.2971E+02
BA	1.2225E+05	6.9405E+04	3.4173E+03	4.7420E+02
MFO	4.1185E+04	3.2561E+04	3.1913E+03	3.6608E+02
	F17		**F18**	
	Avg	Std	Avg	Std
MGWO	1.9162E+03	1.0254E+02	**8.8036E+04**	**6.2562E+04**
GWO	1.9788E+03	1.4376E+02	5.8249E+05	6.9463E+05
SSA	1.9916E+03	1.3147E+02	1.4183E+05	1.1436E+05
DE	**1.8492E+03**	**6.6971E+01**	2.6542E+05	1.0734E+05

PSO	2.3952E+03	2.0462E+02	1.9238E+05	1.2733E+05
WOA	2.5010E+03	2.7952E+02	2.0784E+06	2.6870E+06
FA	2.5076E+03	1.2326E+02	3.5380E+06	1.6507E+06
BA	2.7688E+03	3.0294E+02	2.0863E+05	1.4936E+05
MFO	2.5576E+03	2.3590E+02	5.8556E+06	1.7834E+07
	F19		**F20**	
	Avg	Std	Avg	Std
MGWO	1.7301E+04	1.8314E+04	2.2781E+03	1.1064E+02
GWO	6.4318E+05	1.0971E+06	2.3710E+03	1.2576E+02
SSA	3.2149E+05	1.1641E+05	2.4409E+03	1.3256E+02
DE	**7.8069E+03**	**4.6828E+03**	**2.1314E+03**	**6.6880E+01**
PSO	1.3068E+06	5.8293E+05	2.6304E+03	1.7194E+02
WOA	2.4513E+06	2.0773E+06	2.7314E+03	1.9269E+02
FA	9.5994E+07	3.9093E+07	2.5888E+03	9.3228E+01
BA	6.2920E+05	2.1118E+05	2.9895E+03	2.1683E+02
MFO	5.1073E+07	2.4205E+08	2.6575E+03	2.2331E+02
	F21		**F22**	
	Avg	Std	Avg	Std
MGWO	**2.3543E+03**	1.2723E+01	**3.7721E+03**	1.5577E+03
GWO	2.3893E+03	3.6967E+01	4.4478E+03	1.7001E+03
SSA	2.4094E+03	2.6606E+01	4.6228E+03	2.0188E+03
DE	2.4087E+03	9.2778E+00	4.2827E+03	1.9968E+03
PSO	2.5404E+03	4.0358E+01	5.6485E+03	2.7546E+03
WOA	2.5794E+03	6.9289E+01	6.6739E+03	2.0856E+03
FA	2.5400E+03	**1.0115E+01**	3.8256E+03	**1.7341E+02**
BA	2.6188E+03	8.7349E+01	7.1658E+03	1.1298E+03
MFO	2.5051E+03	3.9461E+01	6.5707E+03	9.4533E+02
	F23		**F24**	
	Avg	Std	Avg	Std
MGWO	**2.7291E+03**	1.8759E+01	**2.9025E+03**	2.4828E+01
GWO	2.7569E+03	2.8567E+01	2.9359E+03	5.6068E+01
SSA	2.7527E+03	2.6210E+01	2.9073E+03	2.6872E+01
DE	2.7569E+03	**9.0662E+00**	2.9585E+03	**1.1556E+01**
PSO	3.1149E+03	1.4894E+02	3.1836E+03	9.3535E+01
WOA	3.0393E+03	1.1066E+02	3.1751E+03	9.9773E+01
FA	2.9114E+03	1.0293E+01	3.0662E+03	1.1569E+01
BA	3.3386E+03	1.5392E+02	3.3761E+03	1.2773E+02
MFO	2.8313E+03	3.9714E+01	2.9800E+03	4.2096E+01
	F25		**F26**	
	Avg	Std	Avg	Std
MGWO	**2.8778E+03**	1.7874E+00	**3.8606E+03**	3.0151E+02

GWO	2.9981E+03	9.2791E+01	4.5804E+03	4.0019E+02
SSA	2.8984E+03	2.0175E+01	4.3976E+03	9.7237E+02
DE	2.8874E+03	**3.4522E-01**	4.6410E+03	1.3883E+02
PSO	2.9042E+03	1.7736E+01	4.9634E+03	1.9113E+03
WOA	2.9521E+03	3.0641E+01	7.4442E+03	1.4462E+03
FA	3.5721E+03	9.0579E+01	6.5103E+03	**1.3797E+02**
BA	2.9168E+03	2.4166E+01	9.0025E+03	1.4452E+03
MFO	3.3783E+03	5.6778E+02	5.9280E+03	4.6117E+02
	F27		**F28**	
	Avg	Std	Avg	Std
MGWO	**3.1926E+03**	1.5907E+01	3.1441E+03	5.7130E+01
GWO	3.2511E+03	2.7653E+01	3.4509E+03	1.5407E+02
SSA	3.2348E+03	1.4878E+01	3.2035E+03	3.3908E+01
DE	3.2053E+03	**3.9009E+00**	3.1907E+03	4.8217E+01
PSO	3.3314E+03	8.4404E+01	3.2557E+03	3.4200E+01
WOA	3.3900E+03	8.4375E+01	3.3053E+03	**2.7038E+01**
FA	3.3352E+03	1.8394E+01	3.8925E+03	1.0143E+02
BA	3.4550E+03	1.6919E+02	**3.1363E+03**	6.2698E+01
MFO	3.2539E+03	2.7842E+01	4.3936E+03	9.8487E+02
	F29		**F30**	
	Avg	Std	Avg	Std
MGWO	**3.4336E+03**	1.1598E+02	**5.7324E+03**	**2.7936E+03**
GWO	3.7762E+03	1.8302E+02	3.9170E+06	2.5684E+06
SSA	3.8809E+03	1.9078E+02	1.1721E+06	7.7875E+05
DE	3.5349E+03	**6.5258E+01**	1.3249E+04	3.6055E+03
PSO	4.3202E+03	2.6293E+02	3.2375E+06	1.2255E+06
WOA	4.8223E+03	3.4477E+02	1.4496E+07	9.3319E+06
FA	4.6609E+03	1.2870E+02	9.1080E+07	3.1435E+07
BA	4.9142E+03	3.6160E+02	1.1166E+06	7.9138E+05
MFO	4.1512E+03	2.9961E+02	9.7656E+05	2.2171E+06

	Wilcoxon signed-rank test		
	+/-/=	Avg	Rank
MGWO	~	**1.53**	**1**
GWO	28/0/2	4.70	4
SSA	25/3/2	3.20	3
DE	19/6/5	2.67	2
PSO	29/0/1	5.67	5
WOA	30/0/0	6.93	8
FA	29/0/1	7.43	9
BA	26/2/2	6.23	6
MFO	30/0/0	6.63	7

Table 9 shows the p-values calculated from the MGWO algorithm results and other comparison algorithms after running independently for 30 times on each benchmark function. There is a statistically significant difference between the MGWO algorithm's performance and the competitor if the corresponding p-value is less than 0.05. The symbol "+" presents that the MGWO algorithm's performance is better than that of the competitor in statistics, while the sign "-" is the opposite. If there is no symbol, it means that no statistically significant difference between the two algorithms. Through the p-values and the symbols, it can be seen that the MGWO algorithm improves the original GWO algorithm on both unimodal and multimodal functions. The original SSA performed better when the objective function is unimodal but not as well as the MGWO algorithm when the objective function is multimodal. Compared with DE, the MGWO algorithm is superior to DE in optimizing composition functions. It improves the ability to deal with hybrid functions to a small extent. The MGWO algorithm's performance on unimodal functions and simple multimodal functions is similar to that of DE. Moreover, compared with the other MAs, the MGWO algorithm can improve the ability to search all kinds of objective functions. We can conclude that the MGWO algorithm has apparent competitiveness through these discussions compared with traditional MAs involved in this experiment.

Table 9. The p-values between the MGWO algorithm and competitors

Function	GWO		SSA		DE		PSO	
F1	1.7344E-06	+	4.9498E-02	-	1.1499E-04	-	1.7344E-06	+
F2	1.7344E-06	+	1.8519E-02	+	1.7344E-06	+	1.7344E-06	+
F3	1.7344E-06	+	1.7344E-06	-	1.7344E-06	+	1.7344E-06	+
F4	1.7344E-06	+	2.3534E-06	+	1.7344E-06	+	1.7344E-06	+
F5	5.3070E-05	+	2.6033E-06	+	1.7344E-06	+	1.7344E-06	+
F6	1.9209E-06	+	1.7344E-06	+	1.7344E-06	-	1.7344E-06	+
F7	9.7110E-05	+	1.7988E-05	+	5.7064E-04	+	1.7344E-06	+
F8	5.2872E-04	+	1.0246E-05	+	2.6033E-06	+	1.7344E-06	+
F9	1.6566E-02	+	5.2165E-06	+	1.7344E-06	-	3.8822E-06	+
F10	1.9646E-03	+	2.6033E-06	+	1.7344E-06	+	1.7344E-06	+
F11	1.7344E-06	+	2.1266E-06	+	6.0350E-03	-	1.7344E-06	+
F12	1.7344E-06	+	1.9209E-06	+	1.7344E-06	+	1.7344E-06	+
F13	6.3391E-06	+	1.1265E-05	+	4.1653E-01		1.7344E-06	+
F14	5.2165E-06	+	6.4242E-03	-	6.9838E-06	+	2.2102E-01	
F15	9.7110E-05	+	7.6909E-06	+	8.2901E-01		1.7344E-06	+
F16	1.1138E-03	+	3.3173E-04	+	5.1931E-02		1.7344E-06	+
F17	1.3591E-01		2.4308E-02	+	2.0671E-02	-	1.7344E-06	+
F18	1.3601E-05	+	3.0010E-02	+	3.5152E-06	+	1.6046E-04	+
F19	3.5152E-06	+	1.7344E-06	+	8.5896E-02		1.7344E-06	+
F20	3.1618E-03	+	8.9187E-05	+	4.2857E-06	-	1.7344E-06	+
F21	6.9838E-06	+	1.7344E-06	+	1.7344E-06	+	1.7344E-06	+
F22	9.7772E-02		9.3676E-02		2.3694E-01		2.4147E-03	+
F23	1.2506E-04	+	9.6266E-04	+	1.9729E-05	+	1.7344E-06	+
F24	2.0671E-02	+	3.7094E-01		1.9209E-06	+	1.7344E-06	+
F25	1.7344E-06	+	1.7344E-06	+	1.7344E-06	+	1.7344E-06	+
F26	1.3601E-05	+	1.1079E-02	+	1.9209E-06	+	1.7518E-02	+

F27	1.7344E-06	+	1.7344E-06	+	5.7517E-06	+	1.7344E-06	+
F28	1.7344E-06	+	8.9187E-05	+	2.5846E-03	+	5.7517E-06	+
F29	2.3534E-06	+	1.9209E-06	+	5.7064E-04	+	1.7344E-06	+
F30	1.7344E-06	+	1.7344E-06	+	1.9209E-06	+	1.7344E-06	+
Function	**WOA**		**FA**		**BA**		**MFO**	
F1	1.7344E-06	+	1.7344E-06	+	1.9209E-06	+	1.7344E-06	+
F2	1.7344E-06	+	1.7344E-06	+	2.6033E-06	-	1.7344E-06	+
F3	1.7344E-06	+	1.7344E-06	+	4.2857E-06	-	1.7344E-06	+
F4	1.9209E-06	+	1.7344E-06	+	1.4773E-04	+	1.7344E-06	+
F5	1.7344E-06	+	1.7344E-06	+	1.7344E-06	+	1.7344E-06	+
F6	1.7344E-06	+	1.7344E-06	+	1.7344E-06	+	1.7344E-06	+
F7	1.7344E-06	+	1.7344E-06	+	1.7344E-06	+	1.7344E-06	+
F8	1.7344E-06	+	1.7344E-06	+	1.7344E-06	+	1.7344E-06	+
F9	1.7344E-06	+	1.7344E-06	+	1.7344E-06	+	1.7344E-06	+
F10	1.7344E-06	+	1.7344E-06	+	1.7344E-06	+	2.3534E-06	+
F11	1.7344E-06	+	1.7344E-06	+	1.7344E-06	+	1.7344E-06	+
F12	1.7344E-06	+	1.7344E-06	+	1.9209E-06	+	1.7344E-06	+
F13	1.9209E-06	+	1.7344E-06	+	1.7344E-06	+	6.3391E-06	+
F14	1.7344E-06	+	1.7344E-06	+	8.1302E-01		1.1265E-05	+
F15	2.8786E-06	+	1.7344E-06	+	1.7344E-06	+	4.8603E-05	+
F16	1.7344E-06	+	1.7344E-06	+	1.7344E-06	+	1.9209E-06	+
F17	1.7344E-06	+	1.7344E-06	+	1.7344E-06	+	1.7344E-06	+
F18	2.3534E-06	+	1.7344E-06	+	9.7110E-05	+	3.4053E-05	+
F19	1.7344E-06	+	1.7344E-06	+	1.7344E-06	+	4.7292E-06	+
F20	1.7344E-06	+	2.1266E-06	+	1.7344E-06	+	1.7344E-06	+
F21	1.7344E-06	+	1.7344E-06	+	1.7344E-06	+	1.7344E-06	+
F22	4.7292E-06	+	8.4508E-01		1.7344E-06	+	4.2857E-06	+
F23	1.7344E-06	+	1.7344E-06	+	1.7344E-06	+	1.7344E-06	+
F24	1.7344E-06	+	1.7344E-06	+	1.7344E-06	+	2.6033E-06	+
F25	1.7344E-06	+	1.7344E-06	+	1.7344E-06	+	1.7344E-06	+
F26	2.3534E-06	+	1.7344E-06	+	1.9209E-06	+	1.7344E-06	+
F27	1.7344E-06	+	1.7344E-06	+	1.7344E-06	+	1.7344E-06	+
F28	1.7344E-06	+	1.7344E-06	+	7.0356E-01		1.7344E-06	+
F29	1.7344E-06	+	1.7344E-06	+	1.7344E-06	+	1.7344E-06	+
F30	1.7344E-06	+	1.7344E-06	+	1.7344E-06	+	1.7344E-06	+

Figure 4 shows the convergence curves of all algorithms on several of the 30 benchmark functions. The convergence curves reflect the algorithms' convergence rate and the final solutions' quality. Considering the quality of the solutions as the first comparison factor, the higher the accuracy and precision of the solution obtained by an algorithm, the algorithm's search ability more robust. The algorithms' ability to jump out of the local optima trap is also very crucial. It reflects the algorithm's performance dealing with the multi-modal functions to a certain extent. The convergence rate reflects the approximate time needed by an algorithm to solve an optimization problem. When the solutions

obtained by the two algorithms are the same, the convergence rate is taken as the index to evaluate the algorithms. F5, F8, and F10 are simple multimodal functions in **Figure 4**. F12 and F18 are hybrid functions; F21, F26, and F30 are composition functions.

The characteristics of the search mechanism limit the MGWO algorithm. During the early stage of iteration, the convergence speed of the MGWO algorithm is relatively low because it pays more attention to explore the search space for improving its exploration ability. At the middle stage of iteration, its convergence speed is improved rapidly, and it approaches the global optimal solution quickly. At the later iteration stage, the MGWO algorithm's convergence curve reflects its ability to jump out of the local optima trap, especially on F30. The MGWO algorithm's search mechanism can make the population jump out of the local optima trap and gain higher-quality solutions. However, the population has already approached convergence. **Table 6** and the categories of benchmark functions show that the MGWO algorithm has better performance on composition functions.

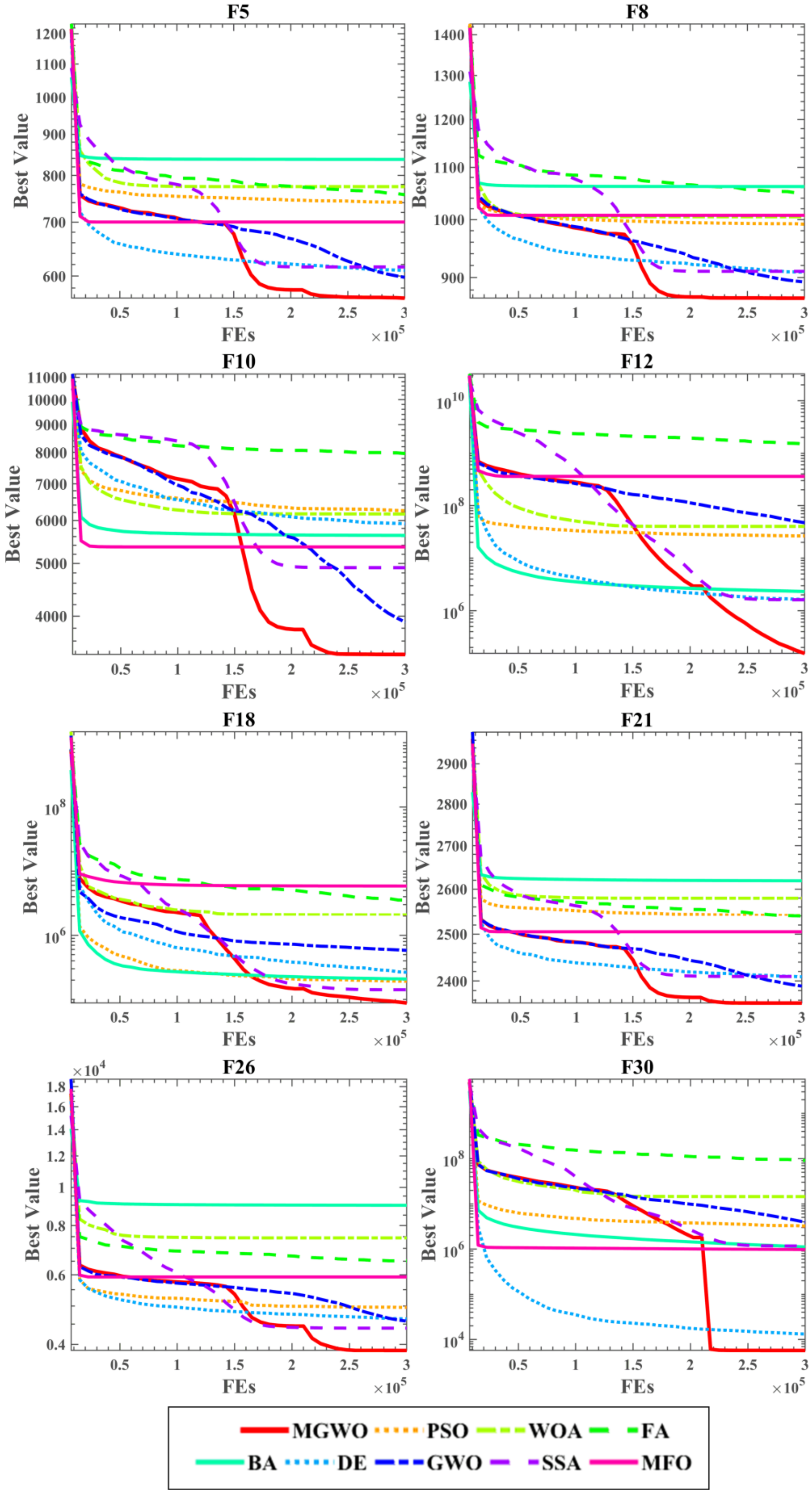

Fig. 4 Convergence curves of the MGWO algorithm and the traditional MAs (First row: F5, F8; second row: F10, F12; third row: F18, F21; fourth row: F26, F30)

4.3 Comparison with the variants of MAs

In this section, the comparative experiments were done with the MGWO algorithm with some advanced optimization algorithms variants of GWO and other MAs on 30 benchmark functions. The GWO algorithm's variants involved in the comparison are hybridizing GWO with differential evolution (HGWO) (Zhu et al., 2015), OBLGWO (Heidari et al., 2019b), IGWO (Cai et al., 2019), CAGWO (Lu et al., 2018). The variants of other MAs involved in the comparison are PSO with an aging leader and challengers (ALCPSO) (Chen et al., 2013), improved WOA (IWOA) (Tubishat et al., 2019), balanced WOA (BWOA) (Chen et al., 2019a), rationalized SCA with efficient searching patterns (CLSCA) (Huang et al., 2020), modified SCA (MSCA) (Qu et al., 2018), chaos-enhanced MFO (CMFO) (Li et al., 2019), enhanced MFO with mutation strategy LGCMFO (Xu et al., 2019c).

Table 10 shows the experimental results of the MGWO algorithm and other variants on each benchmark function. Moreover, **Table 11** shows the p-values between the MGWO algorithm and different variants after each algorithm running independently 30 times on each benchmark function. The Wilcoxon signed-rank test result indicates that the MGWO algorithm ranks first among the 12 optimization algorithms' variants, and the *Avg* is 1.60. Compared with the other four GWO variants, the MGWO algorithm is statistically superior to its competitors on at least 28 benchmark functions. Compared with the ALCPSO, which is recognized as competitive, the MGWO also has apparent advantages on all kinds of benchmark functions, mainly composition functions. The MGWO outperformed the ALCPSO on 22 benchmark functions, and the two algorithms have the same performance on seven benchmark functions. The LGCMFO algorithm ranks second. The MGWO performed significantly better than LGCMFO on 24 benchmark functions but worse than LGCMFO on two benchmark functions. The p-values show that compared with all competitors, the MGWO has a significant performance improvement in dealing with simple multimodal functions and composition functions. The performance on several hybrid benchmark functions is similar to that of the opponents.

Table 10. Comparison of the MGWO algorithm with the variants of MAs

	F1		**F2**	
	Avg	Std	Avg	Std
MGWO	1.4050E+04	2.2976E+04	**2.0000E+02**	**1.1543E-03**
ALCPSO	**7.0936E+03**	**7.1292E+03**	7.2946E+16	2.4936E+17
HGWO	7.9585E+09	1.5217E+09	1.4315E+34	3.1627E+34
OBLGWO	1.4648E+07	8.1057E+06	6.2075E+16	2.0962E+17
IGWO	1.4541E+06	7.3598E+05	1.0717E+14	3.0569E+14
CAGWO	3.5185E+08	3.5594E+08	2.6953E+27	6.9478E+27
IWOA	3.0900E+05	6.7914E+05	6.2720E+14	2.5606E+15
BWOA	1.6045E+08	1.0209E+08	1.4152E+27	5.3294E+27
CLSCA	2.2023E+10	4.3419E+09	6.5277E+35	1.6545E+36
MSCA	1.3591E+04	1.6413E+04	4.6733E+14	2.4725E+15
CMFO	4.1570E+08	1.0034E+09	5.8822E+39	3.2218E+40
LGCMFO	8.5699E+03	7.4305E+03	7.2203E+12	2.6986E+13
	F3		**F4**	

	Avg	Std	Avg	Std
MGWO	**3.0049E+02**	**1.5186E-01**	**4.3432E+02**	2.3582E+01
ALCPSO	2.6755E+04	3.2945E+03	5.0908E+02	2.8806E+01
HGWO	7.8242E+04	5.1464E+03	9.4165E+02	1.2664E+02
OBLGWO	1.9240E+04	4.7991E+03	5.1455E+02	2.8498E+01
IGWO	1.3624E+03	4.7252E+02	4.9634E+02	**2.0564E+01**
CAGWO	4.9025E+04	8.0338E+03	5.5426E+02	2.4731E+01
IWOA	1.2547E+04	5.9647E+03	5.1611E+02	2.7530E+01
BWOA	6.0157E+04	1.1000E+04	6.0321E+02	4.0836E+01
CLSCA	6.2558E+04	6.6907E+03	2.5451E+03	1.1233E+03
MSCA	8.3108E+04	2.3434E+04	4.7423E+02	2.2461E+01
CMFO	1.2036E+05	4.0684E+04	5.8472E+02	9.9239E+01
LGCMFO	6.1712E+03	3.7471E+03	4.8702E+02	2.7433E+01
	F5		**F6**	
	Avg	Std	Avg	Std
MGWO	**5.6488E+02**	1.8126E+01	**6.0045E+02**	**4.2866E-01**
ALCPSO	5.9903E+02	2.6331E+01	6.0546E+02	4.5451E+00
HGWO	7.4589E+02	**1.3048E+01**	6.3831E+02	3.3461E+00
OBLGWO	6.6751E+02	3.9444E+01	6.1698E+02	1.1454E+01
IGWO	6.0628E+02	1.9862E+01	6.2387E+02	7.0343E+00
CAGWO	6.3962E+02	4.8597E+01	6.0364E+02	1.3968E+00
IWOA	6.8655E+02	5.2659E+01	6.1166E+02	6.3170E+00
BWOA	7.7013E+02	2.9355E+01	6.6531E+02	5.5244E+00
CLSCA	8.1612E+02	2.6119E+01	6.6136E+02	6.6027E+00
MSCA	6.9348E+02	4.6186E+01	6.0378E+02	3.6598E+00
CMFO	7.1564E+02	5.0033E+01	6.5152E+02	9.0579E+00
LGCMFO	6.3375E+02	2.9547E+01	6.1594E+02	1.0240E+01
	F7		**F8**	
	Avg	Std	Avg	Std
MGWO	**8.1964E+02**	2.1463E+01	**8.6614E+02**	**1.3088E+01**
ALCPSO	8.6059E+02	2.9611E+01	9.0291E+02	2.4571E+01
HGWO	1.0461E+03	2.7719E+01	9.9899E+02	1.4837E+01
OBLGWO	9.3511E+02	8.1332E+01	9.4009E+02	3.2511E+01
IGWO	8.8518E+02	3.1300E+01	8.8815E+02	1.9350E+01
CAGWO	9.1185E+02	**1.6711E+01**	9.3715E+02	4.5645E+01
IWOA	9.6624E+02	5.5150E+01	9.5896E+02	3.7162E+01
BWOA	1.2586E+03	7.0268E+01	9.7923E+02	3.3249E+01
CLSCA	1.1735E+03	5.9873E+01	1.0667E+03	1.7941E+01
MSCA	9.7057E+02	6.2550E+01	9.9368E+02	5.1084E+01
CMFO	1.2098E+03	1.1443E+02	9.5712E+02	3.1318E+01

LGCMFO	8.8242E+02	4.3264E+01	9.2407E+02	2.6599E+01
	F9		**F10**	
	Avg	Std	Avg	Std
MGWO	1.4406E+03	5.0611E+02	**3.5257E+03**	5.0154E+02
ALCPSO	1.5740E+03	5.9143E+02	4.2544E+03	7.1619E+02
HGWO	3.4282E+03	3.2788E+02	6.7050E+03	**4.5684E+02**
OBLGWO	2.8625E+03	2.2467E+03	5.3452E+03	1.0017E+03
IGWO	2.8519E+03	8.3380E+02	4.5314E+03	6.3886E+02
CAGWO	**1.1257E+03**	**1.9327E+02**	7.1460E+03	1.0715E+03
IWOA	5.4348E+03	1.9018E+03	4.6604E+03	7.0127E+02
BWOA	6.1167E+03	5.9382E+02	6.4963E+03	8.4487E+02
CLSCA	7.6037E+03	1.3875E+03	7.9983E+03	6.1445E+02
MSCA	6.1479E+03	2.2109E+03	3.9639E+03	5.5266E+02
CMFO	5.0452E+03	1.5261E+03	6.9012E+03	1.3005E+03
LGCMFO	3.2600E+03	1.0655E+03	4.8426E+03	5.7143E+02
	F11		**F12**	
	Avg	Std	Avg	Std
MGWO	**1.1893E+03**	**2.4234E+01**	**1.2718E+05**	**8.0791E+04**
ALCPSO	1.2474E+03	5.8175E+01	3.5004E+05	4.6489E+05
HGWO	4.8861E+03	1.0887E+03	5.9765E+08	1.8637E+08
OBLGWO	1.2837E+03	4.7342E+01	1.5779E+07	1.1595E+07
IGWO	1.2597E+03	3.6262E+01	1.4658E+07	9.0911E+06
CAGWO	1.3557E+03	4.0100E+01	2.7840E+07	2.0331E+07
IWOA	1.2544E+03	6.8608E+01	2.9325E+06	1.7660E+06
BWOA	1.8495E+03	4.3614E+02	1.0509E+08	6.9339E+07
CLSCA	2.4276E+03	2.9104E+02	2.1374E+09	5.6160E+08
MSCA	2.0135E+03	1.1340E+03	2.8741E+06	3.6406E+06
CMFO	4.5724E+03	3.6916E+03	3.6265E+07	9.9364E+07
LGCMFO	1.2417E+03	6.4637E+01	1.1864E+06	1.8594E+06
	F13		**F14**	
	Avg	Std	Avg	Std
MGWO	3.5339E+04	2.3677E+04	**5.4269E+03**	**3.2779E+03**
ALCPSO	**1.5256E+04**	**1.7528E+04**	2.5974E+04	4.3411E+04
HGWO	2.7412E+08	1.6462E+08	8.6841E+05	5.6565E+05
OBLGWO	2.4952E+05	2.3767E+05	5.9933E+04	4.4767E+04
IGWO	2.4495E+05	3.9483E+05	4.8559E+04	4.2303E+04
CAGWO	2.8355E+05	3.0699E+05	2.7379E+05	3.0639E+05
IWOA	1.8745E+04	2.0424E+04	6.5492E+04	5.1542E+04
BWOA	2.2862E+05	1.2097E+05	1.0336E+06	9.8562E+05
CLSCA	7.2955E+08	5.1196E+08	3.2676E+05	2.8305E+05

MSCA	3.3801E+04	2.8086E+04	4.3364E+05	5.1742E+05
CMFO	8.6445E+04	1.9114E+05	4.6095E+05	1.0080E+06
LGCMFO	4.4711E+04	2.6952E+04	2.3839E+04	3.3115E+04
	F15		**F16**	
	Avg	Std	Avg	Std
MGWO	1.1713E+04	1.3921E+04	**2.1774E+03**	**2.0105E+02**
ALCPSO	1.7264E+04	1.4089E+04	2.5258E+03	2.7092E+02
HGWO	9.3580E+06	1.0867E+07	3.3001E+03	2.1682E+02
OBLGWO	7.9777E+04	5.7982E+04	2.7728E+03	3.3536E+02
IGWO	5.1197E+04	3.7037E+04	2.4917E+03	2.9689E+02
CAGWO	5.7199E+04	7.7361E+04	2.7016E+03	3.1789E+02
IWOA	9.8257E+03	7.9613E+03	2.8184E+03	3.3391E+02
BWOA	1.2908E+05	1.2245E+05	3.7470E+03	4.2899E+02
CLSCA	6.7657E+06	6.7355E+06	3.8399E+03	2.3636E+02
MSCA	1.6061E+04	2.0472E+04	3.0552E+03	3.6552E+02
CMFO	4.4139E+07	2.4161E+08	3.1017E+03	4.5304E+02
LGCMFO	**6.4455E+03**	**5.5303E+03**	2.7501E+03	3.4735E+02
	F17		**F18**	
	Avg	Std	Avg	Std
MGWO	**1.8931E+03**	**1.0452E+02**	**9.9390E+04**	**7.7089E+04**
ALCPSO	2.1301E+03	2.3042E+02	1.8006E+05	1.3047E+05
HGWO	2.3787E+03	1.3955E+02	2.6460E+06	3.1660E+06
OBLGWO	2.2590E+03	1.8936E+02	1.2184E+06	1.0412E+06
IGWO	1.9815E+03	1.3798E+02	4.2932E+05	3.1651E+05
CAGWO	1.9604E+03	1.4650E+02	5.5804E+05	5.3571E+05
IWOA	2.2660E+03	2.2798E+02	9.2240E+05	9.1387E+05
BWOA	2.7299E+03	2.4421E+02	4.3625E+06	5.2945E+06
CLSCA	2.4640E+03	1.6131E+02	3.0325E+06	2.4007E+06
MSCA	2.5432E+03	2.7536E+02	2.8432E+06	3.3201E+06
CMFO	2.5249E+03	3.9961E+02	6.2235E+06	1.4031E+07
LGCMFO	2.2197E+03	2.6561E+02	2.0324E+05	1.3407E+05
	F19		**F20**	
	Avg	Std	Avg	Std
MGWO	1.6702E+04	1.6775E+04	**2.2592E+03**	**1.0727E+02**
ALCPSO	1.5645E+04	1.6027E+04	2.3175E+03	1.2851E+02
HGWO	1.4553E+07	1.5319E+07	2.6374E+03	1.1468E+02
OBLGWO	3.4984E+05	3.2209E+05	2.4324E+03	1.4107E+02
IGWO	2.9045E+05	5.8218E+05	2.3167E+03	1.3464E+02
CAGWO	1.4685E+05	1.7075E+05	2.3353E+03	8.1805E+01
IWOA	1.0797E+04	8.6896E+03	2.5118E+03	1.8265E+02
BWOA	4.0761E+06	3.5682E+06	2.7344E+03	1.6279E+02

CLSCA	2.3349E+07	1.8161E+07	2.6683E+03	1.3185E+02
MSCA	2.0617E+04	2.0268E+04	2.5718E+03	1.7657E+02
CMFO	7.8288E+04	2.0652E+05	2.7262E+03	2.9358E+02
LGCMFO	**6.0628E+03**	**3.3902E+03**	2.4937E+03	1.6503E+02
	F21		**F22**	
	Avg	Std	Avg	Std
MGWO	**2.3504E+03**	**1.1937E+01**	4.0551E+03	1.4915E+03
ALCPSO	2.4116E+03	3.8045E+01	4.8410E+03	1.7718E+03
HGWO	2.5115E+03	1.2929E+01	3.1643E+03	1.3135E+02
OBLGWO	2.4327E+03	5.2495E+01	3.1321E+03	1.8736E+03
IGWO	2.4029E+03	1.7983E+01	2.3107E+03	**1.7020E+00**
CAGWO	2.4175E+03	4.1047E+01	2.6352E+03	1.2591E+03
IWOA	2.4825E+03	4.5535E+01	5.2293E+03	2.0572E+03
BWOA	2.5621E+03	4.3164E+01	5.7938E+03	2.5801E+03
CLSCA	2.5833E+03	2.7346E+01	4.3657E+03	4.0822E+02
MSCA	2.4864E+03	3.8220E+01	5.6559E+03	8.8108E+02
CMFO	2.4882E+03	4.2586E+01	5.8148E+03	2.9136E+03
LGCMFO	2.4005E+03	4.7885E+01	**2.3011E+03**	1.7728E+00
	F23		**F24**	
	Avg	Std	Avg	Std
MGWO	**2.7285E+03**	2.5783E+01	**2.8958E+03**	**2.2869E+01**
ALCPSO	2.7881E+03	4.2754E+01	2.9710E+03	4.8167E+01
HGWO	2.8991E+03	**1.4820E+01**	3.0658E+03	2.9371E+01
OBLGWO	2.8015E+03	4.0654E+01	2.9817E+03	3.0920E+01
IGWO	2.7806E+03	2.4972E+01	2.9526E+03	3.7740E+01
CAGWO	2.7838E+03	5.0926E+01	2.9303E+03	5.2696E+01
IWOA	2.8463E+03	4.9548E+01	3.0889E+03	7.7158E+01
BWOA	3.1053E+03	1.0048E+02	3.1862E+03	1.0233E+02
CLSCA	3.0067E+03	3.4827E+01	3.1699E+03	4.5972E+01
MSCA	2.8887E+03	4.6610E+01	3.1917E+03	8.5529E+01
CMFO	3.0165E+03	1.0508E+02	3.1667E+03	1.1128E+02
LGCMFO	2.7940E+03	4.3017E+01	2.9300E+03	3.8594E+01
	F25		**F26**	
	Avg	Std	Avg	Std
MGWO	**2.8779E+03**	**1.9704E+00**	3.8979E+03	**2.7413E+02**
ALCPSO	2.8973E+03	1.6852E+01	4.8861E+03	1.0857E+03
HGWO	3.0817E+03	2.3758E+01	5.9288E+03	3.9670E+02
OBLGWO	2.9162E+03	2.2391E+01	5.1742E+03	7.4255E+02
IGWO	2.9050E+03	1.8829E+01	4.7100E+03	2.9439E+02
CAGWO	2.9431E+03	1.8081E+01	4.5633E+03	4.0856E+02

IWOA	2.9056E+03	2.0263E+01	5.3853E+03	1.0977E+03
BWOA	3.0046E+03	2.8486E+01	7.4985E+03	1.1824E+03
CLSCA	3.3574E+03	9.9582E+01	7.0292E+03	8.0248E+02
MSCA	2.8873E+03	1.4578E+01	5.4885E+03	8.4769E+02
CMFO	2.9452E+03	4.1905E+01	6.3364E+03	7.0571E+02
LGCMFO	2.8915E+03	1.4713E+01	**3.4952E+03**	1.1075E+03
	F27		**F28**	
	Avg	Std	Avg	Std
MGWO	**3.1919E+03**	1.6594E+01	**3.1638E+03**	6.6188E+01
ALCPSO	3.2592E+03	3.1074E+01	3.2405E+03	3.8637E+01
HGWO	3.3052E+03	2.9603E+01	3.6205E+03	5.5572E+01
OBLGWO	3.2374E+03	1.7727E+01	3.2760E+03	2.8972E+01
IGWO	3.2381E+03	1.5113E+01	3.2486E+03	2.8290E+01
CAGWO	3.2289E+03	9.1656E+00	3.3617E+03	3.3913E+01
IWOA	3.2365E+03	1.7311E+01	3.2307E+03	2.4131E+01
BWOA	3.3615E+03	1.1199E+02	3.3935E+03	4.2449E+01
CLSCA	3.4015E+03	4.2509E+01	4.3286E+03	3.2869E+02
MSCA	3.2000E+03	**3.2219E-04**	3.2972E+03	**1.5309E+01**
CMFO	3.3695E+03	7.6497E+01	3.3966E+03	3.5692E+02
LGCMFO	3.2866E+03	3.5914E+01	3.2195E+03	2.4671E+01
	F29		**F30**	
	Avg	Std	Avg	Std
MGWO	**3.4537E+03**	**1.4139E+02**	**4.8605E+03**	**2.1452E+03**
ALCPSO	3.8651E+03	2.9222E+02	2.8298E+04	6.0215E+04
HGWO	4.4304E+03	1.6410E+02	7.7549E+07	3.0728E+07
OBLGWO	4.0381E+03	2.7088E+02	3.0724E+06	1.7530E+06
IGWO	3.7668E+03	1.5474E+02	4.1131E+06	2.6105E+06
CAGWO	3.7408E+03	1.8937E+02	7.4164E+06	4.8334E+06
IWOA	3.8438E+03	2.2080E+02	3.5003E+04	3.7935E+04
BWOA	4.9452E+03	4.4656E+02	2.2454E+07	1.8926E+07
CLSCA	4.8534E+03	2.9549E+02	1.0760E+08	4.3832E+07
MSCA	3.8529E+03	2.4542E+02	8.0708E+03	7.1745E+03
CMFO	4.5304E+03	4.2528E+02	1.6876E+06	4.0201E+06
LGCMFO	3.9585E+03	2.1344E+02	6.3356E+04	1.7721E+05

	Wilcoxon signed-rank test		
	+/-/=	Avg	Rank
MGWO	~	**1.60**	**1**
ALCPSO	22/1/7	3.83	3
HGWO	29/1/0	9.67	9
OBLGWO	29/0/1	6.33	7

IGWO	28/1/1	4.33	4
CAGWO	28/2/0	5.67	6
IWOA	26/1/3	5.63	5
BWOA	30/0/0	10.20	11
CLSCA	29/0/1	10.90	12
MSCA	26/0/4	6.53	8
CMFO	28/0/2	9.70	10
LGCMFO	24/2/4	3.60	2

Table 11. The p-values between the MGWO algorithm and the variants of MAs

Function	ALCPSO		HGWO		OBLGWO		IGWO	
F1	1.6503E-01		1.7344E-06	+	1.7344E-06	+	1.7344E-06	+
F2	1.7344E-06	+	1.7344E-06	+	1.7344E-06	+	1.7344E-06	+
F3	1.7344E-06	+	1.7344E-06	+	1.7344E-06	+	1.7344E-06	+
F4	1.7344E-06	+	1.7344E-06	+	1.7344E-06	+	3.8822E-06	+
F5	2.8434E-05	+	1.7344E-06	+	1.7344E-06	+	5.2165E-06	+
F6	2.3534E-06	+	1.7344E-06	+	1.7344E-06	+	1.7344E-06	+
F7	2.3704E-05	+	1.7344E-06	+	2.6033E-06	+	1.7344E-06	+
F8	5.7517E-06	+	1.7344E-06	+	1.7344E-06	+	5.7924E-05	+
F9	4.1653E-01		1.7344E-06	+	6.6392E-04	+	6.3391E-06	+
F10	1.0357E-03	+	1.7344E-06	+	2.1266E-06	+	8.4661E-06	+
F11	4.8603E-05	+	1.7344E-06	+	1.7344E-06	+	2.3534E-06	+
F12	2.7116E-01		1.7344E-06	+	1.7344E-06	+	1.7344E-06	+
F13	1.5927E-03	-	1.7344E-06	+	2.3534E-06	+	3.5152E-06	+
F14	3.8811E-04	+	1.7344E-06	+	2.3534E-06	+	3.5152E-06	+
F15	1.9152E-01		1.7344E-06	+	1.7344E-06	+	6.3391E-06	+
F16	1.7988E-05	+	1.7344E-06	+	2.3534E-06	+	5.7924E-05	+
F17	1.1499E-04	+	1.7344E-06	+	2.6033E-06	+	1.7518E-02	+
F18	4.0702E-02	+	1.7344E-06	+	1.7344E-06	+	3.8822E-06	+
F19	5.9994E-01		1.7344E-06	+	3.1817E-06	+	1.9729E-05	+
F20	5.4463E-02		1.7344E-06	+	2.8308E-04	+	8.9718E-02	
F21	2.3534E-06	+	1.7344E-06	+	2.5967E-05	+	1.7344E-06	+
F22	8.5896E-02		3.8542E-03	-	6.5641E-02		6.1564E-04	-
F23	1.4936E-05	+	1.7344E-06	+	3.5152E-06	+	4.2857E-06	+
F24	1.7988E-05	+	1.7344E-06	+	2.6033E-06	+	1.9209E-06	+
F25	1.7344E-06	+	1.7344E-06	+	1.7344E-06	+	1.7344E-06	+
F26	1.6046E-04	+	1.7344E-06	+	1.2381E-05	+	1.9209E-06	+
F27	1.7344E-06	+	1.7344E-06	+	1.7344E-06	+	1.7344E-06	+
F28	1.4773E-04	+	1.7344E-06	+	1.9209E-06	+	1.7988E-05	+
F29	2.8786E-06	+	1.7344E-06	+	1.7344E-06	+	5.2165E-06	+
F30	1.9209E-06	+	1.7344E-06	+	1.7344E-06	+	1.7344E-06	+
Function	**CAGWO**		**IWOA**		**BWOA**		**CLSCA**	

F1	1.7344E-06	+	5.9836E-02		1.7344E-06	+	1.7344E-06	+
F2	1.7344E-06	+	1.7344E-06	+	1.7344E-06	+	1.7344E-06	+
F3	1.7344E-06	+	1.7344E-06	+	1.7344E-06	+	1.7344E-06	+
F4	1.7344E-06	+	1.9209E-06	+	1.7344E-06	+	1.7344E-06	+
F5	8.4661E-06	+	1.7344E-06	+	1.7344E-06	+	1.7344E-06	+
F6	1.7344E-06	+	1.7344E-06	+	1.7344E-06	+	1.7344E-06	+
F7	1.7344E-06	+	1.7344E-06	+	1.7344E-06	+	1.7344E-06	+
F8	6.3391E-06	+	1.7344E-06	+	1.7344E-06	+	1.7344E-06	+
F9	6.8359E-03	-	1.7344E-06	+	1.7344E-06	+	1.7344E-06	+
F10	1.7344E-06	+	3.1123E-05	+	1.7344E-06	+	1.7344E-06	+
F11	1.7344E-06	+	1.7423E-04	+	1.7344E-06	+	1.7344E-06	+
F12	1.7344E-06	+	1.7344E-06	+	1.7344E-06	+	1.7344E-06	+
F13	1.7344E-06	+	9.8421E-03	-	1.9209E-06	+	1.7344E-06	+
F14	1.7344E-06	+	3.8822E-06	+	1.7344E-06	+	1.7344E-06	+
F15	2.4118E-04	+	7.9710E-01		2.6033E-06	+	1.7344E-06	+
F16	4.2857E-06	+	2.8786E-06	+	1.7344E-06	+	1.7344E-06	+
F17	4.7162E-02	+	2.6033E-06	+	1.7344E-06	+	1.7344E-06	+
F18	1.1265E-05	+	2.8786E-06	+	2.6033E-06	+	1.7344E-06	+
F19	2.3704E-05	+	4.5281E-01		1.7344E-06	+	1.7344E-06	+
F20	8.7297E-03	+	5.7924E-05	+	1.7344E-06	+	1.7344E-06	+
F21	2.8786E-06	+	1.7344E-06	+	1.7344E-06	+	1.7344E-06	+
F22	2.4147E-03	-	2.5637E-02	+	1.0444E-02	+	3.7094E-01	
F23	1.0570E-04	+	2.1266E-06	+	1.7344E-06	+	1.7344E-06	+
F24	6.0350E-03	+	1.7344E-06	+	1.7344E-06	+	1.7344E-06	+
F25	1.7344E-06	+	1.7344E-06	+	1.7344E-06	+	1.7344E-06	+
F26	5.2165E-06	+	1.2381E-05	+	1.7344E-06	+	1.7344E-06	+
F27	1.7344E-06	+	1.7344E-06	+	1.7344E-06	+	1.7344E-06	+
F28	1.7344E-06	+	1.6046E-04	+	1.7344E-06	+	1.7344E-06	+
F29	6.3391E-06	+	5.2165E-06	+	1.7344E-06	+	1.7344E-06	+
F30	1.7344E-06	+	1.7344E-06	+	1.7344E-06	+	1.7344E-06	+

Function	**MSCA**		**CMFO**		**LGCMFO**	
F1	2.6230E-01		1.7344E-06	+	9.2626E-01	
F2	1.9209E-06	+	1.7344E-06	+	1.7344E-06	+
F3	1.7344E-06	+	1.7344E-06	+	1.7344E-06	+
F4	2.1630E-05	+	1.7344E-06	+	4.7292E-06	+
F5	1.7344E-06	+	1.7344E-06	+	1.7344E-06	+
F6	2.1630E-05	+	1.7344E-06	+	1.7344E-06	+
F7	1.7344E-06	+	1.7344E-06	+	2.3534E-06	+
F8	1.7344E-06	+	1.7344E-06	+	1.7344E-06	+
F9	1.7344E-06	+	1.7344E-06	+	3.8822E-06	+
F10	4.6818E-03	+	1.7344E-06	+	2.8786E-06	+
F11	1.7344E-06	+	1.7344E-06	+	4.8969E-04	+
F12	1.9209E-06	+	1.9209E-06	+	4.7292E-06	+

F13	7.6552E-01		9.2626E-01		2.8948E-01	
F14	1.7344E-06	+	2.6033E-06	+	1.2381E-05	+
F15	4.9080E-01		4.1140E-03	+	2.9894E-01	
F16	1.7344E-06	+	1.7344E-06	+	1.9209E-06	+
F17	1.7344E-06	+	1.7344E-06	+	1.1265E-05	+
F18	1.9209E-06	+	9.3157E-06	+	6.6392E-04	+
F19	4.4052E-01		1.0639E-01		1.1079E-02	-
F20	2.8786E-06	+	4.2857E-06	+	6.8923E-05	+
F21	1.7344E-06	+	1.7344E-06	+	3.1123E-05	+
F22	2.0515E-04	+	7.7309E-03	+	2.1630E-05	-
F23	1.7344E-06	+	1.7344E-06	+	1.1265E-05	+
F24	1.7344E-06	+	1.7344E-06	+	9.6266E-04	+
F25	1.4773E-04	+	1.7344E-06	+	1.7344E-06	+
F26	3.1817E-06	+	1.7344E-06	+	7.8647E-02	
F27	8.1878E-05	+	1.7344E-06	+	1.7344E-06	+
F28	2.3534E-06	+	1.7344E-06	+	7.1570E-04	+
F29	1.3601E-05	+	1.9209E-06	+	1.9209E-06	+
F30	2.3038E-02	+	1.7344E-06	+	3.1817E-06	+

Figure 5 shows the convergence curves of all algorithms participating in the comparison on several benchmark functions. F3 is the unimodal function, F8 and F10 are simple multimodal functions, F12, F14, F16, and F18 are hybrid functions, F21, F23, and F30 are composition functions. Many improved algorithms enhance the search ability on complex objective functions and lead to unimodal performance not being as good as some original MAs. However, the MGWO algorithm does not have such trouble, and its implementation on unimodal functions is also considerable. The total number of evaluations controls the search mechanism of the MGWO, so it will not converge as fast as the ALCPSO during the early stage of the search process. Still, it can obtain higher quality solutions than the ALCPSO at the end of the search process. The two times change of the search mechanism can improve the algorithm's convergence speed and enhance the ability to jump out of the local optima traps. It can be proved that an optimization algorithm's performance can be improved by dividing the evaluation process into several stages, considering the emphasis of each step, and using the appropriate search mechanism. According to the different types of objective functions, other search mechanisms focus on various search focus, which can achieve different purposes, whether to get more accurate solutions or faster convergence speed. The above two experiments can prove the superiority of the MGWO algorithm.

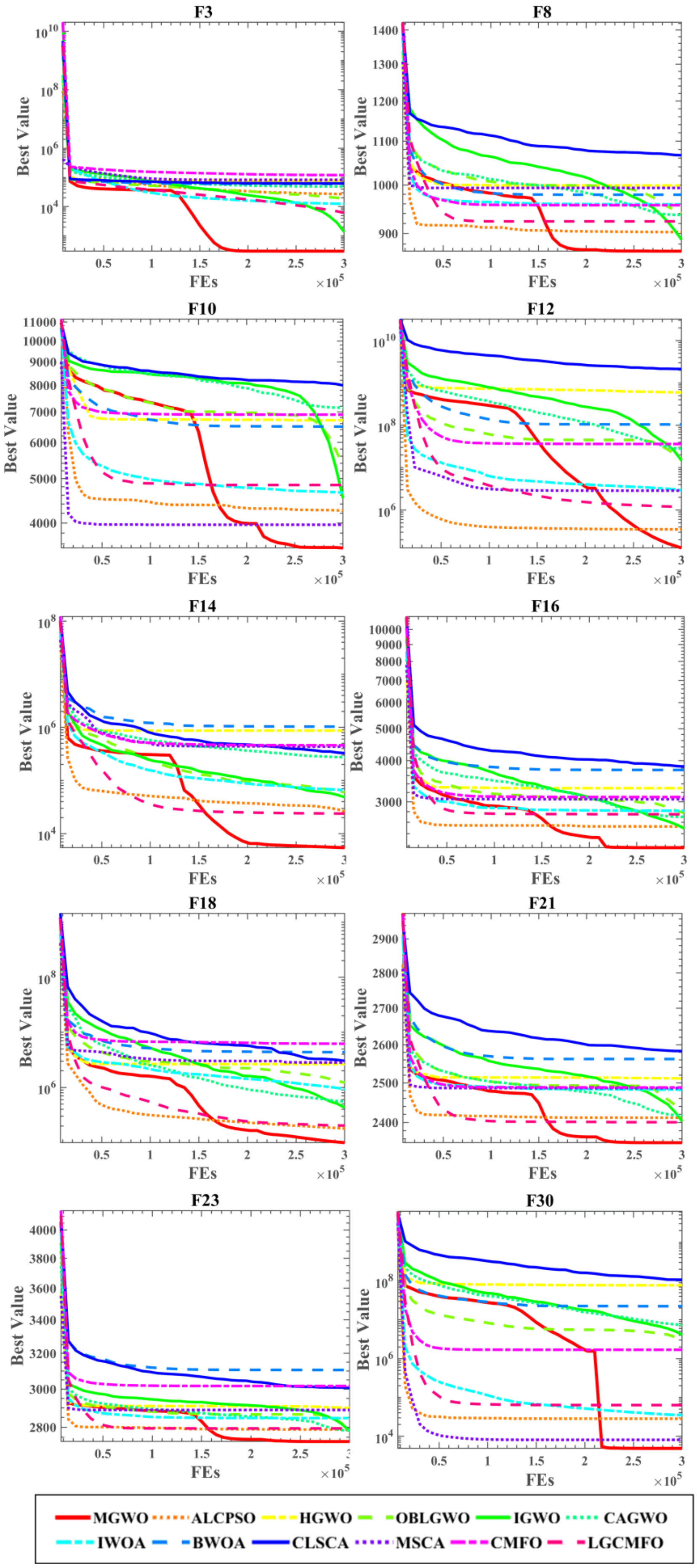

Fig. 5 Convergence curves of the MGWO algorithm and the variants of MAs (First row: F3, F8; second row: F10, F12; third row: F14, F16; fourth row: F18, F21; fifth row: F23, F30)

4.4 Balance and diversity analysis

Its search mechanism determines the meta-heuristic optimization algorithms' performance. However, we cannot evaluate different search mechanisms quantitatively. Instead, we assess an optimization algorithm's performance by the quality of the solution obtained by the algorithm, the convergence rate, and the ability to escape from the local optima trap. Exploration refers to finding different kinds of solutions distributed in other areas of the entire search space. Exploitation emphasizes further exploring the promising areas in the search space and find a better solution with higher quality. An optimization algorithm's exploration and exploitation ability are closely related to its convergence rate. Improving the exploration ability can increase the possibility of finding the global optimum solution, but this behavior is at the cost of reducing the convergence speed.

Conversely, improving the exploitation ability can make the algorithm converge faster and enhance the probability of falling into the local optima trap. Therefore, exploration and exploitation are two mutually exclusive processes, and the quality of the balance between them affects the algorithm's performance. However, it is worth noting that even if two algorithms' ratios are the same, each algorithm's specific search mechanism's quality will significantly affect the performance. Moreover, it is difficult to obtain an appropriate exploration/exploitation ratio suitable for all existing optimization algorithms. Through a large number of experiments, Morales-Castaeda et al. (Morales-Castaeda et al., 2020) concluded that the algorithm's performance is the best when the balance response reaches a balance of 90% exploitation and 10% exploration under the condition of multimodal objective functions. The balance diagram's roughness means the unstable balance change in the evolution process caused by the small and sudden shift in diversity influenced by the search mechanism. These changes slightly improve the algorithm's exploration ability to escape from the local optima trap even at the exploitation stage. That is, the rough balance response shows better algorithm performance.

To further find why the MGWO algorithm's performance improved compared with the original GWO algorithm, the balance and diversity comparison experiments were carried out and analyzed. The two algorithms have been independently run on 30 benchmark functions of CEC2017 30 times, and the results are shown in **Table 12**. %EPL is the average percentage of exploration, and %EPT is the average percentage of exploration, which are used to indicate the time proportion of exploration and exploitation process. Average the exploration and exploration percentages of all benchmark functions, the MGWO obtained a balance of 90.5271% exploitation and 9.4729% exploration. The GWO received compensation of 88.4629% exploitation and 11.5371% exploration. The proportion of time consumed by the two algorithms on exploration and exploitation is not much different. The MGWO took a longer time than the GWO on the exploitation process slightly.

Table 12. Balance analysis of the MGWO algorithm and the GWO algorithm

Algorithm	Function	%EPL	%EPT	Function	%EPL	%EPT
MGWO	F1	9.9461	90.0539	F16	11.3009	88.6991
GWO		13.7245	86.2755		11.6514	88.3486
MGWO	F2	7.5005	92.4995	F17	8.1458	91.8542
GWO		10.1118	89.8882		9.8601	90.1399
MGWO	F3	5.2141	94.7859	F18	11.9452	88.0548
GWO		6.1694	93.8306		9.6552	90.3448

MGWO	F4	10.8746	89.1254	F19	10.0295	89.9705
GWO		14.3744	85.6256		9.4611	90.5389
MGWO	F5	9.2217	90.7783	F20	0.46862	99.5314
GWO		11.0272	88.9728		8.8270	91.1730
MGWO	F6	10.2439	89.7561	F21	9.4143	90.5857
GWO		12.8432	87.1568		12.0452	87.9548
MGWO	F7	4.8249	95.1751	F22	9.4528	90.5472
GWO		5.5620	94.4380		11.8357	88.1643
MGWO	F8	7.1809	92.8191	F23	13.5567	86.4433
GWO		8.5830	91.417		19.5372	80.4628
MGWO	F9	6.8411	93.1589	F24	14.7119	85.2881
GWO		8.5855	91.4145		20.9825	79.0175
MGWO	F10	8.1675	91.8325	F25	6.6237	93.3763
GWO		11.7551	88.2449		8.3162	91.6838
MGWO	F11	5.3464	94.6536	F26	9.8592	90.1408
GWO		6.9407	93.0593		12.9541	87.0459
MGWO	F12	10.2979	89.7021	F27	17.9804	82.0196
GWO		12.0262	87.9738		19.9800	80.0200
MGWO	F13	11.3332	88.6668	F28	8.9843	91.0157
GWO		11.9783	88.0217		12.3044	87.6956
MGWO	F14	11.1794	88.8206	F29	11.2618	88.7382
GWO		9.5581	90.4419		13.3742	86.6258
MGWO	F15	9.3146	90.6854	F30	12.9649	87.0351
GWO		9.7812	90.2188		12.3068	87.6932
MGWO	avg	9.4729	90.5271			
GWO		11.5371	88.4629			

The equilibrium evolution diagrams are shown in **Figures 6** and **7**. The graph of incremental-decremental is a visual feature of the interactive effects of exploration and exploitation. The incremental-decremental graph will generate increment when the exploration effect is greater than or equal to the exploitation effect. Otherwise, it will create a decrement. Moreover, it will reach the vertex when the impacts of exploration and exploitation are the same. In the case of a negative value, it is assumed to be zero. F1 is a unimodal function, F6 is a simple multimodal function, F12 and F19 are hybrid functions, F24 and F26 are composition functions. Apparently, the two algorithms both have the right balance between exploration and exploitation. The exploitation percentage of the MGWO on each benchmark function is slightly higher than that of the GWO, and all of them are more than 80%. At the first stage, the equilibrium response of the MGWO was the same as that of the GWO. The MGWO paid more attention to exploitation at the second stage, so the time proportion of exploitation increased rapidly. At this time, the convergence rate of the MGWO increased. Generally speaking, dividing the search process into several different stages will harm the convergence rate. Still, the convergence rate of the MGWO will increase due to the search mechanism adopted at the second stage. At the last stage, the equilibrium response of the MGWO became rough, especially on F12, F19, and F26. During the GWO's whole search process, the time proportion of exploitation has been rising, the time proportion of exploration has been declining, and the curve has become more and more smooth.

This shows that the MGWO has a more vital ability to jump out of the local optima trap and gain better quality solutions. In the equilibrium evolution diagram of F19, both algorithms' equilibrium responses are about 10% exploration and 90% exploitation. Still, the rough equilibrium diagram shows that the MGWO can better escape the local optima trap better than the GWO. On the benchmark function F24, the quality of the two algorithms' solutions is similar, but the MGWO can converge faster.

Figure 8 shows the evolution of diversity during the optimization procedure. The axis x corresponds to the number of iterations, and the axis y corresponds to the diversity measure. The search process began with high diversity, and the population's diversity gradually decreased with the increase of iterations. GWO gradually lost its population's diversity with the increase of iterations. The MGWO kept a low level on some functions after the rapid decline of the population's diversity at the second stage. On several functions, the population's diversity of the MGWO increased at the third stage and produced a different degree of oscillation. This also proves that the MGWO algorithm has a certain ability to jump out of the local optima trap. We can conclude that the MGWO algorithm has a better balance of exploration and exploitation than the GWO algorithm from the balance and diversity experiments.

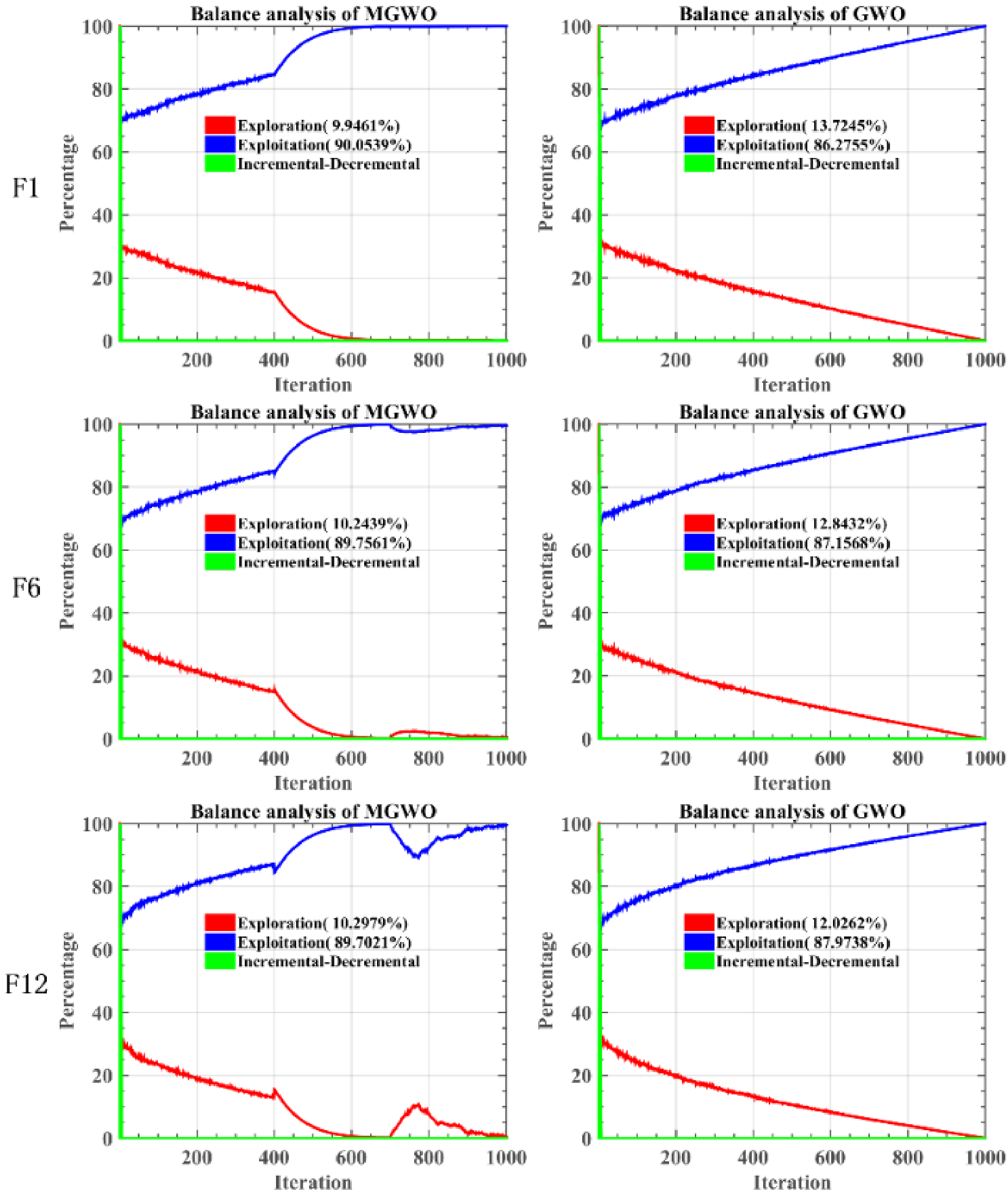

Fig. 6 The balance analysis of MGWO and GWO on F1, F6, F12

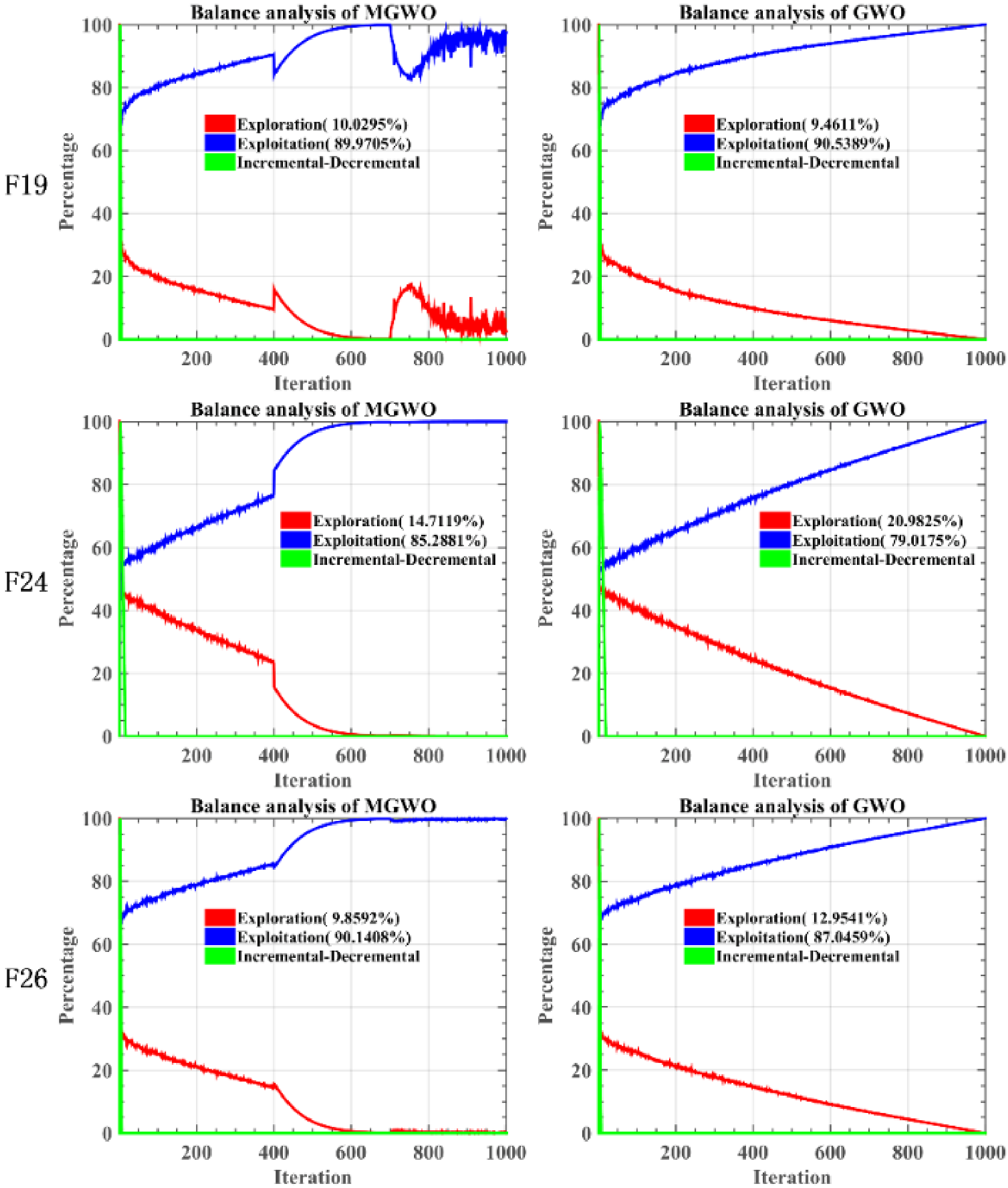

Fig. 7 The balance analysis of MGWO and GWO on F19, F24, F26

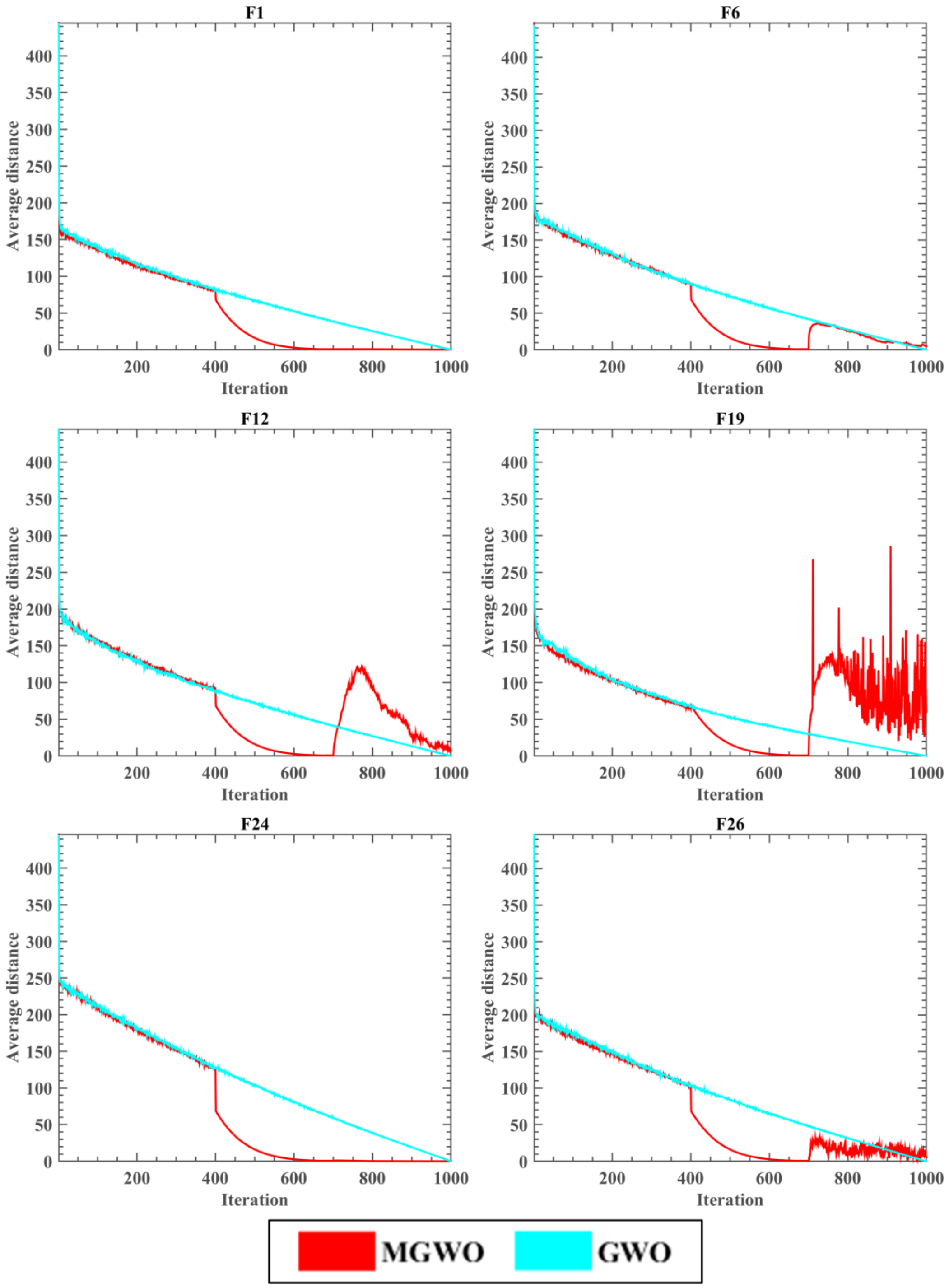

Fig. 8 The diversity analysis of MGWO and GWO

4.5 Experiments on Multi-threshold image segmentation

In this section, MGWO will be used in the practical application of multi-threshold image segmentation. The objective function used is obtained by calculating Kapur's entropy in Section 2.2. The images used are Leaf Spot Diseases on Maize images. MGWO will be compared with nine swarm intelligence optimization algorithms on sixteen images to verify its effectiveness on multi-threshold image segmentation. The algorithms involved in the comparison are as follows: GWO, SSA, WOA, cuckoo search (CS) (Yang and Deb, 2010), HHO, IGWO, comprehensive learning PSO (CLPSO) (Liang et al., 2006), CLSGMFO (Xu et al., 2019b), and LGCMFO. Finally, three evaluation indexes: peak signal to noise ratio (PSNR) (Huynh-Thu and Ghanbari, 2008), structural similarity index (SSIM) (Zhou et al., 2004), and feature similarity index (FSIM) (Zhang et al., 2011) are used to evaluate the segmented results and rank all the comparison algorithms.

4.5.1 Image and parameter setting

Leaf Spot Diseases on Maize images with the size of 400×256 used in the image segmentation experiment are derived from the standard publicly available dataset called the PlantVillage, and the total number of images is sixteen. Sixteen images can be divided into general and serious according to the severity of Leaf Spot Disease. According to different features, images can also be divided into different categories. There is Corn Rust interference on corn leaves in Images 2, 4, 5, 15, and 16, and multiple leaf spot on corn leaves in Images 4, 6, 8, 10, 12, and 13, and no background interference in Images 4 and 14.

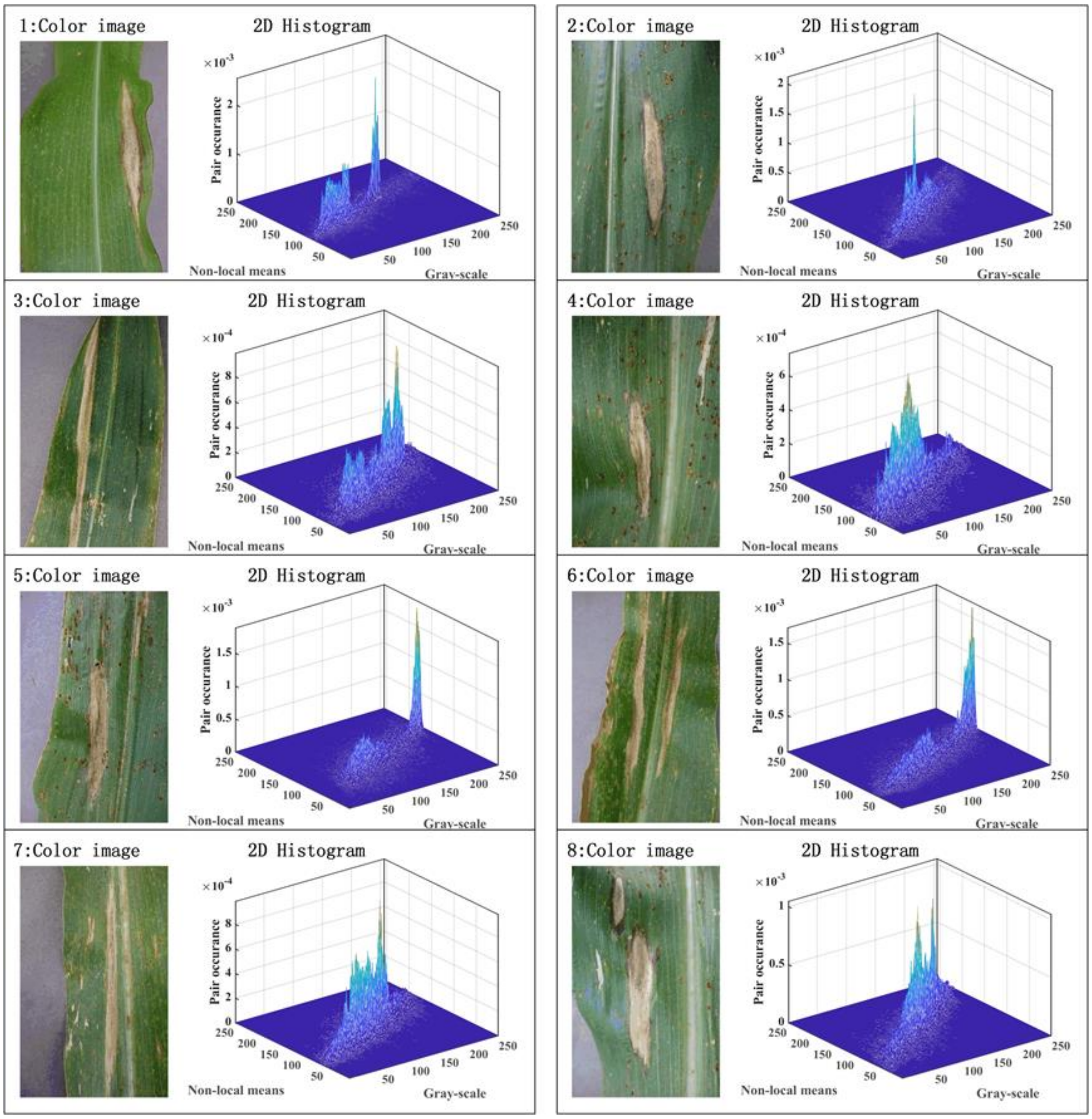

(a)

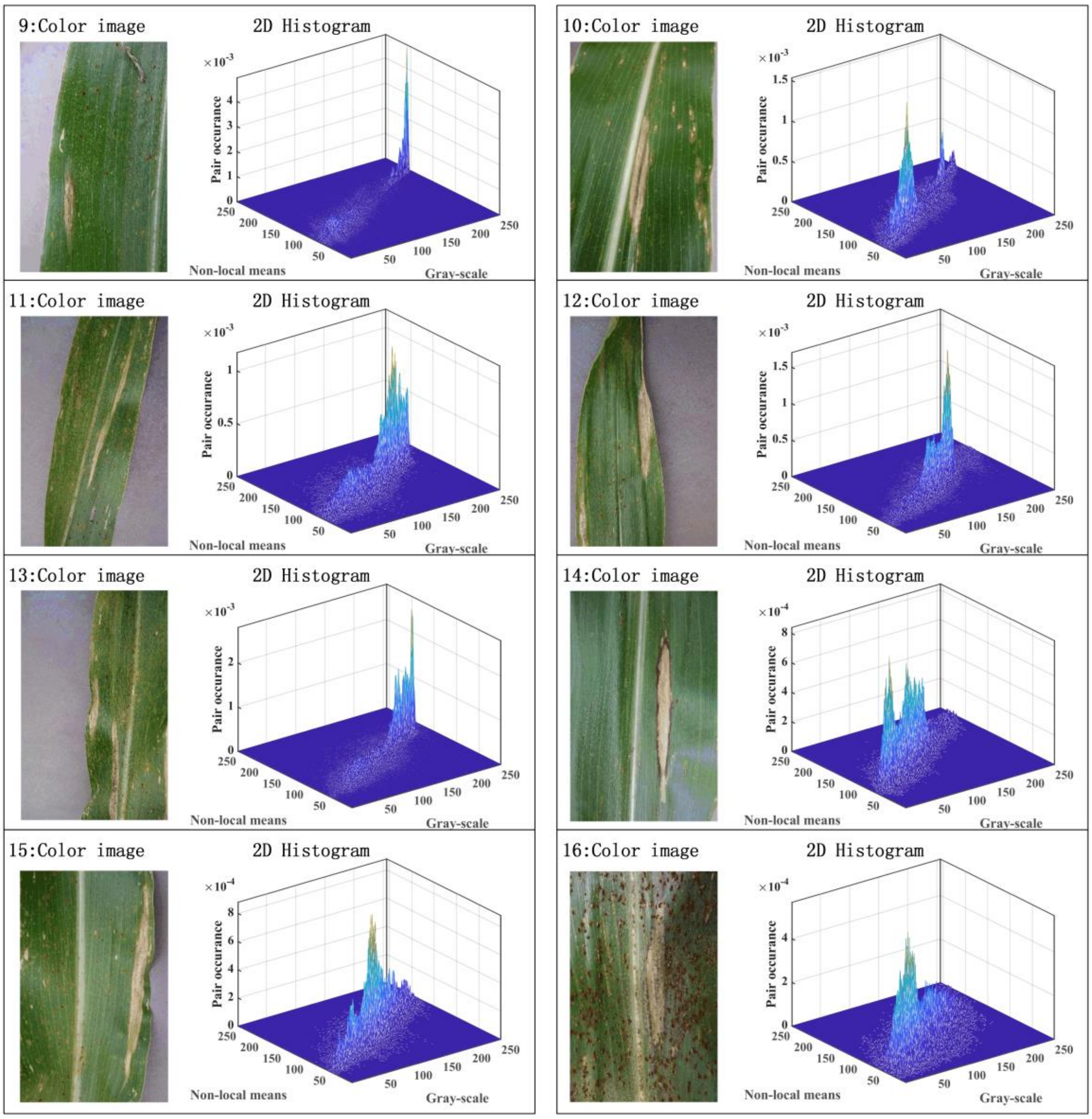

(b)

Fig. 9 Original images and their 2D histograms

Figure 9 shows the eight images and their 2D histograms, respectively. The experiments are carried out under the condition of threshold level is 4,6,8,10 respectively. All comparison algorithms run under the same conditions to ensure the experiments' fairness, where the population size is 20, each algorithm runs 30 times independently.

4.5.2 Performance evaluation parameters

In this section, PSNR, SSIM, and FSIM are briefly introduced, used to evaluate multi-threshold image segmentation results.

PSNR is an index to measure image quality. When used to evaluate the effect of image segmentation, the larger the PSNR is, the better the image segmentation effect is. SSIM is used to measure the similarity between the original image and the segmented image. The closer the value is to 1, the better the image segmentation effect is. When the two images are identical, the SSIM value is 1. FSIM uses feature similarity to evaluate image quality, including phase congruence (PC) and gradient magnitude (GM). The former is used to describe the local structure and extract stable features from the image, while the latter is used to describe changes in the image. The value of FSIM is between 0 and 1, and the closer it is to 1, the better the image segmentation effect is.

4.5.3 Experimental results and analysis

The experimental results of multi-threshold image segmentation are showed through tables and pictures in this section. Comparative experiments were carried out by segmenting eight images under the condition of threshold levels of 4, 6, 8, and 10, to verify the effectiveness of MGWO on image segmentation at different threshold levels. There are ten swarm intelligence optimization algorithms involved in the comparison. PSNR, SSIM, and FSIM were used to evaluate the segmentation effect. In the discussion of experimental results, the Wilcoxon signed-rank tests on PSNR, SSIM, and FSIM are carried out, the mean and standard deviation of the evaluation indexes are calculated. All comparison algorithms are sorted under the condition of each segmentation threshold level.

Tables A.1-A.3 show the *AVG* and *STD* of the PSNR, SSIM, and FSIM, respectively. Where the largest *AVG* and the smallest *STD* are marked in bold. **Table 13** shows the maxima of the objective function. Meanwhile, they are the maximum values of Kapur's entropy found by each algorithm at different threshold levels. At each threshold level, the largest of ten values obtained by comparison algorithms are marked in bold. **Tables 14-16** show the results of the Wilcoxon signed-rank tests on PSNR, SSIM, and FSIM. Where "+" indicates the number of pictures on which the performance of MGWO is better than the comparison algorithm. In contrast, "-" denotes the opposite, and "=" indicates the number of pictures on which the performance of MGWO is almost similar to the comparison algorithm. Mean indicates the mean value of the sort on all pictures, and Rank indicates the final ranking level. One algorithm has different performances when they run on multi-threshold image segmentation at different thresholds.

Compared with nine other algorithms, MGWO has outstanding performance at four threshold levels, as shown in these tables. This advantage did not decrease with the increase of the threshold level. At each threshold level, the three indicators, PSNR, SSIM, and FSIM, obtained by the MGWO algorithm ranked first. When the threshold level is 4, the three indicators obtained by CS ranked second. When the threshold level is 6, the three indicators obtained by GWO ranked second. Although the original GWO and CS have competitiveness at a low threshold level, their advantages decrease rapidly with the increase of threshold level. Compared with SSA, MGWO has a substantial advantage at every threshold level. SSA is not suitable for multi-threshold image segmentation of Leaf Spot Diseases on Maize. Compared with the other competitive MAs, which are HHO and WOA, the performance of MGWO on at least seven images is far ahead when the threshold levels are 4 and 6, and it also has competitiveness when the threshold levels are 8 and 10. Compared with the excellent algorithm CLPSO, MGWO is more suitable for multi-threshold image segmentation at each threshold level with Kapur's entropy as the objective function. Compared to the improved GWO, which is called IGWO, the performance of MGWO on at least six images is far ahead.

Although the other improved algorithms, CLSGMFO and LGCMFO, have advantages at high threshold levels, their performance at low-threshold image segmentation is not outstanding. Around image segmentation with different thresholds, MGWO got the best ranking when the threshold level is six. These can prove the advantages of MGWO when applied to the multi-threshold image segmentation of Leaf Spot Diseases on Maize. **Table A.4** shows the thresholds found by each algorithm at the 4-level threshold. **Table A.5** shows the average running time (*AvgTime*) of all comparison algorithms on each picture at each threshold level after 30 parallel random runs. It can be seen that MGWO can obtain better effects of multi-threshold image segmentation, but the corresponding running time will increase slightly. This is consistent with the time complexity of MGWO analyzed above. Since the multi-stage strategy increases the proportion of the algorithm's exploration time, it increases the algorithm's ability to find approximate solutions closer to the true optimal solution and the ability to get rid of the local optima trap, which will inevitably slow down the algorithm's convergence speed.

Figure 10 shows the 6-level threshold segmentation results obtained by each algorithm on image 1. It can be seen from the segmentation results that when the threshold is six, the MGWO algorithm can better segment the disease spots on maize leaves than other comparative algorithms. These operations can lay a solid foundation for recognizing and classifying the disease spots. The plot style of **Figures 9** and **10** refers to the paper of Zhao et al. (Zhao et al., 2021).

According to the above analysis of multi-threshold image segmentation results, MGWO has noticeable competitiveness over other comparative algorithms in segmentation experiments at four threshold levels of Leaf Spot Diseases on Maize. The proposed MGWO can also be applied to other complex problems, such as optimal control and design (Gong et al., 2019; Luo et al., 2020b; Mi et al., 2021; Zhao et al., 2020a), digital image colorimetry (Jing et al., 2021), neural network modeling (Fan et al., 2021; Zhou et al., 2021), prediction cases (Chen et al., 2021), and remote sensing (Wang et al., 2020b) The potential exploration and exploitation trends of the MGWO also needs more real-world problems to be considered for benchmark purposes. Such domains can be related to both image domain or feature spaces with continuous and binary spaces, for instance, optimal performance design (Meng et al., 2018), active surveillance (Pei et al., 2020), pedestrian dead reckoning (Qiu et al., 2018), evaluation of human lower limb motions (Qiu et al., 2016), image super-resolution (Zhu et al., 2021a; Zhu et al., 2021b), anomaly behavior detection (Guo et al., 2020), image robust representation learning (Hu et al., 2021a), and sentiment classification (Jiang et al., 2020b). Also, another discussion point on the proposed method is to investigate more deeply the root of the equations of MGWO because its source is still GWO, and it still can be seen as a variant of a velocity-free PSO.

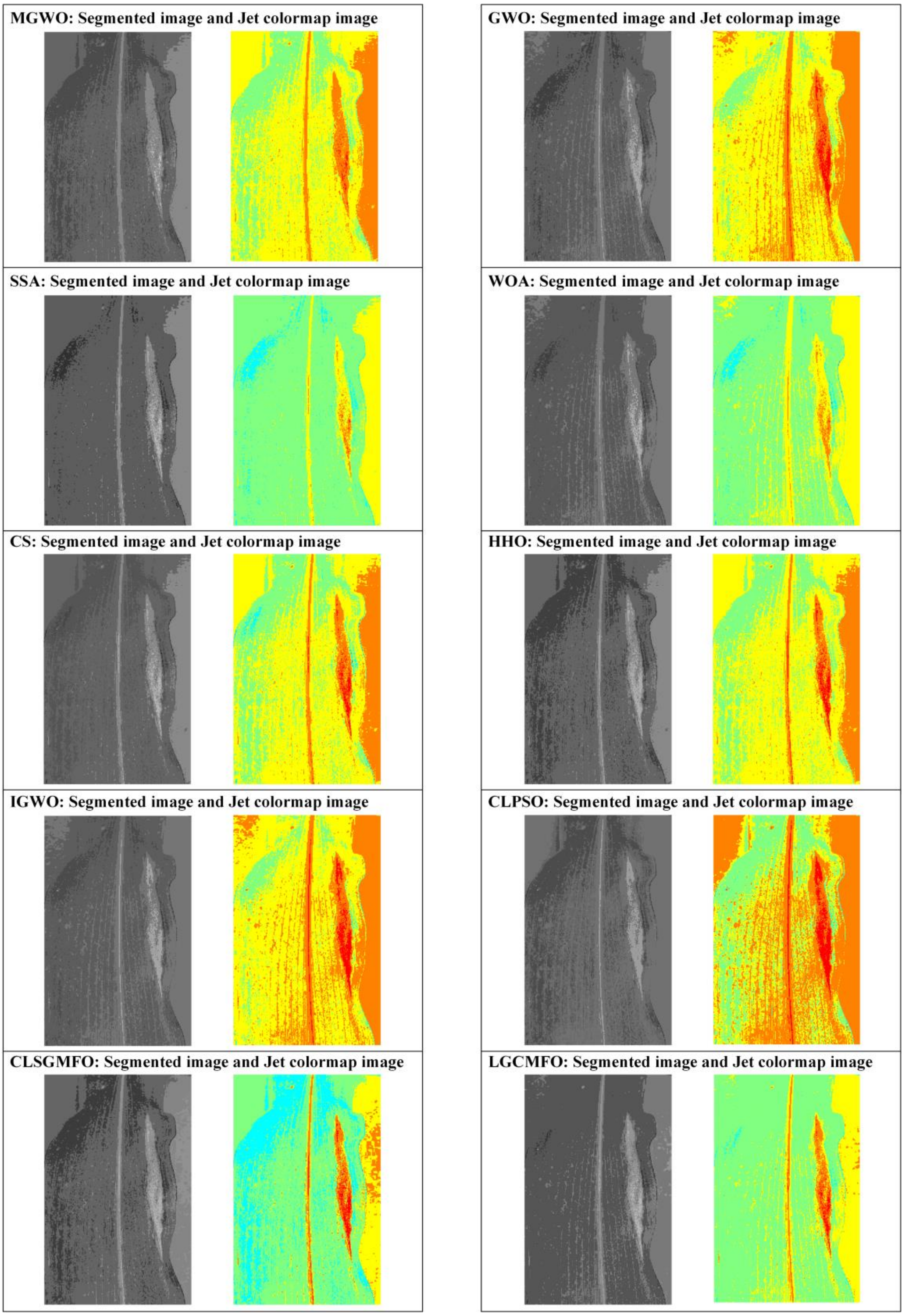

Fig. 10 The segmented results of image 1 at 6-level threshold using all algorithms

Table 13. The fitness value results of each comparative algorithm

Image	Level	MGWO	GWO	HHO	WOA	SSA	CS	IGWO	CLPSO	CLSGMFO	LGCMFO
1	4	**3.87236E+01**	**3.87236E+01**	3.86628E+01	3.87202E+01	3.87190E+01	3.87162E+01	3.87209E+01	**3.87236E+01**	3.87235E+01	**3.87236E+01**
	6	**4.92391E+01**	4.91693E+01	4.87152E+01	4.85520E+01	4.87852E+01	4.87897E+01	4.90972E+01	4.91009E+01	4.91791E+01	4.91125E+01
	8	5.83051E+01	5.79948E+01	5.82075E+01	5.74794E+01	5.76193E+01	5.81497E+01	5.80314E+01	5.82683E+01	5.81475E+01	**5.83611E+01**
	10	6.67144E+01	6.62477E+01	6.58145E+01	6.64673E+01	6.55186E+01	6.63559E+01	6.60820E+01	6.67924E+01	6.65337E+01	**6.68829E+01**
2	4	**3.83643E+01**	**3.83643E+01**	3.76887E+01	3.78365E+01	3.80102E+01	3.83216E+01	3.83228E+01	3.82439E+01	3.81686E+01	3.81320E+01
	6	**4.91931E+01**	4.88145E+01	4.87635E+01	4.87958E+01	4.87868E+01	4.88145E+01	4.87766E+01	4.89523E+01	4.87940E+01	4.87805E+01
	8	**5.87284E+01**	5.86972E+01	5.82170E+01	5.85353E+01	5.81525E+01	5.84841E+01	5.84282E+01	5.87002E+01	5.86186E+01	5.86183E+01
	10	**6.75524E+01**	6.70426E+01	6.65886E+01	6.73350E+01	6.70775E+01	6.71772E+01	6.70029E+01	6.74889E+01	6.74858E+01	6.75092E+01
3	4	**3.81117E+01**	3.81101E+01	3.78047E+01	3.79706E+01	3.80245E+01	3.81023E+01	3.80994E+01	3.81094E+01	3.80372E+01	3.80426E+01
	6	4.91241E+01	4.91228E+01	4.90126E+01	4.90891E+01	4.91029E+01	4.91238E+01	4.90919E+01	**4.91251E+01**	4.91217E+01	4.91243E+01
	8	5.86171E+01	5.86307E+01	5.84205E+01	5.84841E+01	5.85263E+01	5.86700E+01	5.85634E+01	**5.87147E+01**	5.86761E+01	5.87073E+01
	10	**6.76433E+01**	6.74781E+01	6.70014E+01	6.71695E+01	6.64575E+01	6.72646E+01	6.69258E+01	6.74338E+01	6.74501E+01	6.73349E+01
4	4	**3.77794E+01**	3.77642E+01	3.74015E+01	3.75482E+01	3.76268E+01	3.76492E+01	3.76559E+01	3.76678E+01	**3.77794E+01**	3.76678E+01
	6	**4.86005E+01**	4.85915E+01	4.84293E+01	4.84349E+01	4.85223E+01	4.85796E+01	4.85261E+01	4.85864E+01	4.85940E+01	4.85460E+01
	8	5.82836E+01	5.79433E+01	5.76649E+01	5.80695E+01	5.76362E+01	5.81764E+01	5.80471E+01	5.82802E+01	5.82256E+01	**5.82986E+01**
	10	**6.69785E+01**	6.67008E+01	6.64174E+01	6.64311E+01	6.66338E+01	6.68702E+01	6.64105E+01	6.69684E+01	6.68248E+01	6.68312E+01
5	4	**3.87176E+01**	**3.87176E+01**	3.64547E+01	3.83469E+01	3.86811E+01	3.86156E+01	3.87131E+01	3.82588E+01	3.82002E+01	**3.87176E+01**
	6	**5.01104E+01**	4.80769E+01	4.72590E+01	4.79040E+01	4.98301E+01	4.96679E+01	4.98715E+01	4.95776E+01	4.98197E+01	4.74629E+01
	8	5.78868E+01	5.80425E+01	5.86305E+01	5.75067E+01	5.76847E+01	5.87361E+01	**5.94031E+01**	5.88065E+01	5.79084E+01	5.79254E+01
	10	6.65272E+01	6.62523E+01	6.60540E+01	**6.84627E+01**	6.58633E+01	6.72150E+01	6.76775E+01	6.80145E+01	6.66480E+01	6.65838E+01
6	4	**3.86862E+01**	**3.86862E+01**	3.83839E+01	3.84233E+01	3.86662E+01	3.86778E+01	3.86464E+01	3.86678E+01	3.86678E+01	3.86678E+01
	6	**4.95379E+01**	4.95333E+01	4.94970E+01	4.93464E+01	4.94014E+01	4.94775E+01	4.94853E+01	4.95321E+01	4.94863E+01	4.95237E+01
	8	**5.92285E+01**	5.92082E+01	5.90918E+01	5.91073E+01	5.90128E+01	5.91403E+01	5.89391E+01	5.91750E+01	5.91893E+01	5.91611E+01

	10	**6.79754E+01**	6.77934E+01	6.70965E+01	6.77954E+01	6.76587E+01	6.77046E+01	6.75139E+01	6.79056E+01	6.77986E+01	6.79226E+01
7	4	**3.86223E+01**	**3.86223E+01**	3.85947E+01	3.82018E+01	3.85747E+01	3.86000E+01	3.86068E+01	3.85817E+01	3.86222E+01	3.78972E+01
	6	4.91918E+01	4.90300E+01	4.82483E+01	4.83083E+01	4.89328E+01	4.91031E+01	4.93880E+01	4.90095E+01	4.91617E+01	**4.94927E+01**
	8	5.83897E+01	**5.86869E+01**	5.81200E+01	5.80846E+01	5.81231E+01	5.83093E+01	5.81525E+01	5.84307E+01	5.81912E+01	5.82136E+01
	10	6.72101E+01	6.66578E+01	6.69333E+01	6.66390E+01	6.66193E+01	6.70748E+01	6.60809E+01	6.71354E+01	**6.73203E+01**	6.68097E+01
8	4	**3.80724E+01**	3.80706E+01	3.69146E+01	3.75672E+01	3.80246E+01	3.79834E+01	3.80572E+01	3.80684E+01	3.76467E+01	3.78877E+01
	6	4.84338E+01	4.84616E+01	4.83788E+01	**4.85939E+01**	4.77207E+01	4.84458E+01	4.85856E+01	4.82815E+01	4.79643E+01	4.80536E+01
	8	5.79134E+01	5.81419E+01	5.76264E+01	5.78271E+01	5.77951E+01	**5.81609E+01**	5.77329E+01	5.79631E+01	5.79245E+01	5.78370E+01
	10	6.67107E+01	6.64815E+01	6.64165E+01	6.67736E+01	6.64028E+01	6.67575E+01	6.64408E+01	**6.67899E+01**	6.67263E+01	6.67707E+01
9	4	**3.81114E+01**	**3.81114E+01**	3.80914E+01	3.80979E+01	3.80393E+01	3.80907E+01	3.81071E+01	3.81060E+01	3.81044E+01	**3.81114E+01**
	6	4.87744E+01	4.87715E+01	4.84106E+01	4.86559E+01	4.85865E+01	4.86390E+01	4.87339E+01	**4.87979E+01**	4.87368E+01	4.87732E+01
	8	5.78833E+01	5.78114E+01	5.74416E+01	5.76716E+01	5.76622E+01	5.77968E+01	5.77487E+01	**5.81742E+01**	5.80447E+01	5.78195E+01
	10	6.59979E+01	6.57051E+01	6.54943E+01	6.56711E+01	6.53996E+01	6.59869E+01	6.54091E+01	6.62838E+01	6.63169E+01	**6.65110E+01**
10	4	**3.83150E+01**	3.83136E+01	3.77201E+01	3.82876E+01	3.81559E+01	3.82941E+01	3.83072E+01	3.82959E+01	3.82959E+01	3.82875E+01
	6	**4.90623E+01**	4.90619E+01	4.87813E+01	4.88601E+01	4.87972E+01	4.89838E+01	4.89987E+01	4.90548E+01	4.90535E+01	4.90254E+01
	8	5.85589E+01	5.86865E+01	5.82441E+01	5.82365E+01	5.80789E+01	5.84424E+01	5.83173E+01	5.87591E+01	**5.89757E+01**	5.83237E+01
	10	6.78978E+01	6.71499E+01	6.68694E+01	6.77215E+01	6.69408E+01	6.75803E+01	6.64702E+01	6.70776E+01	6.78365E+01	**6.80234E+01**
11	4	**3.83227E+01**	3.83215E+01	3.81482E+01	3.83088E+01	3.82902E+01	3.83187E+01	3.83203E+01	**3.83227E+01**	**3.83227E+01**	**3.83227E+01**
	6	**4.91058E+01**	4.90957E+01	4.86644E+01	4.90011E+01	4.89908E+01	4.90972E+01	4.89970E+01	**4.91058E+01**	4.91052E+01	**4.91058E+01**
	8	5.82029E+01	5.81988E+01	5.75641E+01	5.79840E+01	5.83843E+01	5.83562E+01	5.81642E+01	**5.85802E+01**	5.83642E+01	5.84636E+01
	10	6.64080E+01	6.64896E+01	6.61945E+01	6.64994E+01	6.67249E+01	6.66655E+01	6.63975E+01	**6.70396E+01**	6.67167E+01	6.67949E+01
12	4	**3.86035E+01**	**3.86035E+01**	3.81119E+01	3.85826E+01	3.84922E+01	3.85891E+01	3.85930E+01	3.85934E+01	3.86028E+01	3.85869E+01
	6	**4.94920E+01**	4.94911E+01	4.92989E+01	4.88541E+01	4.91089E+01	4.90770E+01	4.94809E+01	4.93636E+01	4.93953E+01	4.91538E+01
	8	5.84978E+01	5.91500E+01	5.81536E+01	5.81292E+01	5.80099E+01	5.84438E+01	5.87501E+01	5.86385E+01	5.90108E+01	**5.92634E+01**
	10	6.69279E+01	6.68128E+01	6.63388E+01	6.65494E+01	6.63047E+01	6.67866E+01	6.63544E+01	6.70779E+01	6.65787E+01	**6.71120E+01**

13	4	**3.84181E+01**	**3.84181E+01**	3.81687E+01	3.83817E+01	3.83411E+01	3.84179E+01	3.84094E+01	**3.84181E+01**	3.84179E+01	**3.84181E+01**
	6	4.89348E+01	4.88653E+01	4.88004E+01	4.88172E+01	4.88308E+01	4.89367E+01	4.88974E+01	**4.89827E+01**	4.89432E+01	4.89370E+01
	8	**5.86741E+01**	5.82909E+01	5.79310E+01	5.81847E+01	5.81999E+01	5.82863E+01	5.80879E+01	5.85518E+01	5.84914E+01	5.82779E+01
	10	6.68173E+01	6.65666E+01	6.59483E+01	6.66975E+01	6.64136E+01	6.68488E+01	6.63403E+01	**6.69890E+01**	6.68999E+01	6.69123E+01
14	4	3.81120E+01	3.79835E+01	3.79265E+01	3.78512E+01	3.79445E+01	3.81542E+01	3.81650E+01	3.81531E+01	3.80013E+01	**3.81751E+01**
	6	**4.88832E+01**	4.88454E+01	4.82469E+01	4.87376E+01	4.86521E+01	4.88443E+01	4.88746E+01	4.87559E+01	4.88384E+01	4.87311E+01
	8	**5.86977E+01**	5.82983E+01	5.81345E+01	5.79704E+01	5.81076E+01	5.82672E+01	5.82021E+01	5.84907E+01	5.85674E+01	5.85123E+01
	10	6.71634E+01	6.71117E+01	6.64496E+01	6.69977E+01	6.65257E+01	6.70051E+01	6.64179E+01	6.71138E+01	6.68377E+01	**6.72633E+01**
15	4	3.79185E+01	**3.79245E+01**	3.74904E+01	3.78939E+01	3.74040E+01	3.78741E+01	3.79058E+01	3.76793E+01	3.75698E+01	3.79185E+01
	6	4.82882E+01	4.82700E+01	4.79728E+01	4.80404E+01	4.83037E+01	4.81384E+01	4.83454E+01	4.84851E+01	**4.84986E+01**	4.83211E+01
	8	5.81818E+01	5.80355E+01	5.79056E+01	5.82496E+01	5.79751E+01	5.83904E+01	5.79723E+01	**5.84027E+01**	5.83242E+01	5.83835E+01
	10	6.71115E+01	6.66467E+01	6.65467E+01	**6.74789E+01**	6.69868E+01	6.70648E+01	6.64364E+01	6.74295E+01	6.70576E+01	6.69616E+01
16	4	**3.79592E+01**	3.79474E+01	3.78386E+01	3.79581E+01	3.79431E+01	3.79532E+01	3.79283E+01	3.78659E+01	3.78857E+01	**3.79592E+01**
	6	4.87831E+01	**4.88296E+01**	4.78266E+01	4.84949E+01	4.85905E+01	4.86942E+01	4.86961E+01	4.87631E+01	4.85147E+01	4.87320E+01
	8	**5.87003E+01**	5.85368E+01	5.78142E+01	5.77165E+01	5.80198E+01	5.83612E+01	5.82046E+01	5.85903E+01	5.81853E+01	5.84665E+01
	10	6.71653E+01	6.69418E+01	6.69429E+01	6.63894E+01	6.63531E+01	6.67650E+01	6.64496E+01	**6.73162E+01**	6.70938E+01	6.70661E+01

Table 14. The PSNR comparison results at each threshold level

Level		MGWO	GWO	HHO	WOA	SSA	CS	IGWO	CLPSO	CLSGMFO	LGCMFO
4	+/-/=	~	4/0/12	12/0/4	11/0/5	10/0/6	2/1/13	7/0/9	9/2/5	9/2/5	8/2/6
	Mean	**3.13**	3.81	8.88	8.38	7.94	3.63	4.69	4.56	5.25	4.75
	Rank	**1**	3	10	9	8	2	5	4	7	6
6	+/-/=	~	4/0/12	7/0/9	8/0/8	13/0/3	7/0/9	7/0/9	10/0/6	6/0/10	7/1/8
	Mean	**2.25**	3.81	7.06	7.56	9.31	5.06	5.94	5.12	4.63	4.25
	Rank	**1**	2	8	9	10	5	7	6	4	3

8	+/-/=	~	8/0/8	5/0/11	7/0/9	13/0/3	6/0/10	6/0/10	9/0/7	4/0/12	5/1/10
	Mean	**2.44**	6.19	5.94	5.63	9.69	6.13	6.81	4.94	3.88	3.38
	Rank	**1**	8	6	5	10	7	9	4	3	2
10	+/-/=	~	11/0/5	2/0/14	2/3/11	14/0/2	4/0/12	7/0/9	3/0/13	3/0/13	2/0/14
	Mean	**2.75**	6.81	6.50	4.19	9.69	5.31	7.31	3.94	4.50	4.00
	Rank	**1**	8	7	4	10	6	9	2	5	3

Table 15. The SSIM comparison results at each threshold level

Level		MGWO	GWO	HHO	WOA	SSA	CS	IGWO	CLPSO	CLSGMFO	LGCMFO
4	+/-/=	~	5/0/11	12/0/4	12/0/4	13/0/3	3/1/12	6/1/9	11/0/5	10/0/6	9/1/6
	Mean	**2.25**	3.75	9.00	9.00	7.94	3.19	4.13	5.00	5.50	5.25
	Rank	**1**	3	9	9	8	2	4	5	7	6
6	+/-/=	~	4/0/12	9/0/7	11/0/5	12/0/4	8/0/8	8/0/8	9/0/7	9/1/6	8/1/7
	Mean	**2.25**	3.88	7.00	7.69	9.13	5.06	5.50	5.19	4.69	4.63
	Rank	**1**	2	8	9	10	5	7	6	4	3
8	+/-/=	~	9/0/7	3/0/13	3/0/13	12/0/4	7/0/9	6/0/10	6/0/10	4/0/12	5/0/11
	Mean	**2.13**	6.69	5.38	5.25	9.63	6.19	6.75	5.13	4.19	3.69
	Rank	**1**	8	6	5	10	7	9	4	3	2
10	+/-/=	~	12/0/4	1/0/15	2/3/11	14/0/2	4/0/12	7/0/9	6/0/10	7/0/9	3/0/13
	Mean	**2.31**	6.81	6.75	3.94	9.69	5.50	6.63	4.31	4.56	4.50
	Rank	**1**	9	8	2	10	6	7	3	5	4

Table 16. The FSIM comparison results at each threshold level

Level		MGWO	GWO	HHO	WOA	SSA	CS	IGWO	CLPSO	CLSGMFO	LGCMFO
4	+/-/=	~	6/0/10	12/0/4	13/0/3	10/0/6	2/3/11	6/1/9	9/2/5	8/2/6	7/2/7
	Mean	**2.94**	4.44	8.94	8.81	7.94	3.63	4.44	4.56	4.69	4.63
	Rank	**1**	3	10	9	8	2	3	5	7	6
6	+/-/=	~	5/0/11	7/1/8	11/0/5	14/0/2	7/0/9	7/0/9	11/0/5	7/0/9	7/1/8
	Mean	**2.31**	4.00	6.69	7.31	9.31	5.44	5.56	5.44	4.75	4.19
	Rank	**1**	2	8	9	10	5	7	5	4	3
8	+/-/=	~	9/0/7	6/0/10	4/0/12	12/0/4	6/0/10	8/0/8	7/1/8	6/0/10	4/2/10
	Mean	**2.38**	6.25	6.44	5.44	9.56	5.81	7.19	4.81	3.75	3.38
	Rank	**1**	7	8	5	10	6	9	4	3	2
10	+/-/=	~	8/0/8	4/0/12	2/3/11	14/0/2	3/0/13	7/0/9	3/2/11	2/0/14	2/0/14
	Mean	**2.88**	6.75	7.38	4.56	9.56	5.13	7.50	3.19	4.44	3.63
	Rank	**1**	7	8	5	10	6	9	2	4	3

5. Conclusions and future works

In this paper, an improved GWO called MGWO was proposed based on multiple stages. The search phase is divided into three stages to reach a higher balance between exploration and exploitation than the original GWO. At the first stage, take full advantage of the primary GWO's strong exploration capability. At the second stage, the SSA algorithm is a part of the position update formula is used to increase the primary GWO. In the last step, the algorithm exploits promising areas by performing Cauchy mutation on each dimension of the current optimal solution.

Experiments with other swarm intelligence optimization algorithms on benchmark functions show that MGWO can obtain more accurate solutions than different algorithms and has an excellent ability to jump out of the local optima trap. The balance and diversity experiment proves that MGWO has a better balance of exploitation and exploration than the original GWO. Its rough curves also verify the ability to jump out of the local optima trap. Then, the MGWO was applied to the multi-threshold image segmentation of Leaf Spot Diseases on Maize. Comparing the results of three evaluation indexes proved that MGWO is superior to other comparative algorithms when applied to this application.

Aiming at the shortcoming of the MGWO, which is the slight rising of the time complexity, further research is to find and develop strategies to relieve the time complexity without reducing the algorithm's performance. MGWO can be applied to image segmentation and disease identification of more different kinds of maize diseases to guide farmers to take corresponding disease control measures. Devote research results to agriculture and agricultural modernization. Furthermore, the performance of MGWO solving optimization problems in other fields also needs to be further verified.

Acknowledgment

This research was supported by the National Natural Science Foundation of China (U19A2061, U1809209, 62076185), Science and Technology Development Project of Jilin Province (20190301024NY), Jilin Provincial Industrial Innovation Special Fund Project (2018C039-3), Taif University Researchers Supporting Project Number (TURSP-2020/114), Taif University, Taif, Saudi Arabia.

Appendix A

Table A.1 The AVG and STD comparison results of PSNR

Image	Level	Item	MGWO	GWO	HHO	WOA	SSA	CS	IGWO	CLPSO	CLSGMFO	LGCMFO
1	4	AVG	2.04910E+01	2.06574E+01	1.90316E+01	1.90630E+01	2.02817E+01	**2.09634E+01**	2.06030E+01	2.06956E+01	2.03771E+01	2.05653E+01
		STD	6.89233E-01	7.60515E-01	3.31344E+00	3.97881E+00	1.64771E+00	**5.58762E-01**	1.81802E+00	7.18742E-01	1.24961E+00	1.28660E+00
	6	AVG	**2.29509E+01**	2.23672E+01	2.24207E+01	2.19137E+01	2.13100E+01	2.22866E+01	2.18777E+01	2.20443E+01	2.20662E+01	2.22368E+01
		STD	1.16810E+00	1.02823E+00	2.72418E+00	2.52018E+00	1.81716E+00	2.25377E+00	2.27246E+00	**7.63041E-01**	1.15950E+00	1.06676E+00
	8	AVG	2.37554E+01	2.33624E+01	2.29584E+01	2.34027E+01	2.27604E+01	2.32676E+01	2.27662E+01	2.34337E+01	**2.38852E+01**	2.34926E+01
		STD	2.09917E+00	1.61048E+00	3.49044E+00	2.29358E+00	2.97931E+00	2.14061E+00	2.22529E+00	**1.49545E+00**	1.76889E+00	2.18407E+00
	10	AVG	2.48198E+01	2.48311E+01	2.52238E+01	2.42834E+01	2.41808E+01	2.51683E+01	2.49624E+01	**2.54412E+01**	2.52590E+01	2.51817E+01
		STD	**1.24716E+00**	1.50883E+00	3.31098E+00	2.94233E+00	2.13486E+00	1.74716E+00	2.46837E+00	1.35960E+00	1.79684E+00	1.73702E+00
2	4	AVG	**1.94603E+01**	1.92775E+01	1.70244E+01	1.75290E+01	1.86550E+01	1.94403E+01	1.91809E+01	1.88077E+01	1.86787E+01	1.89977E+01
		STD	8.98355E-01	1.51311E+00	3.39711E+00	2.26718E+00	1.13832E+00	1.44388E+00	1.17502E+00	7.87874E-01	1.24745E+00	**6.62462E-01**
	6	AVG	2.11042E+01	2.11846E+01	2.02639E+01	2.05508E+01	2.04864E+01	**2.13470E+01**	2.09025E+01	2.13465E+01	2.12571E+01	2.09462E+01
		STD	8.27170E-01	**6.60747E-01**	2.26247E+00	1.74120E+00	1.07377E+00	9.41888E-01	1.14773E+00	8.37407E-01	8.22692E-01	9.49238E-01
	8	AVG	2.25989E+01	2.25227E+01	2.28308E+01	2.27120E+01	2.21609E+01	2.26895E+01	2.24935E+01	2.25153E+01	2.28476E+01	**2.30452E+01**
		STD	1.14427E+00	**5.71911E-01**	1.40643E+00	1.52551E+00	9.12631E-01	8.77319E-01	1.68072E+00	7.46818E-01	8.44563E-01	7.47844E-01
	10	AVG	2.41250E+01	2.38165E+01	2.39757E+01	**2.49201E+01**	2.38401E+01	2.43769E+01	2.45966E+01	2.46066E+01	2.42795E+01	2.44019E+01
		STD	1.03154E+00	**8.38249E-01**	2.48942E+00	1.05966E+00	1.10695E+00	1.15151E+00	1.40494E+00	9.08237E-01	1.11607E+00	1.26219E+00
3	4	AVG	**1.97267E+01**	1.96023E+01	1.75560E+01	1.72109E+01	1.79549E+01	1.94764E+01	1.88705E+01	1.87893E+01	1.83841E+01	1.84057E+01
		STD	**7.80986E-01**	9.56826E-01	2.21790E+00	2.00162E+00	1.36081E+00	1.05276E+00	1.42963E+00	1.06748E+00	1.37368E+00	1.23646E+00
	6	AVG	2.09863E+01	2.06499E+01	2.03115E+01	2.07888E+01	2.05671E+01	2.07115E+01	2.05907E+01	**2.10723E+01**	2.05259E+01	2.07598E+01
		STD	9.96331E-01	1.33744E+00	1.67261E+00	1.60487E+00	1.00001E+00	**2.91393E-01**	1.12072E+00	6.60804E-01	1.07881E+00	1.08090E+00
	8	AVG	2.26103E+01	2.25684E+01	2.27457E+01	2.28262E+01	2.20611E+01	2.28636E+01	2.26300E+01	2.30665E+01	2.28606E+01	**2.31286E+01**
		STD	9.17250E-01	**6.18214E-01**	1.83950E+00	1.54438E+00	1.25180E+00	7.57289E-01	1.14504E+00	6.70018E-01	9.89327E-01	1.30192E+00

	10	AVG	**2.46697E+01**	2.38648E+01	2.38971E+01	2.44121E+01	2.38007E+01	2.42728E+01	2.39886E+01	2.42070E+01	2.46393E+01	2.44898E+01
		STD	8.84055E-01	8.14498E-01	2.63194E+00	1.69632E+00	1.14793E+00	1.04229E+00	1.62711E+00	**7.56687E-01**	1.26549E+00	1.20474E+00
4	4	AVG	**1.92769E+01**	1.92490E+01	1.76923E+01	1.71125E+01	1.86104E+01	1.89601E+01	1.90449E+01	1.86956E+01	1.92099E+01	1.86303E+01
		STD	9.92471E-01	1.00793E+00	2.18421E+00	2.51581E+00	1.13593E+00	6.85544E-01	1.15080E+00	**4.88085E-01**	8.05115E-01	7.18522E-01
	6	AVG	**2.16721E+01**	2.12672E+01	2.07581E+01	2.08159E+01	2.06305E+01	2.09690E+01	2.13040E+01	2.13068E+01	2.10139E+01	2.12638E+01
		STD	4.69193E-01	4.13557E-01	2.13570E+00	9.07284E-01	1.30500E+00	1.06288E+00	9.84023E-01	**2.96296E-01**	6.49847E-01	6.74239E-01
	8	AVG	**2.30976E+01**	2.24708E+01	2.26824E+01	2.24517E+01	2.15759E+01	2.22748E+01	2.29327E+01	2.26969E+01	2.28023E+01	2.29639E+01
		STD	7.50988E-01	**6.57900E-01**	1.62198E+00	2.03259E+00	1.26213E+00	1.12426E+00	1.54819E+00	6.86973E-01	7.51964E-01	8.51373E-01
	10	AVG	**2.49169E+01**	2.40774E+01	2.46492E+01	2.43403E+01	2.36575E+01	2.43914E+01	2.41593E+01	2.45870E+01	2.45410E+01	2.45684E+01
		STD	9.31506E-01	8.18797E-01	2.05436E+00	1.36414E+00	1.27736E+00	1.10488E+00	1.82330E+00	**6.76923E-01**	9.65002E-01	9.10442E-01
5	4	AVG	1.87793E+01	1.84495E+01	1.73065E+01	1.73994E+01	1.80933E+01	**1.90014E+01**	1.82835E+01	1.73758E+01	1.88627E+01	1.86778E+01
		STD	1.63923E+00	1.41450E+00	2.89914E+00	2.52844E+00	2.35845E+00	1.79316E+00	1.81134E+00	2.21382E+00	1.66642E+00	**1.19851E+00**
	6	AVG	2.07058E+01	2.01074E+01	2.03929E+01	2.05709E+01	1.89048E+01	2.02936E+01	2.06805E+01	1.87781E+01	2.12048E+01	**2.12831E+01**
		STD	**1.20869E+00**	1.81855E+00	2.73965E+00	1.89276E+00	2.57759E+00	1.89622E+00	1.56206E+00	2.36651E+00	1.34850E+00	2.02512E+00
	8	AVG	2.28943E+01	2.23825E+01	2.28419E+01	2.31621E+01	2.15600E+01	2.25952E+01	2.13221E+01	2.19793E+01	2.35526E+01	**2.37811E+01**
		STD	1.63067E+00	1.08501E+00	2.23947E+00	2.02862E+00	1.92602E+00	1.62574E+00	2.09695E+00	**1.00220E+00**	1.15008E+00	1.40349E+00
	10	AVG	2.45109E+01	2.38207E+01	2.44422E+01	**2.52398E+01**	2.27736E+01	2.35684E+01	2.34885E+01	2.45042E+01	2.45446E+01	2.44112E+01
		STD	1.31198E+00	1.26414E+00	2.96561E+00	1.69277E+00	1.86870E+00	2.39385E+00	1.91294E+00	**1.02375E+00**	1.18027E+00	1.21217E+00
6	4	AVG	1.93423E+01	1.82850E+01	1.77527E+01	1.82782E+01	1.78340E+01	**1.93860E+01**	1.80138E+01	1.88665E+01	1.80365E+01	1.80554E+01
		STD	1.66479E+00	1.68764E+00	2.51018E+00	2.16296E+00	1.71804E+00	**9.53974E-01**	1.99025E+00	1.35731E+00	1.87561E+00	1.70994E+00
	6	AVG	2.04429E+01	2.03770E+01	**2.09541E+01**	2.04477E+01	2.00899E+01	1.94956E+01	2.07697E+01	2.05986E+01	2.07631E+01	2.02958E+01
		STD	9.43350E-01	**8.88626E-01**	1.62899E+00	1.42138E+00	1.45359E+00	1.07315E+00	1.10303E+00	1.00589E+00	1.14467E+00	1.09219E+00
	8	AVG	2.23978E+01	2.19690E+01	2.25851E+01	2.21845E+01	2.17748E+01	2.23924E+01	2.24360E+01	**2.26985E+01**	2.25564E+01	2.21654E+01
		STD	8.59659E-01	7.89122E-01	1.53315E+00	1.38181E+00	1.22186E+00	9.60963E-01	1.16594E+00	**5.84969E-01**	8.71779E-01	9.02706E-01
	10	AVG	2.41319E+01	2.34870E+01	2.37975E+01	2.42642E+01	2.31981E+01	2.39592E+01	2.36399E+01	**2.44178E+01**	2.39464E+01	2.39707E+01
		STD	**6.01485E-01**	7.53197E-01	2.19991E+00	1.26079E+00	1.21474E+00	9.90321E-01	1.73257E+00	6.92263E-01	1.06411E+00	9.74675E-01

7	4	AVG	**1.90140E+01**	1.89309E+01	1.74042E+01	1.74382E+01	1.77531E+01	1.86471E+01	1.86728E+01	1.88002E+01	1.84127E+01	1.87164E+01
		STD	9.42053E-01	8.81485E-01	2.36562E+00	1.30762E+00	1.18714E+00	1.06438E+00	1.43551E+00	1.11892E+00	1.07794E+00	**7.94537E-01**
	6	AVG	**2.08589E+01**	2.06358E+01	2.05176E+01	1.99434E+01	1.93964E+01	2.07488E+01	1.98611E+01	2.00703E+01	2.02310E+01	2.04012E+01
		STD	**9.88988E-01**	1.59314E+00	1.79210E+00	2.01410E+00	1.37431E+00	1.50945E+00	1.83321E+00	1.27860E+00	1.16527E+00	1.63912E+00
	8	AVG	2.26612E+01	2.18018E+01	2.21488E+01	**2.27503E+01**	2.16380E+01	2.24004E+01	2.24304E+01	2.22418E+01	2.24563E+01	2.25001E+01
		STD	1.43607E+00	9.36478E-01	2.27988E+00	1.73957E+00	1.60018E+00	9.80848E-01	1.62524E+00	**8.59418E-01**	1.10517E+00	1.26112E+00
	10	AVG	**2.45137E+01**	2.33402E+01	2.37529E+01	2.43578E+01	2.28217E+01	2.36434E+01	2.35324E+01	2.35522E+01	2.36859E+01	2.39146E+01
		STD	1.42102E+00	1.42484E+00	1.94326E+00	1.67529E+00	1.30030E+00	1.29287E+00	1.97020E+00	8.15421E-01	1.63621E+00	**7.98753E-01**
8	4	AVG	1.82235E+01	1.78419E+01	1.79818E+01	1.80481E+01	1.87741E+01	1.89561E+01	1.85867E+01	1.90974E+01	1.89659E+01	**1.97277E+01**
		STD	1.45809E+00	1.57917E+00	2.39629E+00	2.22192E+00	1.69228E+00	1.37124E+00	2.07683E+00	1.25964E+00	1.78104E+00	**9.44299E-01**
	6	AVG	2.18449E+01	**2.20175E+01**	2.07036E+01	2.02721E+01	1.99255E+01	2.02341E+01	2.00505E+01	2.13321E+01	2.10328E+01	2.08241E+01
		STD	1.31321E+00	1.13026E+00	1.32642E+00	1.90333E+00	1.53136E+00	1.97390E+00	1.84965E+00	1.14391E+00	**1.05661E+00**	1.16407E+00
	8	AVG	**2.32767E+01**	2.24970E+01	2.26560E+01	2.22779E+01	2.17450E+01	2.22513E+01	2.18777E+01	2.25292E+01	2.27381E+01	2.26987E+01
		STD	1.14836E+00	1.29795E+00	1.54364E+00	2.01124E+00	1.45466E+00	1.04886E+00	1.16272E+00	**5.78891E-01**	1.16421E+00	9.15403E-01
	10	AVG	2.42128E+01	2.33626E+01	2.39758E+01	**2.47111E+01**	2.31037E+01	2.37011E+01	2.32892E+01	2.40416E+01	2.42379E+01	2.42783E+01
		STD	1.19745E+00	9.45431E-01	1.80191E+00	9.46906E-01	1.63707E+00	1.01270E+00	2.10322E+00	**7.18268E-01**	8.92147E-01	9.09419E-01
9	4	AVG	1.86040E+01	1.86763E+01	1.89703E+01	1.87232E+01	1.86326E+01	1.84274E+01	1.86461E+01	1.90856E+01	1.91966E+01	**1.93082E+01**
		STD	8.92050E-01	**1.87054E-01**	1.31017E+00	1.02244E+00	1.21006E+00	7.22932E-01	8.90737E-01	3.39063E-01	5.55437E-01	5.09076E-01
	6	AVG	2.17537E+01	2.18681E+01	1.99858E+01	2.09579E+01	2.02654E+01	2.18965E+01	2.11701E+01	2.20380E+01	2.15689E+01	**2.20408E+01**
		STD	1.00473E+00	9.97029E-01	2.75699E+00	1.74933E+00	1.90623E+00	7.22184E-01	1.36524E+00	**4.50816E-01**	1.07125E+00	6.37709E-01
	8	AVG	**2.37026E+01**	2.34680E+01	2.24725E+01	2.28960E+01	2.20151E+01	2.29164E+01	2.29480E+01	2.36286E+01	2.33081E+01	2.33379E+01
		STD	8.42243E-01	**5.53913E-01**	1.67402E+00	1.85059E+00	1.36041E+00	2.28182E+00	1.47673E+00	6.90129E-01	1.05716E+00	1.15465E+00
	10	AVG	2.46697E+01	2.46695E+01	2.38339E+01	2.48183E+01	2.32615E+01	2.48710E+01	2.44481E+01	**2.49633E+01**	2.44051E+01	2.47587E+01
		STD	1.20773E+00	**6.62515E-01**	2.05530E+00	1.48311E+00	1.46908E+00	9.29742E-01	1.69354E+00	1.29831E+00	1.16640E+00	9.68561E-01
10	4	AVG	1.90136E+01	1.86877E+01	1.73493E+01	1.80657E+01	1.84503E+01	1.87513E+01	**1.92804E+01**	1.81481E+01	1.89463E+01	1.89419E+01
		STD	7.19417E-01	**6.08222E-01**	2.47393E+00	2.01195E+00	1.99865E+00	8.59559E-01	1.10487E+00	1.15229E+00	1.17943E+00	8.50391E-01

	6	AVG	**2.21525E+01**	2.17753E+01	2.04424E+01	1.97836E+01	2.08881E+01	2.16228E+01	2.06653E+01	2.19201E+01	2.12602E+01	2.13529E+01
		STD	1.01045E+00	**8.65923E-01**	2.37088E+00	2.42403E+00	1.46662E+00	1.41145E+00	2.16651E+00	9.02851E-01	1.24883E+00	1.43558E+00
	8	AVG	**2.43008E+01**	2.38535E+01	2.18137E+01	2.19290E+01	2.22116E+01	2.24605E+01	2.24561E+01	2.35672E+01	2.33779E+01	2.35386E+01
		STD	**6.76520E-01**	8.72756E-01	3.37401E+00	2.41538E+00	1.54093E+00	2.23869E+00	2.05096E+00	1.41794E+00	1.28975E+00	1.08897E+00
	10	AVG	**2.59562E+01**	2.51819E+01	2.34834E+01	2.39772E+01	2.35616E+01	2.39837E+01	2.36850E+01	2.49768E+01	2.47684E+01	2.46782E+01
		STD	**9.34442E-01**	1.17192E+00	2.54479E+00	2.11173E+00	1.56527E+00	2.00532E+00	2.26157E+00	1.10574E+00	1.46809E+00	1.36495E+00
11	4	AVG	**2.05605E+01**	2.04227E+01	1.84114E+01	1.83837E+01	1.81423E+01	2.01061E+01	1.97906E+01	1.99462E+01	1.95387E+01	1.96978E+01
		STD	1.54409E-01	**1.29267E-01**	1.87657E+00	2.09246E+00	1.88197E+00	7.35080E-01	1.11126E+00	9.41050E-01	1.17096E+00	1.15270E+00
	6	AVG	**2.22913E+01**	2.13504E+01	2.09217E+01	2.07241E+01	2.08372E+01	2.15549E+01	2.17894E+01	2.14145E+01	2.14934E+01	2.17422E+01
		STD	1.17424E+00	9.97055E-01	1.93504E+00	1.47051E+00	1.22830E+00	4.80301E-01	1.35642E+00	**2.24434E-01**	9.63250E-01	1.09994E+00
	8	AVG	**2.39459E+01**	2.36644E+01	2.24398E+01	2.36234E+01	2.18219E+01	2.35987E+01	2.36298E+01	2.33020E+01	2.35191E+01	2.34744E+01
		STD	**7.33190E-01**	8.20044E-01	2.32677E+00	1.57583E+00	1.59471E+00	9.66175E-01	1.24040E+00	8.52974E-01	1.20236E+00	1.43052E+00
	10	AVG	**2.53847E+01**	2.53754E+01	2.49490E+01	2.43663E+01	2.41200E+01	2.50255E+01	2.52066E+01	2.51490E+01	2.49372E+01	2.47787E+01
		STD	1.02036E+00	8.04488E-01	2.00771E+00	1.62933E+00	1.16279E+00	1.04698E+00	1.45586E+00	**7.60142E-01**	1.19249E+00	1.57277E+00
12	4	AVG	2.04026E+01	2.01891E+01	1.86627E+01	1.84615E+01	1.89768E+01	**2.04201E+01**	1.97248E+01	1.98734E+01	1.96362E+01	1.94954E+01
		STD	5.82244E-01	**2.84988E-01**	2.46150E+00	1.69845E+00	2.08208E+00	8.58364E-01	7.01365E-01	1.00707E+00	1.05909E+00	1.09447E+00
	6	AVG	**2.20913E+01**	2.19652E+01	2.18690E+01	2.08854E+01	2.07951E+01	2.16975E+01	2.15735E+01	2.11363E+01	2.16324E+01	2.14247E+01
		STD	1.03086E+00	**7.30936E-01**	2.00861E+00	2.46673E+00	1.31734E+00	1.19999E+00	1.31577E+00	9.39077E-01	1.24381E+00	8.13992E-01
	8	AVG	2.38868E+01	2.32063E+01	2.37282E+01	**2.39386E+01**	2.25868E+01	2.37628E+01	2.31097E+01	2.33188E+01	2.33383E+01	2.34767E+01
		STD	1.02484E+00	**9.95443E-01**	2.10453E+00	1.22257E+00	1.31912E+00	1.23734E+00	1.71558E+00	1.16546E+00	1.09861E+00	1.04011E+00
	10	AVG	2.50415E+01	2.44198E+01	2.43794E+01	2.48515E+01	2.42033E+01	2.48945E+01	2.49955E+01	2.48310E+01	**2.52655E+01**	2.50359E+01
		STD	1.10534E+00	**6.32333E-01**	3.18066E+00	1.99925E+00	1.40095E+00	1.35913E+00	1.46844E+00	9.88925E-01	1.33984E+00	1.24102E+00
13	4	AVG	2.05905E+01	2.06127E+01	1.94887E+01	1.95792E+01	1.91010E+01	**2.07019E+01**	2.01980E+01	2.05694E+01	2.00783E+01	2.02293E+01
		STD	4.20479E-01	5.50142E-01	1.23021E+00	1.60297E+00	1.48277E+00	**3.38930E-01**	7.08494E-01	3.46208E-01	3.80900E-01	5.20066E-01
	6	AVG	**2.23928E+01**	2.19102E+01	2.15444E+01	2.09499E+01	2.07835E+01	2.16152E+01	2.16158E+01	2.12582E+01	2.18732E+01	2.17286E+01

		STD	7.44006E-01	1.34668E+00	1.87048E+00	1.99302E+00	1.65989E+00	6.72280E-01	1.32893E+00	**4.77203E-01**	1.10670E+00	9.88198E-01
	8	AVG	2.40181E+01	2.32347E+01	2.26921E+01	2.28297E+01	2.28347E+01	2.38021E+01	2.36041E+01	2.39566E+01	2.35833E+01	**2.42744E+01**
		STD	8.52587E-01	**6.95639E-01**	2.22837E+00	1.99286E+00	1.07393E+00	9.06253E-01	1.62249E+00	8.25172E-01	9.34062E-01	8.27527E-01
	10	AVG	2.54602E+01	2.47466E+01	2.39439E+01	2.48591E+01	2.39478E+01	2.51623E+01	2.47114E+01	2.51415E+01	**2.56226E+01**	2.54440E+01
		STD	1.20019E+00	1.03738E+00	2.52854E+00	2.04126E+00	1.48485E+00	1.09904E+00	1.30301E+00	**8.33028E-01**	1.15711E+00	9.94066E-01
14	4	AVG	1.99356E+01	**2.01137E+01**	1.70635E+01	1.76184E+01	1.85163E+01	1.94654E+01	1.90062E+01	1.82273E+01	1.83651E+01	1.91957E+01
		STD	1.10085E+00	9.03634E-01	2.10080E+00	2.08914E+00	1.99631E+00	**8.96698E-01**	1.85948E+00	1.98258E+00	1.94880E+00	1.07292E+00
	6	AVG	2.16050E+01	**2.16694E+01**	1.95422E+01	2.01492E+01	1.98921E+01	2.11676E+01	2.08412E+01	2.05169E+01	2.08702E+01	2.10429E+01
		STD	1.21129E+00	**8.14507E-01**	3.13933E+00	1.87047E+00	1.56307E+00	1.23232E+00	1.42454E+00	1.39633E+00	1.30465E+00	1.28717E+00
	8	AVG	**2.36593E+01**	2.33019E+01	2.23683E+01	2.22955E+01	2.18636E+01	2.25879E+01	2.20040E+01	2.30882E+01	2.32587E+01	2.29777E+01
		STD	1.00562E+00	**7.66351E-01**	2.63242E+00	2.70018E+00	1.47703E+00	1.72940E+00	1.89948E+00	1.01221E+00	1.00039E+00	1.07409E+00
	10	AVG	2.47298E+01	2.45522E+01	2.40452E+01	2.42802E+01	2.34744E+01	2.43673E+01	2.34266E+01	2.45759E+01	2.41603E+01	**2.49561E+01**
		STD	1.25807E+00	1.09953E+00	2.56644E+00	1.48991E+00	1.11040E+00	1.65070E+00	2.31907E+00	1.23358E+00	1.26330E+00	**8.93405E-01**
15	4	AVG	**2.00834E+01**	1.89567E+01	1.76378E+01	1.77153E+01	1.82965E+01	1.99145E+01	1.94721E+01	1.95827E+01	1.88222E+01	1.94558E+01
		STD	1.58265E+00	1.98162E+00	2.08179E+00	2.17786E+00	1.28318E+00	**1.19086E+00**	1.70482E+00	1.24094E+00	1.50934E+00	1.43964E+00
	6	AVG	**2.17421E+01**	2.16564E+01	1.97958E+01	1.99495E+01	1.97300E+01	2.00867E+01	2.01778E+01	2.05065E+01	2.11271E+01	2.07640E+01
		STD	**9.18070E-01**	1.05126E+00	2.01126E+00	1.88960E+00	1.38539E+00	1.16953E+00	1.76564E+00	1.28051E+00	1.19280E+00	1.11297E+00
	8	AVG	**2.33273E+01**	2.21825E+01	2.28139E+01	2.22444E+01	2.17268E+01	2.19566E+01	2.22910E+01	2.22523E+01	2.26004E+01	2.27746E+01
		STD	8.49849E-01	9.24668E-01	1.74676E+00	1.93088E+00	9.41642E-01	1.01572E+00	1.33378E+00	7.17689E-01	1.10404E+00	**7.02510E-01**
	10	AVG	2.44879E+01	2.35050E+01	2.40938E+01	**2.44988E+01**	2.34104E+01	2.43705E+01	2.32433E+01	2.44144E+01	2.39109E+01	2.43114E+01
		STD	9.02426E-01	**6.64763E-01**	2.13997E+00	1.59073E+00	1.06766E+00	7.83260E-01	1.96375E+00	7.36137E-01	1.09793E+00	9.09256E-01
16	4	AVG	1.89424E+01	1.90308E+01	1.90246E+01	1.90036E+01	1.88030E+01	1.84262E+01	**1.92486E+01**	1.90960E+01	1.91327E+01	1.90045E+01
		STD	4.90940E-01	6.10721E-01	5.75332E-01	8.84106E-01	9.73061E-01	4.61206E-01	6.64245E-01	**4.12869E-01**	6.58914E-01	4.61441E-01
	6	AVG	2.16208E+01	2.15429E+01	2.12364E+01	2.13741E+01	2.08541E+01	2.14114E+01	2.14773E+01	2.13651E+01	2.16719E+01	**2.17164E+01**
		STD	**2.72783E-01**	3.66357E-01	1.50817E+00	5.84375E-01	1.68763E+00	3.23254E-01	9.89728E-01	4.57642E-01	4.46951E-01	3.86858E-01

	8	AVG	**2.41679E+01**	2.33094E+01	2.36459E+01	2.35247E+01	2.22772E+01	2.32352E+01	2.31445E+01	2.34247E+01	2.34373E+01	2.36372E+01
		STD	6.17682E-01	5.59371E-01	1.33938E+00	6.61492E-01	1.23158E+00	8.69088E-01	1.50358E+00	**4.13581E-01**	7.50130E-01	6.13357E-01
	10	AVG	**2.56036E+01**	2.52178E+01	2.54387E+01	2.55171E+01	2.41268E+01	2.49223E+01	2.46689E+01	2.48661E+01	2.49568E+01	2.51075E+01
		STD	5.89463E-01	6.10466E-01	1.09800E+00	6.85113E-01	1.13460E+00	7.04718E-01	1.28946E+00	**5.41312E-01**	9.14676E-01	8.53843E-01

Table A.2 The AVG and STD comparison results of SSIM

Image	Level	Item	MGWO	GWO	HHO	WOA	SSA	CS	IGWO	CLPSO	CLSGMFO	LGCMFO
1	4	AVG	7.22754E-01	7.28014E-01	6.40556E-01	6.17548E-01	6.96218E-01	**7.35822E-01**	7.12588E-01	7.17492E-01	7.15356E-01	7.03118E-01
		STD	2.00117E-02	1.77381E-02	1.10135E-01	1.50752E-01	4.26547E-02	**1.35366E-02**	7.23892E-02	2.07083E-02	2.47955E-02	6.19779E-02
	6	AVG	**7.64751E-01**	7.40381E-01	7.28916E-01	7.24700E-01	7.05628E-01	7.32433E-01	7.30187E-01	7.28567E-01	7.27508E-01	7.33609E-01
		STD	**2.82684E-02**	4.87181E-02	8.12117E-02	5.87714E-02	5.32150E-02	5.80110E-02	5.87192E-02	3.01523E-02	3.09020E-02	3.20283E-02
	8	AVG	**7.75966E-01**	7.72667E-01	7.56344E-01	7.57131E-01	7.39725E-01	7.64108E-01	7.52094E-01	7.52890E-01	7.72824E-01	7.59532E-01
		STD	5.82989E-02	**3.22854E-02**	8.19300E-02	6.35735E-02	7.49839E-02	4.77408E-02	5.47286E-02	4.95945E-02	4.15091E-02	5.30229E-02
	10	AVG	8.02380E-01	8.05032E-01	8.00896E-01	7.91781E-01	7.79727E-01	8.00491E-01	8.07211E-01	**8.08592E-01**	8.07086E-01	8.06306E-01
		STD	3.53157E-02	3.32547E-02	8.07677E-02	7.73009E-02	5.54490E-02	4.71795E-02	5.95148E-02	**3.29779E-02**	4.59894E-02	4.49212E-02
2	4	AVG	6.40146E-01	6.38429E-01	5.34571E-01	5.62501E-01	6.10680E-01	**6.42616E-01**	6.28346E-01	6.17372E-01	6.08956E-01	6.19133E-01
		STD	3.23137E-02	5.45801E-02	1.62522E-01	1.03069E-01	3.62086E-02	4.72738E-02	4.02541E-02	2.90380E-02	3.66146E-02	**2.20045E-02**
	6	AVG	6.87865E-01	6.87334E-01	6.62029E-01	6.70557E-01	6.71077E-01	6.95418E-01	6.82470E-01	**6.96576E-01**	6.92308E-01	6.82052E-01
		STD	2.64422E-02	**2.04144E-02**	7.05022E-02	5.94589E-02	3.31387E-02	2.91596E-02	3.69783E-02	2.42721E-02	2.61899E-02	3.09649E-02
	8	AVG	7.36145E-01	7.32836E-01	7.45450E-01	7.40019E-01	7.25360E-01	7.38238E-01	7.35847E-01	7.33668E-01	7.41796E-01	**7.48468E-01**
		STD	3.45416E-02	**1.85422E-02**	4.48182E-02	3.99124E-02	2.72051E-02	2.54576E-02	4.95541E-02	2.08255E-02	2.67688E-02	2.23538E-02
	10	AVG	7.81355E-01	7.72126E-01	7.78424E-01	**8.04853E-01**	7.75647E-01	7.89200E-01	7.97269E-01	7.96070E-01	7.86422E-01	7.88753E-01
		STD	3.06448E-02	**2.49351E-02**	7.04408E-02	2.97708E-02	3.27754E-02	3.29669E-02	3.83247E-02	2.78470E-02	3.34277E-02	3.81494E-02
3	4	AVG	**6.67176E-01**	6.55704E-01	5.77356E-01	5.51178E-01	5.94138E-01	6.48472E-01	6.31299E-01	6.26859E-01	6.02561E-01	6.02621E-01
		STD	**3.60479E-02**	4.12276E-02	9.60869E-02	7.98635E-02	6.28209E-02	4.84458E-02	4.62027E-02	4.62150E-02	6.34923E-02	5.69490E-02
	6	AVG	7.19256E-01	7.03555E-01	6.85482E-01	7.06268E-01	6.99727E-01	7.11679E-01	**7.07589E-01**	7.19424E-01	6.95700E-01	7.05283E-01

		STD	2.83950E-02	4.33779E-02	5.52180E-02	5.33175E-02	3.57227E-02	1.75102E-02	**3.36725E-02**	1.55755E-02	3.89476E-02	3.27967E-02
	8	AVG	7.67927E-01	7.61908E-01	7.67057E-01	7.65523E-01	7.47750E-01	7.67258E-01	7.62650E-01	7.76596E-01	7.68152E-01	**7.77373E-01**
		STD	2.43892E-02	**1.90032E-02**	4.95343E-02	4.48334E-02	3.40316E-02	2.55694E-02	3.37123E-02	1.90374E-02	2.93627E-02	3.64886E-02
	10	AVG	**8.21774E-01**	8.01061E-01	8.00220E-01	8.10460E-01	7.95993E-01	8.10401E-01	8.05904E-01	8.06706E-01	8.18015E-01	8.14420E-01
		STD	2.28749E-02	2.36904E-02	6.98680E-02	4.69643E-02	3.01692E-02	2.94000E-02	3.90115E-02	**2.10515E-02**	2.83572E-02	3.09748E-02
4	4	AVG	**6.08282E-01**	6.03907E-01	5.51926E-01	5.28840E-01	5.85381E-01	5.92847E-01	6.00085E-01	5.83301E-01	6.04795E-01	5.86647E-01
		STD	3.70852E-02	3.48836E-02	8.64859E-02	1.04984E-01	3.96486E-02	2.49146E-02	4.33512E-02	**1.68173E-02**	2.60968E-02	2.39228E-02
	6	AVG	**6.92162E-01**	6.76985E-01	6.64378E-01	6.69895E-01	6.58302E-01	6.69264E-01	6.84042E-01	6.75590E-01	6.73571E-01	6.81048E-01
		STD	1.93076E-02	1.23704E-02	7.82549E-02	2.99116E-02	4.61863E-02	3.56192E-02	3.10041E-02	**1.10868E-02**	2.12335E-02	2.16571E-02
	8	AVG	**7.45522E-01**	7.25943E-01	7.37432E-01	7.28727E-01	6.99388E-01	7.20108E-01	7.40825E-01	7.35471E-01	7.37022E-01	7.42069E-01
		STD	2.37734E-02	**1.99648E-02**	5.54626E-02	6.34890E-02	3.98992E-02	3.63236E-02	4.96262E-02	2.17083E-02	2.39734E-02	2.69762E-02
	10	AVG	**8.05392E-01**	7.77813E-01	7.96549E-01	7.89239E-01	7.68089E-01	7.89128E-01	7.79792E-01	7.94338E-01	7.92459E-01	7.93543E-01
		STD	2.78393E-02	2.49603E-02	5.84194E-02	3.98166E-02	3.70055E-02	3.38474E-02	5.33341E-02	**2.00821E-02**	2.93366E-02	2.71122E-02
5	4	AVG	6.37374E-01	6.35242E-01	5.68551E-01	5.84005E-01	6.05787E-01	**6.52992E-01**	6.24336E-01	5.88860E-01	6.29413E-01	6.24596E-01
		STD	5.03317E-02	**4.05658E-02**	1.09330E-01	9.09226E-02	8.99662E-02	5.59655E-02	7.18523E-02	7.28655E-02	5.98243E-02	4.11993E-02
	6	AVG	6.91631E-01	6.97790E-01	7.00928E-01	7.11004E-01	6.55805E-01	7.00925E-01	7.06970E-01	6.40517E-01	**7.31110E-01**	7.30672E-01
		STD	**4.61619E-02**	5.90066E-02	1.06747E-01	6.76691E-02	9.42106E-02	6.28737E-02	6.68605E-02	8.88153E-02	5.09876E-02	7.07153E-02
	8	AVG	7.80644E-01	7.68091E-01	7.85586E-01	7.86568E-01	7.42833E-01	7.70518E-01	7.37057E-01	7.55152E-01	7.89186E-01	**8.01753E-01**
		STD	5.17062E-02	**3.05270E-02**	6.84649E-02	6.78381E-02	6.51008E-02	5.14245E-02	6.37462E-02	3.77362E-02	3.90996E-02	3.87083E-02
	10	AVG	8.24726E-01	8.03526E-01	8.22459E-01	**8.45818E-01**	7.78774E-01	7.96676E-01	7.96425E-01	8.18423E-01	8.22660E-01	8.18225E-01
		STD	3.65308E-02	3.19692E-02	6.96529E-02	4.48310E-02	5.93039E-02	6.73914E-02	6.14434E-02	**2.60647E-02**	3.17599E-02	3.67699E-02
6	4	AVG	**6.66779E-01**	6.34622E-01	5.88529E-01	6.22268E-01	6.11655E-01	6.56505E-01	6.27738E-01	6.42071E-01	6.30764E-01	6.32747E-01
		STD	4.60927E-02	2.99713E-02	1.04875E-01	7.98385E-02	5.32780E-02	**2.83122E-02**	5.56329E-02	3.30057E-02	5.46578E-02	4.29004E-02
	6	AVG	6.90864E-01	6.90247E-01	**7.14761E-01**	7.01857E-01	6.87465E-01	6.72387E-01	7.04167E-01	6.92398E-01	7.07811E-01	6.88802E-01
		STD	3.92702E-02	3.71381E-02	5.80217E-02	5.75749E-02	5.38749E-02	**3.47668E-02**	4.12613E-02	4.60753E-02	4.20204E-02	4.32193E-02
	8	AVG	7.69449E-01	7.55756E-01	7.71066E-01	7.57490E-01	7.51552E-01	7.63568E-01	7.70791E-01	**7.74429E-01**	7.66327E-01	7.60174E-01

		STD	2.62300E-02	**2.25819E-02**	5.79846E-02	5.41247E-02	4.82641E-02	3.83761E-02	3.41146E-02	2.82163E-02	2.91530E-02	3.92169E-02
	10	AVG	8.20006E-01	7.97931E-01	8.04452E-01	8.12933E-01	7.89574E-01	8.14604E-01	8.06002E-01	**8.25854E-01**	8.12822E-01	8.11624E-01
		STD	2.39794E-02	2.16062E-02	6.07145E-02	3.85375E-02	4.18867E-02	3.32987E-02	5.61532E-02	**1.73134E-02**	3.75097E-02	3.25717E-02
7	4	AVG	**6.16241E-01**	6.08276E-01	5.64969E-01	5.69915E-01	5.79205E-01	6.10120E-01	6.09920E-01	6.15869E-01	6.00025E-01	6.03074E-01
		STD	3.23743E-02	3.02188E-02	8.88074E-02	3.68535E-02	3.82421E-02	2.68622E-02	4.15613E-02	3.78781E-02	3.37278E-02	**2.55540E-02**
	6	AVG	**6.74083E-01**	6.72794E-01	6.65454E-01	6.46974E-01	6.31160E-01	6.69530E-01	6.45578E-01	6.51444E-01	6.56830E-01	6.59409E-01
		STD	**3.11267E-02**	4.54291E-02	5.63982E-02	6.10327E-02	4.11015E-02	4.95287E-02	5.30151E-02	3.73286E-02	3.61352E-02	4.50354E-02
	8	AVG	7.25213E-01	6.93895E-01	7.11702E-01	**7.30010E-01**	7.01172E-01	7.15011E-01	7.22096E-01	7.15172E-01	7.23687E-01	7.21949E-01
		STD	4.55980E-02	**2.94845E-02**	6.66211E-02	5.48169E-02	4.73646E-02	3.80981E-02	5.04045E-02	3.52327E-02	3.44833E-02	4.12398E-02
	10	AVG	**7.83461E-01**	7.49564E-01	7.67027E-01	7.81861E-01	7.36867E-01	7.57585E-01	7.53145E-01	7.54096E-01	7.57850E-01	7.64862E-01
		STD	4.07970E-02	4.08098E-02	4.96720E-02	4.68751E-02	3.64918E-02	3.71117E-02	5.84618E-02	**2.38496E-02**	4.67148E-02	2.49440E-02
8	4	AVG	6.20800E-01	6.07890E-01	5.92792E-01	6.00047E-01	6.28192E-01	6.36984E-01	6.25061E-01	6.35756E-01	6.28561E-01	**6.52304E-01**
		STD	4.33220E-02	4.38277E-02	8.63144E-02	7.69137E-02	4.37711E-02	3.19674E-02	6.64861E-02	2.67346E-02	5.57445E-02	**2.55125E-02**
	6	AVG	7.19522E-01	**7.23786E-01**	6.85805E-01	6.73132E-01	6.60880E-01	6.69322E-01	6.63310E-01	7.01660E-01	6.91911E-01	6.86052E-01
		STD	3.69581E-02	3.63092E-02	4.04547E-02	4.96336E-02	4.47180E-02	5.75706E-02	5.47976E-02	3.43358E-02	**3.22467E-02**	3.74762E-02
	8	AVG	**7.62379E-01**	7.35898E-01	7.47668E-01	7.37292E-01	7.17760E-01	7.34195E-01	7.21840E-01	7.41761E-01	7.43445E-01	7.45423E-01
		STD	3.37199E-02	4.06857E-02	4.25852E-02	5.65382E-02	4.35941E-02	3.08179E-02	3.16599E-02	**1.68812E-02**	3.60073E-02	2.86086E-02
	10	AVG	7.87380E-01	7.67819E-01	7.83567E-01	**8.03924E-01**	7.57510E-01	7.73583E-01	7.64340E-01	7.81281E-01	7.87466E-01	7.89445E-01
		STD	3.49670E-02	2.36400E-02	4.56069E-02	**1.99432E-02**	4.46785E-02	2.72288E-02	5.15204E-02	2.07921E-02	2.54384E-02	2.72655E-02
9	4	AVG	**7.23034E-01**	7.08781E-01	7.05494E-01	6.81252E-01	6.86587E-01	7.11553E-01	7.20895E-01	6.89751E-01	6.99859E-01	7.12999E-01
		STD	2.34023E-02	**1.30225E-02**	6.62335E-02	6.23160E-02	6.50777E-02	3.12238E-02	3.15671E-02	1.83760E-02	3.40687E-02	3.39406E-02
	6	AVG	**7.98099E-01**	7.76532E-01	7.20158E-01	7.52465E-01	7.21293E-01	7.76294E-01	7.64770E-01	7.82633E-01	7.73459E-01	7.79742E-01
		STD	3.07137E-02	2.81660E-02	1.01876E-01	5.88451E-02	7.63734E-02	2.85819E-02	6.48092E-02	**1.64591E-02**	3.12542E-02	1.81308E-02
	8	AVG	**8.38567E-01**	8.26183E-01	8.04312E-01	8.27771E-01	7.91389E-01	8.11476E-01	8.18712E-01	8.33861E-01	8.26699E-01	8.22978E-01
		STD	2.06935E-02	**1.68179E-02**	6.94115E-02	3.44006E-02	5.50133E-02	8.03999E-02	4.81907E-02	2.46847E-02	2.86720E-02	3.39208E-02
	10	AVG	**8.70800E-01**	8.56715E-01	8.46440E-01	8.70267E-01	8.20869E-01	8.68939E-01	8.57001E-01	8.69870E-01	8.55431E-01	8.64042E-01

		STD	3.29043E-02	2.04622E-02	6.00298E-02	3.58192E-02	3.77154E-02	2.83124E-02	3.71382E-02	2.81750E-02	3.32530E-02	**1.96506E-02**
10	4	AVG	6.38141E-01	6.32099E-01	5.38144E-01	5.78312E-01	5.89439E-01	6.27014E-01	**6.43542E-01**	6.01586E-01	6.15931E-01	6.19049E-01
		STD	**2.91013E-02**	3.16484E-02	1.19717E-01	9.99042E-02	9.61930E-02	3.71529E-02	4.86106E-02	4.92690E-02	4.36167E-02	3.21340E-02
	6	AVG	**7.21206E-01**	7.15783E-01	6.69739E-01	6.46485E-01	6.84089E-01	7.02421E-01	6.77817E-01	7.12425E-01	6.91133E-01	6.98733E-01
		STD	3.67498E-02	3.91473E-02	9.28870E-02	9.43250E-02	4.81714E-02	4.45532E-02	8.11560E-02	**3.38260E-02**	4.97231E-02	4.90314E-02
	8	AVG	**7.85181E-01**	7.75564E-01	7.03957E-01	7.20482E-01	7.31009E-01	7.30856E-01	7.35131E-01	7.66972E-01	7.58680E-01	7.67516E-01
		STD	**2.20537E-02**	2.84746E-02	1.37960E-01	7.27304E-02	4.54455E-02	7.41778E-02	6.50623E-02	4.67757E-02	4.23838E-02	3.52860E-02
	10	AVG	**8.36592E-01**	8.13415E-01	7.67339E-01	7.79806E-01	7.70782E-01	7.77748E-01	7.71533E-01	8.08926E-01	8.01434E-01	7.98312E-01
		STD	**2.48997E-02**	3.15664E-02	7.63937E-02	5.75172E-02	4.39442E-02	5.51747E-02	6.34932E-02	3.27555E-02	4.14515E-02	3.77020E-02
11	4	AVG	**7.04443E-01**	6.99285E-01	6.35389E-01	6.39059E-01	6.32827E-01	6.89597E-01	6.84811E-01	6.82469E-01	6.72232E-01	6.78077E-01
		STD	7.59153E-03	**5.28029E-03**	7.47175E-02	6.91519E-02	5.56527E-02	2.76581E-02	3.54250E-02	2.93122E-02	3.97208E-02	3.89110E-02
	6	AVG	**7.58073E-01**	7.26486E-01	7.17412E-01	7.15727E-01	7.17456E-01	7.33998E-01	7.42847E-01	7.25543E-01	7.34672E-01	7.37129E-01
		STD	3.55948E-02	2.98082E-02	5.82182E-02	5.07112E-02	3.83669E-02	2.20750E-02	4.10948E-02	**7.93752E-03**	2.87438E-02	3.42031E-02
	8	AVG	**8.03074E-01**	7.93498E-01	7.65066E-01	7.97404E-01	7.49792E-01	7.95613E-01	7.94585E-01	7.83890E-01	7.90056E-01	7.89259E-01
		STD	**2.03000E-02**	2.33832E-02	5.99980E-02	4.10612E-02	4.49835E-02	2.78209E-02	3.26452E-02	2.48004E-02	3.10657E-02	3.70582E-02
	10	AVG	**8.40367E-01**	8.36614E-01	8.27490E-01	8.13323E-01	8.07879E-01	8.29869E-01	8.34723E-01	8.29600E-01	8.26428E-01	8.20231E-01
		STD	1.92294E-02	2.01650E-02	4.85910E-02	4.15171E-02	3.37577E-02	2.61614E-02	3.42559E-02	**1.88043E-02**	2.93287E-02	4.08943E-02
12	4	AVG	**7.15228E-01**	7.03300E-01	6.13259E-01	6.16366E-01	6.31630E-01	6.96545E-01	6.72726E-01	6.71443E-01	6.50930E-01	6.45395E-01
		STD	2.97725E-02	**2.94765E-02**	1.03546E-01	7.03860E-02	6.94180E-02	4.19265E-02	3.51826E-02	4.80729E-02	4.00301E-02	4.94613E-02
	6	AVG	**7.28103E-01**	7.21886E-01	7.19246E-01	6.86989E-01	6.89170E-01	7.22202E-01	7.13727E-01	7.12637E-01	7.05399E-01	7.02478E-01
		STD	3.05404E-02	3.45806E-02	6.02168E-02	7.15151E-02	4.23626E-02	3.62459E-02	3.87897E-02	2.79316E-02	3.79185E-02	**2.31124E-02**
	8	AVG	7.72745E-01	7.54479E-01	7.66672E-01	**7.76032E-01**	7.37711E-01	7.73262E-01	7.58636E-01	7.62871E-01	7.50263E-01	7.61050E-01
		STD	3.21585E-02	3.13175E-02	6.22360E-02	3.39506E-02	4.00679E-02	3.80843E-02	5.62114E-02	3.68270E-02	3.91978E-02	**2.75630E-02**
	10	AVG	8.06329E-01	7.83591E-01	7.81885E-01	8.04995E-01	7.87160E-01	8.04749E-01	8.05788E-01	7.96085E-01	**8.09756E-01**	8.00317E-01
		STD	2.56791E-02	**2.37339E-02**	9.35700E-02	4.82748E-02	3.77622E-02	3.51438E-02	3.80779E-02	2.86746E-02	3.39493E-02	3.36288E-02

13	4	AVG	7.24861E-01	7.21377E-01	7.21930E-01	7.05913E-01	6.92378E-01	7.23866E-01	7.23073E-01	**7.27830E-01**	7.23881E-01	7.22271E-01
		STD	**1.12962E-02**	1.63298E-02	4.78009E-02	5.43388E-02	5.12798E-02	1.38117E-02	3.02998E-02	1.20174E-02	1.83602E-02	2.19227E-02
	6	AVG	7.71449E-01	7.61443E-01	**7.71606E-01**	7.46941E-01	7.40483E-01	7.56731E-01	7.54788E-01	7.49631E-01	7.62429E-01	7.53907E-01
		STD	2.85338E-02	2.55317E-02	3.95478E-02	4.41567E-02	3.84903E-02	1.66466E-02	4.81645E-02	**1.14999E-02**	2.40991E-02	2.21607E-02
	8	AVG	**8.12973E-01**	7.93365E-01	7.90802E-01	7.81152E-01	7.88946E-01	8.01537E-01	7.97072E-01	8.05045E-01	8.03696E-01	8.12472E-01
		STD	2.14571E-02	1.95382E-02	6.88951E-02	5.59517E-02	2.58816E-02	1.88765E-02	4.04634E-02	**1.56985E-02**	2.26927E-02	2.31707E-02
	10	AVG	8.38251E-01	8.18180E-01	8.09995E-01	8.33165E-01	8.12013E-01	8.40469E-01	8.27016E-01	8.28469E-01	**8.42293E-01**	8.39917E-01
		STD	2.12102E-02	**1.82449E-02**	6.71102E-02	3.89279E-02	3.16817E-02	1.92664E-02	3.08750E-02	1.91249E-02	2.70222E-02	2.09127E-02
14	4	AVG	6.34337E-01	**6.35238E-01**	5.37663E-01	5.52340E-01	5.88110E-01	6.18435E-01	5.96970E-01	5.78549E-01	5.84164E-01	6.10836E-01
		STD	3.70154E-02	3.20264E-02	8.23084E-02	7.84000E-02	6.82925E-02	**2.34426E-02**	6.73427E-02	7.26279E-02	7.01611E-02	3.31244E-02
	6	AVG	**6.91891E-01**	6.90668E-01	6.30986E-01	6.52187E-01	6.42136E-01	6.83353E-01	6.71082E-01	6.65713E-01	6.75632E-01	6.80446E-01
		STD	4.04268E-02	**3.24465E-02**	1.14446E-01	5.68409E-02	4.95726E-02	4.42016E-02	4.40330E-02	4.08792E-02	3.78164E-02	3.90842E-02
	8	AVG	**7.61331E-01**	7.51062E-01	7.29085E-01	7.25391E-01	7.06509E-01	7.28817E-01	7.15132E-01	7.43164E-01	7.47511E-01	7.38564E-01
		STD	3.23629E-02	**2.29482E-02**	7.78695E-02	7.82835E-02	4.63803E-02	5.45394E-02	5.58496E-02	3.60501E-02	3.56254E-02	3.40850E-02
	10	AVG	7.95998E-01	7.88968E-01	7.78313E-01	7.85988E-01	7.55440E-01	7.83334E-01	7.66629E-01	7.91511E-01	7.78507E-01	**8.01597E-01**
		STD	3.92939E-02	3.35832E-02	7.77028E-02	4.03150E-02	3.81090E-02	4.71503E-02	5.50605E-02	3.52921E-02	3.61836E-02	**2.62529E-02**
15	4	AVG	**6.36360E-01**	6.02544E-01	5.34587E-01	5.44697E-01	5.65985E-01	6.29996E-01	6.07923E-01	6.04568E-01	5.74359E-01	6.00080E-01
		STD	4.55349E-02	5.32134E-02	8.78915E-02	7.87191E-02	3.70454E-02	**3.60118E-02**	5.34394E-02	3.91106E-02	5.52377E-02	4.98540E-02
	6	AVG	**6.86167E-01**	6.82304E-01	6.26511E-01	6.27464E-01	6.17675E-01	6.38190E-01	6.38134E-01	6.42205E-01	6.59411E-01	6.49526E-01
		STD	3.97653E-02	**3.89445E-02**	7.68222E-02	6.19415E-02	4.53047E-02	3.93184E-02	5.50710E-02	5.10128E-02	4.58495E-02	4.15164E-02
	8	AVG	**7.45139E-01**	7.04744E-01	7.37601E-01	7.17530E-01	6.95770E-01	7.06529E-01	7.13119E-01	7.16507E-01	7.19807E-01	7.29167E-01
		STD	2.91676E-02	3.33557E-02	5.52354E-02	5.62263E-02	2.80122E-02	3.57220E-02	4.92552E-02	**2.38836E-02**	3.82647E-02	2.47833E-02
	10	AVG	**7.87880E-01**	7.54362E-01	7.73589E-01	7.87759E-01	7.49161E-01	7.82915E-01	7.49752E-01	7.82977E-01	7.63991E-01	7.78722E-01
		STD	2.78134E-02	2.49951E-02	6.21233E-02	4.38821E-02	3.86839E-02	**2.21020E-02**	5.79820E-02	2.23019E-02	4.12357E-02	2.85286E-02
16	4	AVG	6.51953E-01	6.56720E-01	6.56195E-01	6.55192E-01	6.44224E-01	6.29636E-01	**6.65927E-01**	6.60283E-01	6.61437E-01	6.55668E-01

		STD	2.34119E-02	2.87226E-02	2.61553E-02	4.07179E-02	4.53812E-02	2.04302E-02	2.85412E-02	**1.86636E-02**	3.03406E-02	2.23488E-02
	6	AVG	7.64759E-01	7.62502E-01	7.46144E-01	7.54511E-01	7.32394E-01	7.54716E-01	7.58573E-01	7.55007E-01	7.65337E-01	**7.67956E-01**
		STD	**1.02264E-02**	1.27613E-02	6.12651E-02	2.27908E-02	6.98065E-02	1.23753E-02	3.64829E-02	1.66384E-02	1.80152E-02	1.44411E-02
	8	AVG	**8.45693E-01**	8.21918E-01	8.26956E-01	8.25834E-01	7.85810E-01	8.16308E-01	8.11935E-01	8.22555E-01	8.23686E-01	8.29901E-01
		STD	1.53076E-02	1.81733E-02	4.44089E-02	2.02838E-02	4.10387E-02	2.75759E-02	5.02462E-02	**1.36813E-02**	2.29453E-02	1.88379E-02
	10	AVG	**8.81568E-01**	8.70692E-01	8.72314E-01	8.77246E-01	8.41482E-01	8.61638E-01	8.52846E-01	8.62041E-01	8.63832E-01	8.66716E-01
		STD	**1.22331E-02**	1.52555E-02	3.14448E-02	1.71810E-02	3.08755E-02	1.67826E-02	3.67540E-02	1.22938E-02	2.27592E-02	2.27730E-02

Table A.3 The AVG and STD comparison results of FSIM

Image	Level	Item	MGWO	GWO	HHO	WOA	SSA	CS	IGWO	CLPSO	CLSGMFO	LGCMFO
1	4	AVG	7.42262E-01	7.44669E-01	6.88959E-01	6.87987E-01	7.25708E-01	**7.55771E-01**	7.39063E-01	7.40487E-01	7.44114E-01	7.30716E-01
		STD	1.86652E-02	1.75398E-02	6.46795E-02	7.68435E-02	3.61907E-02	**1.13916E-02**	4.85919E-02	1.79488E-02	1.76647E-02	5.47709E-02
	6	AVG	**7.86750E-01**	7.67404E-01	7.74445E-01	7.63601E-01	7.47214E-01	7.68575E-01	7.63617E-01	7.65959E-01	7.67582E-01	7.70479E-01
		STD	2.20434E-02	3.42375E-02	5.47301E-02	5.52734E-02	4.20420E-02	4.87932E-02	4.38969E-02	**1.76477E-02**	2.73635E-02	2.41462E-02
	8	AVG	8.12236E-01	8.08048E-01	7.95505E-01	8.06395E-01	7.95849E-01	8.11114E-01	8.03443E-01	8.00371E-01	**8.21432E-01**	8.10446E-01
		STD	4.97104E-02	**2.82296E-02**	6.78987E-02	4.84688E-02	5.13149E-02	4.25593E-02	4.21554E-02	4.10788E-02	4.05079E-02	4.90429E-02
	10	AVG	8.42171E-01	8.40082E-01	8.42344E-01	8.41325E-01	8.22229E-01	8.46969E-01	8.45545E-01	**8.58234E-01**	8.56445E-01	8.53396E-01
		STD	3.10713E-02	3.15410E-02	7.06856E-02	5.20549E-02	4.62434E-02	4.03225E-02	4.70472E-02	**2.51753E-02**	3.66517E-02	3.83602E-02
2	4	AVG	**7.05111E-01**	6.90556E-01	6.44304E-01	6.57965E-01	6.78333E-01	7.00415E-01	6.95110E-01	6.88894E-01	6.87098E-01	6.97664E-01
		STD	1.98951E-02	2.94455E-02	6.62242E-02	4.60971E-02	3.11401E-02	2.70589E-02	2.62069E-02	**1.36305E-02**	3.06113E-02	1.81943E-02
	6	AVG	7.59323E-01	7.64889E-01	7.35297E-01	7.52265E-01	7.39242E-01	**7.71915E-01**	7.58797E-01	7.71240E-01	7.68073E-01	7.56548E-01
		STD	2.98581E-02	**2.22162E-02**	6.19286E-02	4.13135E-02	3.04852E-02	3.03712E-02	3.50191E-02	2.42376E-02	2.73212E-02	2.80485E-02
	8	AVG	8.05450E-01	8.05376E-01	8.13104E-01	8.13646E-01	7.93739E-01	8.11910E-01	8.02986E-01	8.04538E-01	8.15208E-01	**8.21693E-01**
		STD	3.33660E-02	**1.68921E-02**	4.01763E-02	3.20471E-02	2.75000E-02	2.64875E-02	4.69754E-02	2.12874E-02	2.36397E-02	2.19119E-02
	10	AVG	8.49092E-01	8.41716E-01	8.43815E-01	**8.72443E-01**	8.41327E-01	8.57053E-01	8.59588E-01	8.64060E-01	8.55533E-01	8.58161E-01

		STD	2.84320E-02	**2.30028E-02**	6.19284E-02	2.42430E-02	2.67317E-02	2.96192E-02	3.35346E-02	2.35321E-02	2.86665E-02	3.23150E-02
3	4	AVG	**7.74458E-01**	7.60653E-01	6.95796E-01	6.80884E-01	6.94481E-01	7.48207E-01	7.27345E-01	7.15029E-01	7.07165E-01	7.04973E-01
		STD	**3.88603E-02**	5.35517E-02	7.00641E-02	6.29216E-02	6.31104E-02	6.04169E-02	5.74923E-02	6.10030E-02	5.49356E-02	5.32615E-02
	6	AVG	**8.12414E-01**	8.01411E-01	7.95453E-01	8.08984E-01	7.93382E-01	8.03117E-01	8.01212E-01	8.10626E-01	7.97811E-01	8.04777E-01
		STD	2.64258E-02	3.77928E-02	4.11486E-02	4.26402E-02	3.03191E-02	**1.14096E-02**	3.00940E-02	1.79611E-02	3.12507E-02	2.98317E-02
	8	AVG	8.57862E-01	8.54602E-01	8.55094E-01	8.60379E-01	8.39010E-01	8.62989E-01	8.54932E-01	**8.71517E-01**	8.64660E-01	8.70983E-01
		STD	2.20024E-02	1.71040E-02	4.29246E-02	3.48447E-02	3.42730E-02	2.00526E-02	2.81408E-02	**1.55599E-02**	2.35212E-02	2.97234E-02
	10	AVG	**9.04011E-01**	8.88767E-01	8.75999E-01	8.94403E-01	8.83973E-01	8.95854E-01	8.86877E-01	8.95733E-01	9.03216E-01	9.00348E-01
		STD	1.77254E-02	1.84497E-02	5.08332E-02	3.93316E-02	2.67304E-02	2.10909E-02	3.27769E-02	**1.46842E-02**	2.24910E-02	2.48808E-02
4	4	AVG	6.90763E-01	6.93962E-01	6.50047E-01	6.47175E-01	6.76248E-01	6.86965E-01	**6.96084E-01**	6.75185E-01	6.94451E-01	6.88739E-01
		STD	1.92545E-02	2.16984E-02	4.99518E-02	5.34978E-02	3.16525E-02	2.02665E-02	2.36341E-02	**1.37018E-02**	1.44336E-02	1.57402E-02
	6	AVG	**7.66151E-01**	7.53672E-01	7.41386E-01	7.47383E-01	7.35433E-01	7.47585E-01	7.59796E-01	7.52546E-01	7.52016E-01	7.59489E-01
		STD	1.39900E-02	1.14732E-02	4.54797E-02	2.45453E-02	3.84182E-02	2.50865E-02	2.48896E-02	**1.03798E-02**	1.78679E-02	2.02345E-02
	8	AVG	**8.09193E-01**	7.94734E-01	7.93180E-01	8.00862E-01	7.63734E-01	7.91142E-01	8.03790E-01	8.02091E-01	8.03304E-01	8.09042E-01
		STD	2.10183E-02	**1.83052E-02**	3.87424E-02	3.73583E-02	2.98438E-02	2.53959E-02	4.08494E-02	1.92872E-02	2.06432E-02	2.40588E-02
	10	AVG	**8.55586E-01**	8.35848E-01	8.52356E-01	8.47903E-01	8.24817E-01	8.49921E-01	8.40126E-01	8.52673E-01	8.51502E-01	8.51853E-01
		STD	2.05859E-02	1.95029E-02	4.02337E-02	2.41174E-02	2.81269E-02	2.60101E-02	3.51079E-02	**1.48027E-02**	2.46008E-02	2.09207E-02
5	4	AVG	7.33317E-01	7.22874E-01	6.83276E-01	6.91249E-01	7.15288E-01	**7.43070E-01**	7.18165E-01	6.95745E-01	7.32808E-01	7.25490E-01
		STD	5.28859E-02	4.57898E-02	8.39906E-02	6.69462E-02	6.27805E-02	5.41613E-02	6.11746E-02	6.17690E-02	5.22439E-02	**3.91841E-02**
	6	AVG	7.88650E-01	7.84489E-01	7.90306E-01	7.91429E-01	7.47076E-01	7.84052E-01	7.90212E-01	7.40261E-01	8.08082E-01	**8.13845E-01**
		STD	**3.92756E-02**	5.08392E-02	7.28987E-02	5.30187E-02	6.98011E-02	5.24575E-02	5.25158E-02	6.42047E-02	4.11076E-02	5.64539E-02
	8	AVG	8.55773E-01	8.45612E-01	8.53626E-01	8.60562E-01	8.21505E-01	8.44765E-01	8.17958E-01	8.32462E-01	8.68496E-01	**8.76754E-01**
		STD	4.34516E-02	**2.67958E-02**	5.94451E-02	5.11652E-02	5.34587E-02	4.21002E-02	5.47307E-02	2.95321E-02	3.12571E-02	3.19100E-02
	10	AVG	8.94774E-01	8.79788E-01	8.85665E-01	**9.04563E-01**	8.50109E-01	8.67636E-01	8.68319E-01	8.93841E-01	8.93891E-01	8.92388E-01
		STD	2.93897E-02	2.83277E-02	5.94755E-02	3.77586E-02	4.99569E-02	5.94286E-02	4.43632E-02	**2.19590E-02**	2.64340E-02	2.66145E-02
6	4	AVG	**7.27879E-01**	6.94065E-01	6.74322E-01	6.94154E-01	6.79757E-01	7.26647E-01	6.88295E-01	7.07533E-01	6.90343E-01	6.90226E-01

		STD	4.67994E-02	4.41469E-02	6.10399E-02	5.51931E-02	4.43792E-02	**2.61237E-02**	5.76140E-02	3.36665E-02	5.30029E-02	4.91235E-02
	6	AVG	7.56838E-01	7.53431E-01	**7.83459E-01**	7.70584E-01	7.60154E-01	7.43491E-01	7.67175E-01	7.67087E-01	7.74079E-01	7.60221E-01
		STD	3.12951E-02	2.85080E-02	4.45144E-02	4.55529E-02	3.95020E-02	**2.82038E-02**	3.46831E-02	3.25951E-02	3.51969E-02	3.10601E-02
	8	AVG	8.31062E-01	8.13617E-01	8.36309E-01	8.24705E-01	8.14962E-01	8.28049E-01	8.32517E-01	**8.39789E-01**	8.33058E-01	8.23599E-01
		STD	2.34553E-02	1.95159E-02	4.65438E-02	4.25260E-02	3.70720E-02	2.79190E-02	2.56645E-02	**1.86664E-02**	2.46894E-02	2.96627E-02
	10	AVG	8.77128E-01	8.57186E-01	8.60214E-01	8.74697E-01	8.51269E-01	8.73396E-01	8.64163E-01	**8.85284E-01**	8.73782E-01	8.74057E-01
		STD	1.73666E-02	1.58787E-02	5.51721E-02	2.85639E-02	3.34040E-02	2.74682E-02	4.44869E-02	**1.42587E-02**	2.87122E-02	2.61035E-02
7	4	AVG	6.68663E-01	6.56391E-01	6.33430E-01	6.30745E-01	6.33433E-01	6.58345E-01	6.62612E-01	**6.73466E-01**	6.59385E-01	6.67427E-01
		STD	3.70091E-02	3.48142E-02	4.42390E-02	3.63166E-02	3.18523E-02	**2.39836E-02**	4.31242E-02	3.38711E-02	3.70041E-02	3.12566E-02
	6	AVG	**7.31540E-01**	7.27776E-01	7.23686E-01	7.15571E-01	6.88164E-01	7.17629E-01	7.11749E-01	7.04417E-01	7.16366E-01	7.19824E-01
		STD	3.39968E-02	4.95942E-02	5.16821E-02	4.90962E-02	3.76814E-02	3.99546E-02	5.06414E-02	4.03340E-02	**3.37051E-02**	4.30497E-02
	8	AVG	7.83212E-01	7.56703E-01	7.68690E-01	**7.97389E-01**	7.59043E-01	7.79973E-01	7.79923E-01	7.78475E-01	7.88110E-01	7.90848E-01
		STD	4.25417E-02	2.97724E-02	6.24773E-02	4.59364E-02	4.28191E-02	3.15821E-02	4.78002E-02	**2.72182E-02**	3.42261E-02	3.49940E-02
	10	AVG	8.38298E-01	8.09689E-01	8.20551E-01	**8.43409E-01**	7.99982E-01	8.22538E-01	8.10181E-01	8.22834E-01	8.24241E-01	8.32246E-01
		STD	3.65146E-02	3.86762E-02	4.90802E-02	3.89862E-02	3.09477E-02	2.93555E-02	4.99931E-02	2.07402E-02	3.86288E-02	**2.07102E-02**
8	4	AVG	6.50816E-01	6.38466E-01	6.56789E-01	6.61362E-01	6.73025E-01	6.72910E-01	6.67048E-01	6.78231E-01	6.81130E-01	**6.97210E-01**
		STD	4.38705E-02	4.08674E-02	4.66461E-02	4.37606E-02	3.79156E-02	3.28203E-02	4.15800E-02	2.84443E-02	3.57504E-02	**2.26616E-02**
	6	AVG	7.56792E-01	**7.59559E-01**	7.30153E-01	7.23491E-01	7.06194E-01	7.18673E-01	7.24364E-01	7.45978E-01	7.38345E-01	7.32320E-01
		STD	3.70076E-02	3.39074E-02	3.81534E-02	3.57594E-02	4.35491E-02	4.28611E-02	3.98255E-02	2.99695E-02	**2.97366E-02**	3.89707E-02
	8	AVG	**7.98068E-01**	7.79406E-01	7.91108E-01	7.85331E-01	7.58886E-01	7.81328E-01	7.69274E-01	7.83826E-01	7.88242E-01	7.90603E-01
		STD	3.00876E-02	3.73142E-02	3.42569E-02	4.84792E-02	3.82135E-02	2.20064E-02	2.88560E-02	**1.48058E-02**	3.52130E-02	2.69022E-02
	10	AVG	8.21516E-01	8.07742E-01	8.22752E-01	**8.41110E-01**	7.96359E-01	8.19305E-01	8.07257E-01	8.23595E-01	8.29173E-01	8.30696E-01
		STD	3.31640E-02	2.63066E-02	3.96516E-02	2.94681E-02	3.87886E-02	2.45126E-02	3.91885E-02	**1.98085E-02**	2.17715E-02	2.67618E-02
9	4	AVG	7.61948E-01	7.53175E-01	7.52435E-01	7.30697E-01	7.41684E-01	7.51307E-01	**7.64556E-01**	7.35844E-01	7.54731E-01	7.64164E-01
		STD	1.78195E-02	**1.14657E-02**	5.66618E-02	5.29522E-02	5.22622E-02	2.35027E-02	2.86109E-02	1.58349E-02	3.27733E-02	3.18385E-02
	6	AVG	**8.43730E-01**	8.26638E-01	7.71568E-01	8.03700E-01	7.75938E-01	8.27825E-01	8.14455E-01	8.35315E-01	8.23724E-01	8.34215E-01

		STD	2.26529E-02	2.49529E-02	8.59645E-02	5.10199E-02	5.29688E-02	2.46594E-02	5.00541E-02	**1.52716E-02**	3.12845E-02	1.81579E-02
	8	AVG	**8.80328E-01**	8.73387E-01	8.49262E-01	8.65780E-01	8.32516E-01	8.62718E-01	8.64172E-01	8.80001E-01	8.71843E-01	8.69332E-01
		STD	1.70136E-02	**1.43318E-02**	5.50762E-02	3.36069E-02	4.41523E-02	5.59097E-02	3.98146E-02	1.92908E-02	3.02629E-02	2.81873E-02
	10	AVG	9.03781E-01	8.99666E-01	8.74279E-01	9.01213E-01	8.62757E-01	9.06207E-01	8.92236E-01	**9.08340E-01**	8.96297E-01	9.02655E-01
		STD	2.53254E-02	**1.39331E-02**	5.78860E-02	3.68938E-02	3.26020E-02	2.23541E-02	3.12454E-02	2.02525E-02	2.79130E-02	1.99641E-02
10	4	AVG	7.09740E-01	7.14411E-01	6.85854E-01	7.00007E-01	7.13788E-01	7.31810E-01	7.24819E-01	**7.34460E-01**	7.32227E-01	7.25446E-01
		STD	2.70257E-02	2.90598E-02	4.91937E-02	4.27686E-02	3.23631E-02	2.20540E-02	3.22047E-02	1.76958E-02	**1.40216E-02**	2.24138E-02
	6	AVG	8.02796E-01	7.98716E-01	7.66883E-01	7.64235E-01	7.75280E-01	7.92007E-01	7.79331E-01	**8.03048E-01**	7.85527E-01	7.86426E-01
		STD	2.95952E-02	2.44073E-02	4.09368E-02	4.46732E-02	3.23476E-02	3.24380E-02	4.70429E-02	**1.84850E-02**	3.45287E-02	3.51228E-02
	8	AVG	**8.60766E-01**	8.45814E-01	8.19284E-01	8.13488E-01	8.13883E-01	8.22500E-01	8.21938E-01	8.46154E-01	8.43131E-01	8.44869E-01
		STD	**1.24879E-02**	1.93716E-02	6.09662E-02	4.02991E-02	3.10222E-02	4.63147E-02	4.61539E-02	3.47648E-02	2.94759E-02	2.73333E-02
	10	AVG	**8.89278E-01**	8.83226E-01	8.43108E-01	8.54013E-01	8.51062E-01	8.58582E-01	8.50943E-01	8.77922E-01	8.75132E-01	8.76125E-01
		STD	**1.75917E-02**	2.05670E-02	4.30388E-02	4.20300E-02	2.51905E-02	3.52047E-02	3.63640E-02	2.01676E-02	2.42605E-02	2.08953E-02
11	4	AVG	**7.90725E-01**	7.84722E-01	7.28001E-01	7.23196E-01	7.17225E-01	7.76446E-01	7.66972E-01	7.74188E-01	7.57755E-01	7.66794E-01
		STD	6.43628E-03	**6.05395E-03**	6.21744E-02	6.64949E-02	5.57614E-02	2.61568E-02	3.62186E-02	2.60986E-02	4.10784E-02	3.83050E-02
	6	AVG	**8.42391E-01**	8.16297E-01	7.99489E-01	7.99750E-01	8.03041E-01	8.23823E-01	8.28721E-01	8.18787E-01	8.22053E-01	8.27670E-01
		STD	2.91118E-02	2.81170E-02	5.99510E-02	4.38823E-02	3.37737E-02	1.50680E-02	3.56230E-02	**6.18048E-03**	2.93382E-02	3.11101E-02
	8	AVG	**8.87337E-01**	8.79769E-01	8.42145E-01	8.73997E-01	8.30838E-01	8.76579E-01	8.74141E-01	8.70589E-01	8.74716E-01	8.73471E-01
		STD	**1.73305E-02**	2.03707E-02	5.66431E-02	3.71286E-02	4.20270E-02	2.26436E-02	2.62541E-02	2.17422E-02	2.80925E-02	3.34311E-02
	10	AVG	**9.14227E-01**	9.12919E-01	8.95289E-01	8.84972E-01	8.86077E-01	9.04853E-01	9.04132E-01	9.08447E-01	9.04083E-01	8.98340E-01
		STD	1.76249E-02	1.63114E-02	4.06101E-02	3.68118E-02	2.90336E-02	2.04569E-02	3.03860E-02	**1.35317E-02**	2.21383E-02	3.46632E-02
12	4	AVG	**7.69507E-01**	7.56571E-01	6.84486E-01	6.78688E-01	6.90480E-01	7.55879E-01	7.26862E-01	7.32139E-01	7.12536E-01	7.11215E-01
		STD	3.28887E-02	**2.80366E-02**	6.63502E-02	5.87618E-02	6.23119E-02	3.13796E-02	3.37834E-02	4.29893E-02	4.24738E-02	4.63815E-02
	6	AVG	**7.98049E-01**	7.98025E-01	7.85473E-01	7.57261E-01	7.61540E-01	7.88132E-01	7.82046E-01	7.78698E-01	7.78113E-01	7.75773E-01
		STD	2.76789E-02	2.71507E-02	5.70063E-02	6.31360E-02	3.96310E-02	3.67279E-02	3.47496E-02	3.30591E-02	3.57620E-02	**2.27361E-02**

	8	AVG	**8.50054E-01**	8.29212E-01	8.37948E-01	8.44771E-01	8.09973E-01	8.41512E-01	8.25241E-01	8.30980E-01	8.27619E-01	8.34657E-01
		STD	**2.53911E-02**	2.80227E-02	5.33200E-02	3.00159E-02	3.64784E-02	3.65449E-02	4.49090E-02	3.28834E-02	3.03321E-02	2.60258E-02
	10	AVG	8.76886E-01	8.60080E-01	8.50389E-01	8.67417E-01	8.53421E-01	8.76717E-01	8.69656E-01	8.72006E-01	**8.80039E-01**	8.72968E-01
		STD	2.21727E-02	2.16217E-02	7.94792E-02	4.17962E-02	3.25363E-02	2.61660E-02	3.31208E-02	**2.01098E-02**	2.87511E-02	2.85546E-02
13	4	AVG	7.62535E-01	7.59066E-01	7.43284E-01	7.40736E-01	7.21019E-01	**7.63924E-01**	7.54061E-01	7.60134E-01	7.45329E-01	7.48735E-01
		STD	1.85562E-02	2.73603E-02	3.80954E-02	4.61834E-02	4.26588E-02	**1.13370E-02**	2.81793E-02	1.25754E-02	1.68431E-02	2.15607E-02
	6	AVG	**8.19623E-01**	8.07293E-01	8.04627E-01	7.91394E-01	7.75397E-01	7.97054E-01	7.99533E-01	7.85062E-01	8.04361E-01	7.98338E-01
		STD	2.44719E-02	2.64231E-02	4.58195E-02	4.34391E-02	4.52621E-02	1.93550E-02	4.08747E-02	**1.43264E-02**	2.82921E-02	2.63893E-02
	8	AVG	8.63776E-01	8.43475E-01	8.32960E-01	8.27570E-01	8.34108E-01	8.55084E-01	8.46735E-01	8.60818E-01	8.54147E-01	**8.67426E-01**
		STD	1.95635E-02	**1.64261E-02**	5.42454E-02	5.89026E-02	2.80823E-02	2.02161E-02	4.51556E-02	1.75062E-02	2.29389E-02	2.06477E-02
	10	AVG	8.94145E-01	8.79414E-01	8.55489E-01	8.81226E-01	8.61522E-01	8.92378E-01	8.74334E-01	8.87932E-01	**8.98788E-01**	8.95076E-01
		STD	2.38238E-02	2.09916E-02	6.88507E-02	4.23204E-02	3.38737E-02	1.96984E-02	2.90661E-02	**1.53226E-02**	2.40540E-02	2.00209E-02
14	4	AVG	7.06918E-01	**7.09833E-01**	6.47742E-01	6.50700E-01	6.77945E-01	7.03898E-01	6.86417E-01	6.83741E-01	6.85514E-01	6.94071E-01
		STD	2.20435E-02	**1.61976E-02**	3.83074E-02	4.62849E-02	2.61333E-02	1.77407E-02	3.32482E-02	3.22357E-02	2.91149E-02	2.63902E-02
	6	AVG	7.71045E-01	**7.72526E-01**	7.26644E-01	7.39500E-01	7.23682E-01	7.63222E-01	7.56260E-01	7.54316E-01	7.56071E-01	7.58952E-01
		STD	3.26710E-02	**1.91023E-02**	6.52241E-02	3.61188E-02	3.77530E-02	3.52502E-02	3.19723E-02	2.93655E-02	2.72228E-02	3.04133E-02
	8	AVG	**8.28214E-01**	8.24846E-01	7.96339E-01	8.02969E-01	7.77958E-01	8.06780E-01	7.93140E-01	8.19880E-01	8.19842E-01	8.13225E-01
		STD	2.44999E-02	**1.87294E-02**	5.83320E-02	5.34934E-02	3.57573E-02	3.97187E-02	4.33413E-02	2.72321E-02	2.42835E-02	2.62752E-02
	10	AVG	8.55081E-01	8.53418E-01	8.36027E-01	8.49411E-01	8.25584E-01	8.53694E-01	8.32636E-01	8.54237E-01	8.46114E-01	**8.65176E-01**
		STD	3.37592E-02	2.45591E-02	6.10827E-02	3.12214E-02	2.89731E-02	3.38634E-02	3.75507E-02	2.36192E-02	3.27917E-02	**2.03536E-02**
15	4	AVG	**7.13128E-01**	6.80917E-01	6.51046E-01	6.52800E-01	6.63377E-01	7.10917E-01	6.88880E-01	7.01688E-01	6.78809E-01	6.93839E-01
		STD	4.21273E-02	5.50695E-02	4.74420E-02	5.05985E-02	**3.57673E-02**	4.08533E-02	5.00496E-02	4.16083E-02	5.18749E-02	5.39054E-02
	6	AVG	7.71650E-01	**7.73608E-01**	7.19292E-01	7.26011E-01	7.08564E-01	7.25095E-01	7.26451E-01	7.26418E-01	7.46853E-01	7.40669E-01
		STD	3.48040E-02	3.36605E-02	5.29347E-02	4.14945E-02	3.92446E-02	**3.00735E-02**	4.43477E-02	3.86426E-02	3.84280E-02	3.18813E-02
	8	AVG	**8.09375E-01**	7.83389E-01	8.02810E-01	7.93675E-01	7.71100E-01	7.82352E-01	7.84592E-01	7.89385E-01	7.94292E-01	8.02991E-01

		STD	2.56185E-02	2.71677E-02	2.99182E-02	3.79148E-02	2.75919E-02	2.25201E-02	3.00185E-02	**1.71159E-02**	3.03201E-02	2.03186E-02
	10	AVG	8.39592E-01	8.20649E-01	8.39252E-01	8.48248E-01	8.18922E-01	8.42150E-01	8.16917E-01	**8.48495E-01**	8.35676E-01	8.46100E-01
		STD	2.34926E-02	2.04047E-02	5.03573E-02	3.02018E-02	3.08075E-02	1.72584E-02	4.08611E-02	**1.59715E-02**	2.90864E-02	2.06943E-02
16	4	AVG	7.66905E-01	7.65892E-01	7.62120E-01	7.63795E-01	7.62749E-01	7.59181E-01	**7.72847E-01**	7.70303E-01	7.70664E-01	7.68496E-01
		STD	9.31640E-03	1.37309E-02	1.81846E-02	2.05185E-02	2.17582E-02	1.05657E-02	1.33500E-02	**8.07622E-03**	1.25384E-02	9.86654E-03
	6	AVG	8.50321E-01	8.49296E-01	8.33078E-01	8.39374E-01	8.22497E-01	8.44611E-01	8.43410E-01	8.42001E-01	8.49757E-01	**8.51446E-01**
		STD	**7.53502E-03**	1.02172E-02	3.95610E-02	1.59781E-02	4.88204E-02	8.63441E-03	2.45924E-02	1.25898E-02	1.15325E-02	9.77473E-03
	8	AVG	**9.09570E-01**	8.93533E-01	8.92214E-01	8.95645E-01	8.61000E-01	8.90131E-01	8.83870E-01	8.97422E-01	8.96163E-01	9.01152E-01
		STD	1.24658E-02	1.23815E-02	3.54269E-02	1.37420E-02	3.35154E-02	1.88688E-02	3.64086E-02	**7.63055E-03**	1.58713E-02	1.30629E-02
	10	AVG	**9.33066E-01**	9.29639E-01	9.26695E-01	9.30794E-01	9.03364E-01	9.22407E-01	9.10491E-01	9.24332E-01	9.24326E-01	9.26269E-01
		STD	1.11545E-02	8.97652E-03	2.26448E-02	1.05612E-02	2.55431E-02	1.39922E-02	2.77495E-02	**8.17151E-03**	1.42180E-02	1.51670E-02

Table A.4 Threshold values at 4-level threshold of sixteen images

Image	MGWO	GWO	HHO	WOA	SSA	IGWO	CS	CLPSO	CLSGMFO	LGCMFO
1	42	42	40 48	45	44	45	44	42	43	42
	76	76	78 82	78	77	79	76	76	76	76
	108	108	108 120	108	108	108	108	108	108	108
	158	158	157 166	157	155	159	157	158	158	158
2	41	41	54	54	54	41	41	41	41	41
	67	67	106	105	98	68	66	68	69	69
	91	91	148	147	161	90	91	82	108	101
	138	138	175	184	194	136	149	122	158	154
3	43	45	38	57	47	43	46	44	41	40
	92	92	74	119	89	92	93	92	75	90
	133	133	110	184	127	134	133	133	105	128
	158	158	158	254	158	158	158	158	156	158

4	27	26	53	26	27	30	30	30	27	30
	62	60	104	98	87	79	86	81	62	81
	95	95	148	139	139	139	139	139	95	139
	150	150	185	179	185	175	179	179	150	179
5	7	7	54	13	7	7	7	12	12	7
	25	25	93	25	25	25	25	25	25	25
	68	68	135	48	68	67	68	42	84	68
	132	132	166	118	136	138	127	101	142	132
6	42	42	55	26	45	39	45	45	45	45
	77	77	97	86	98	75	95	97	97	97
	109	109	150	109	149	109	149	149	149	149
	159	159	191	159	184	158	188	184	184	184
7	27	27	30	14	28	26	28	27	27	79
	54	54	55	46	55	54	53	54	53	116
	79	79	83	79	83	79	79	83	79	154
	134	134	134	139	135	134	131	138	134	191
8	30	30	38	29	30	27	31	27	38	27
	56	56	85	80	59	51	54	53	81	56
	80	80	134	117	87	80	80	80	122	87
	140	134	178	160	144	157	139	134	160	144
9	18	18	18	18	18	18	18	18	18	18
	64	64	59	58	58	60	64	63	66	64
	111	111	108	109	103	105	109	110	113	111
	155	155	155	155	151	153	155	154	155	155

10	25	25	42	23	85	73	26	73	73	26
	48	48	75	50	122	115	49	117	117	52
	77	77	104	77	146	155	77	155	155	77
	138	135	147	136	176	190	140	189	190	138
11	36	36	36	36	34	35	36	36	36	36
	81	83	78	78	79	81	80	81	81	81
	126	128	116	128	129	126	126	126	126	126
	162	162	157	162	162	162	162	162	162	162
12	45	45	28	48	35	42	45	44	45	39
	73	73	43	72	63	73	74	72	73	71
	100	100	88	100	98	100	100	100	100	100
	153	153	141	153	146	154	152	154	153	153
13	43	43	49	48	43	44	43	43	44	43
	90	90	101	96	90	90	86	90	90	90
	133	133	148	133	136	133	133	133	133	133
	164	164	187	164	175	164	164	164	164	164
14	47	48	48	77	44	48	49	50	50	49
	79	92	83	127	86	82	86	89	104	87
	109	136	135	159	131	124	126	127	160	126
	159	177	179	191	173	170	175	171	186	170
15	18	18	38	18	60	18	18	29	45	18
	42	40	82	48	104	41	44	52	94	42
	66	61	113	73	137	66	66	72	137	66
	130	124	144	133	165	121	123	135	169	130

16	62	64	59	62	54	60	56	60	62	62
	115	112	121	113	109	111	112	112	115	115
	156	156	156	156	156	156	156	155	156	156
	175	175	175	175	175	175	175	182	182	175

Table A.5 The AvgTime and TotalFEs comparison results of each comparative algorithm

Image	Level	Indicator	MGWO	GWO	HHO	WOA	SSA	IGWO	CS	CLPSO	CLSGMFO	LGCMFO
1	4	AvgTime	154.9234	152.5871	179.1730	169.6470	144.9167	159.0589	161.6585	171.9037	156.5564	142.3748
		TotalFEs	12960	19680	19887	6260	12660	19380	19950	16627	9400	10560
	6	AvgTime	249.5636	247.0515	233.715	244.9851	250.7201	225.5887	226.9999	200.5202	137.7026	137.5816
		TotalFEs	19440	19920	19992	12720	13040	19820	19980	19839	14100	15480
	8	AvgTime	177.7133	176.5234	180.9007	183.9733	178.8880	183.1208	181.5039	163.6025	180.2242	223.5238
		TotalFEs	14660	19920	20022	11300	13340	19300	20000	19962	12700	17400
	10	AvgTime	218.6663	214.0107	207.3771	208.3218	202.2803	204.9758	203.7416	219.4611	224.3336	226.2565
		TotalFEs	13140	19940	19962	10740	13080	17940	19980	19741	19884	18600
2	4	AvgTime	176.6371	153.6543	173.8880	173.2430	143.5651	158.2951	148.9436	165.8035	156.6713	143.3262
		TotalFEs	12760	19700	19888	12560	12720	19660	19950	17012	10900	13800
	6	AvgTime	239.9176	230.6307	236.3050	239.3803	223.5045	225.3387	232.0967	196.2542	137.1575	140.0934
		TotalFEs	13040	19920	19999	10980	13020	19740	19950	18021	10300	16320
	8	AvgTime	176.3844	177.6730	179.8153	178.3227	177.6527	180.9151	180.4788	163.6669	178.7708	220.4802
		TotalFEs	13140	19980	19846	16200	13160	16500	19980	19716	12800	16080
	10	AvgTime	216.5341	215.4503	216.6150	220.0406	204.5551	204.9974	201.7499	219.6817	225.0822	226.0562
		TotalFEs	13160	19940	19998	16680	13240	19500	19980	19438	11500	18360
3	4	AvgTime	178.1587	156.2252	158.3856	173.6238	181.5445	160.4174	149.5992	168.0912	188.7533	143.9711
		TotalFEs	12520	19620	19975	13880	12600	16180	19920	18204	6600	10800

	6	AvgTime	240.3747	223.8496	231.1908	241.2584	218.1550	216.5620	230.5555	199.0585	135.7957	139.3120
		TotalFEs	12920	19900	20012	11760	12800	19220	19950	19136	13100	12600
	8	AvgTime	176.3842	176.8738	180.1617	177.0697	177.6478	179.7240	180.5008	163.5053	178.4643	222.4727
		TotalFEs	13120	19860	20014	17240	13240	19340	19980	19351	13100	15960
	10	AvgTime	216.2810	214.5769	217.4525	215.6490	215.1732	210.2037	203.3118	219.4943	219.5571	230.8111
		TotalFEs	20280	19940	19990	16340	13160	17740	19980	20017	14200	20000
4	4	AvgTime	179.9989	156.5390	158.7941	172.0772	179.8138	162.2833	148.0853	165.4535	181.1855	145.3084
		TotalFEs	12780	19820	19810	10820	13140	18900	19950	18378	9000	12720
	6	AvgTime	239.0669	223.2915	224.8014	238.5020	230.5270	205.7344	229.4984	198.2411	137.0133	139.6507
		TotalFEs	17620	19940	19994	15480	13100	19820	19950	15654	10400	12720
	8	AvgTime	175.4814	176.8166	179.6501	177.1561	177.6656	180.2641	181.8291	163.5110	176.1168	222.9050
		TotalFEs	13060	19960	19972	11200	13120	19500	19980	19989	12200	18360
	10	AvgTime	216.0722	214.5449	216.1943	214.1504	215.2816	217.7361	212.5516	219.8176	221.2635	232.2387
		TotalFEs	18600	19960	19950	17220	13020	19860	19920	18645	15900	18000
5	4	AvgTime	176.2205	155.5472	159.8248	173.5351	179.9372	164.2350	154.1500	166.4346	184.3373	146.5202
		TotalFEs	12880	19560	20015	7920	13100	19860	19980	14422	18100	17160
	6	AvgTime	240.0563	224.4574	213.7847	239.4546	228.5214	192.6416	229.3125	176.3845	137.4936	141.2379
		TotalFEs	13160	19860	19880	13680	13100	18300	19980	18912	13300	14760
	8	AvgTime	174.9361	176.9041	179.5240	176.9589	177.5307	179.0783	182.4244	163.8352	175.2178	215.0024
		TotalFEs	15340	19920	19793	17160	13140	19020	20000	19992	15700	18600
	10	AvgTime	214.9538	212.7343	216.6245	214.3244	214.4553	218.0101	215.5063	219.2640	223.1245	232.8435
		TotalFEs	13160	19940	19987	17480	13280	19060	20000	18718	18900	17640
6	4	AvgTime	176.7627	157.3665	158.1981	172.8129	177.7439	159.6954	154.5604	167.0300	182.7134	144.3313
		TotalFEs	12860	19720	19991	10240	13000	18140	19950	18789	10400	12000
	6	AvgTime	236.2198	220.2522	195.3929	231.9360	227.2157	193.6902	223.1746	161.0589	136.9819	139.8622

		TotalFEs	13060	19860	19919	11880	12800	16140	19980	20006	10000	17040
	8	AvgTime	175.0433	176.4726	179.2354	177.0614	177.4383	179.7565	181.0367	163.6538	172.9231	209.2556
		TotalFEs	13120	19900	19925	18200	13280	19860	20000	17682	13600	14880
	10	AvgTime	214.7096	212.0976	214.4754	213.2261	214.5111	215.6383	215.601	219.4242	219.6858	230.9419
		TotalFEs	13160	19940	19956	17780	13140	19660	19980	15084	19883	18360
7	4	AvgTime	174.3329	153.1080	154.6144	176.1309	178.5566	156.8796	153.6356	166.2123	180.8378	134.0925
		TotalFEs	12700	19640	19493	11020	12940	18980	19980	17870	14500	11640
	6	AvgTime	224.2201	227.2998	198.2818	226.3366	225.0983	204.1113	218.8590	160.3601	137.5512	138.6859
		TotalFEs	16320	19860	19908	13680	13020	19940	19980	19229	11700	15000
	8	AvgTime	175.8818	176.3704	179.1662	177.1312	177.2817	177.8515	180.3625	161.9442	166.0704	203.0961
		TotalFEs	13160	19880	19988	15700	13140	19140	19950	17724	11200	14520
	10	AvgTime	214.0743	212.4712	213.2455	211.2664	212.0080	215.1807	216.9899	219.8064	216.8070	227.6848
		TotalFEs	20280	19920	19710	13180	13320	19220	20000	18495	15900	18120
8	4	AvgTime	170.3637	148.9915	152.8988	170.2212	176.1424	157.6520	146.4353	170.5692	177.4988	130.9832
		TotalFEs	12920	19640	19901	15960	12980	19060	19950	17681	10500	10800
	6	AvgTime	229.5800	227.8293	247.4165	238.9169	225.2947	237.1388	212.6487	160.3864	136.7850	139.8429
		TotalFEs	13140	19840	20027	12820	13140	19780	19980	18571	13300	12960
	8	AvgTime	175.8220	176.6427	179.8250	176.8269	177.3237	176.6626	179.3767	158.2092	167.2338	213.1513
		TotalFEs	13080	19920	19901	16620	13160	19940	20000	17747	13100	15120
	10	AvgTime	208.7039	209.8565	213.6103	211.6021	211.6941	212.0131	216.8582	219.8396	216.9253	226.9047
		TotalFEs	13060	19940	20031	19760	13100	19580	19980	19960	19992	18120
9	4	AvgTime	167.0479	157.8912	151.0749	170.4797	170.4506	157.4365	144.7754	171.5018	172.0351	129.9561
		TotalFEs	12960	19820	19706	9280	12920	18940	19890	15682	14600	8520
	6	AvgTime	252.2561	227.1694	242.0889	249.6409	225.2724	237.0806	212.2029	160.4441	134.6267	138.4968
		TotalFEs	13000	19900	19973	9880	13140	19900	19980	19660	13700	16920

	8	AvgTime	175.6797	176.1543	179.4174	176.0527	176.6556	175.6749	176.9268	158.1769	168.4783	203.8058
		TotalFEs	13120	19920	20024	17600	13080	19140	19980	19253	14700	14400
	10	AvgTime	207.3806	205.5349	211.7615	209.8536	211.5845	211.3728	214.5124	219.5376	215.4135	227.7201
		TotalFEs	20280	19920	19982	15920	13100	19340	19980	18708	13400	13440
10	4	AvgTime	167.4221	159.3054	163.6806	164.7463	169.0766	157.2806	142.3595	169.5340	171.1470	127.1964
		TotalFEs	12840	19160	20026	4980	13000	19260	19980	14731	7600	10200
	6	AvgTime	251.1264	227.9480	243.4955	251.0912	224.9903	238.1436	212.4692	160.9346	134.8469	138.8537
		TotalFEs	13100	19840	19897	17260	13020	19380	19980	18002	12200	18120
	8	AvgTime	175.4814	176.5760	178.1970	175.4429	175.3033	175.5000	176.5865	159.1139	170.0847	196.0826
		TotalFEs	13160	19940	19923	12440	13280	18100	19950	19705	15500	17880
	10	AvgTime	207.4385	205.9789	206.1219	204.2492	208.3405	211.5881	214.3177	219.5471	217.2459	228.5501
		TotalFEs	13140	19940	19999	15640	13100	19300	20000	18271	19867	17640
11	4	AvgTime	168.1119	160.2424	174.5372	171.9716	171.7383	157.1731	155.7038	170.9709	171.8106	174.4041
		TotalFEs	13060	19820	20003	9600	12960	19660	19950	16754	10300	12600
	6	AvgTime	240.4507	226.0129	246.8113	231.9307	222.9562	237.1491	205.2302	161.0806	135.2503	138.8847
		TotalFEs	13040	19900	19986	12320	13160	18980	19980	16163	10800	15000
	8	AvgTime	175.9231	176.4430	177.1996	175.9029	175.1979	175.8765	178.4559	160.7333	179.2138	195.2281
		TotalFEs	13120	19880	19925	10520	13020	19900	19980	18156	19881	16080
	10	AvgTime	208.1931	205.4226	206.8706	204.5097	204.3255	209.5973	216.6925	219.4597	216.2265	224.8146
		TotalFEs	13060	19940	19748	16380	13080	18660	19980	20001	13600	17640
12	4	AvgTime	164.2614	147.6439	172.8351	168.7421	169.2812	145.6492	157.9931	170.0627	171.9393	176.4814
		TotalFEs	12820	19580	19923	15280	12960	19100	20000	18328	8900	11400
	6	AvgTime	227.2133	215.6583	242.1441	229.1988	210.1417	234.7597	214.6293	160.8905	134.5221	138.9669
		TotalFEs	13060	13060	13060	13060	13060	13060	13060	13060	13060	13060
	8	AvgTime	176.1368	174.9037	178.5466	175.3170	175.2162	175.5468	176.7589	164.2134	180.2916	194.9073

		TotalFEs	19080	19940	20007	13780	13180	18620	19980	18313	18900	20000
	10	AvgTime	208.2893	205.1346	207.5288	204.2516	204.3991	207.5567	215.4420	219.8605	242.8631	223.6579
		TotalFEs	13120	19940	19820	15060	13060	19940	19980	16122	12100	19560
13	4	AvgTime	165.3520	155.7053	173.3201	160.0643	170.1582	146.8116	158.4632	157.8666	171.4807	176.1746
		TotalFEs	12840	19800	19691	8480	12960	19340	19980	18641	8200	12480
	6	AvgTime	227.7321	210.6643	245.8686	228.5638	196.6379	238.2016	210.9724	161.3813	135.0011	139.2394
		TotalFEs	13000	19860	19856	9100	13020	18740	19950	19857	11300	14880
	8	AvgTime	174.7296	174.5593	179.5502	175.0944	175.5914	175.5430	176.9418	171.1644	181.0751	195.4191
		TotalFEs	19760	19920	20007	13880	13000	19860	19980	19534	19883	20000
	10	AvgTime	208.7484	205.8200	207.0673	204.8203	204.4478	205.2022	215.3778	219.2607	253.6221	224.1636
		TotalFEs	13160	19960	19933	13060	13240	19860	19980	19552	15000	18000
14	4	AvgTime	168.8986	157.9086	174.5855	156.4941	168.5932	146.0208	160.5004	151.7966	172.0092	165.6785
		TotalFEs	12840	19800	19878	9120	13060	19980	19920	18633	15100	14520
	6	AvgTime	226.2278	201.8415	237.2138	227.3985	195.7837	233.8595	207.2786	162.0263	134.4707	138.5171
		TotalFEs	13040	19920	20009	8700	12900	19540	19830	19189	14900	13920
	8	AvgTime	174.3732	174.2643	177.5293	175.2632	175.4018	176.0676	175.4239	171.3215	180.6559	194.9979
		TotalFEs	13120	19960	19963	6440	13060	17340	19980	19849	11500	13200
	10	AvgTime	208.5563	205.4247	206.7395	204.7643	204.5186	204.6558	214.9021	214.7257	249.7561	219.0757
		TotalFEs	13060	19960	20022	14560	13120	19820	19980	19118	20000	18720
15	4	AvgTime	165.6107	174.3738	172.3796	157.0834	169.2826	168.3957	158.7938	152.8883	165.9702	173.5058
		TotalFEs	13020	19500	19989	4720	13240	19180	19950	18298	9300	19560
	6	AvgTime	232.3251	215.7025	231.4406	227.9410	202.0509	226.2282	208.2418	161.7264	135.3839	139.4236
		TotalFEs	19180	19920	19943	13120	13320	14060	19980	19476	9600	16800
	8	AvgTime	174.6209	173.9734	177.5948	175.3777	175.7219	176.2887	175.6783	171.0196	181.0013	202.3942
		TotalFEs	13140	19920	19995	14680	13020	19740	19980	19819	10500	18240

	10	AvgTime	208.9602	205.6561	206.6962	204.587	205.3699	204.5558	213.3815	209.5956	252.3300	214.6098
		TotalFEs	14400	19900	19917	13800	13060	19740	19980	18535	19881	16440
16	4	AvgTime	164.5955	172.8102	166.1303	153.7239	162.7833	175.7627	154.8224	147.2568	162.0973	159.6797
		TotalFEs	12620	19880	19858	12220	13060	18020	19980	17414	8100	11280
	6	AvgTime	230.8987	235.5789	228.7306	224.2174	227.7747	219.6852	202.8677	156.9456	130.9228	133.7493
		TotalFEs	13120	19920	19778	8740	13040	19140	19980	16890	10200	17640
	8	AvgTime	173.3341	173.0123	177.0397	175.6685	174.8055	176.6388	177.2760	167.4290	179.6321	204.9172
		TotalFEs	12980	19940	19972	13460	13240	19420	19860	18844	11500	16560
	10	AvgTime	207.3721	204.6058	205.7041	205.2786	205.0498	206.0172	212.5774	209.4890	236.7116	208.9480
		TotalFEs	16500	19940	20029	14440	13140	19700	19980	19898	19882	19320
avg	4	AvgTime	169.9186	157.4937	165.2700	167.7873	169.5990	158.3154	153.1550	164.5860	172.9402	**150.8740**
		TotalFEs	12836.25	19671.25	19877.13	**10146.25**	12956.25	18977.50	19955.00	17341.50	10718.75	12502.50
	6	AvgTime	236.7018	224.0774	231.1676	235.672	220.9153	222.8696	217.3148	171.1058	**135.7191**	138.8999
		TotalFEs	14327.50	19463.75	19514.56	12198.75	13042.50	18472.50	19530.63	18229.06	**11997.50**	15201.25
	8	AvgTime	175.4953	175.8852	178.9596	176.7887	176.5826	177.7818	178.8476	**164.0688**	175.9659	207.3525
		TotalFEs	14135.00	19922.5	19954.81	14151.25	**13153.75**	19045.00	19973.75	19102.25	14172.75	16705.00
	10	AvgTime	211.5584	209.3325	210.8803	209.4309	**208.6247**	209.9563	212.7196	218.0166	228.1842	225.3298
		TotalFEs	15097.50	19938.75	19939.63	15502.50	**13140.00**	19307.5	19980.00	18768.94	16868.06	17997.50

References

A, A.A.H., Mirjalili, S., Faris, H., Aljarah, I., Mafarja, M., Chen, H., 2019. Harris hawks optimization: Algorithm and applications. Future Generation Computer Systems 97, 849-872.

Ahmadianfar, I., Asghar Heidari, A., Gandomi, A.H., Chu, X., Chen, H., 2021. RUN Beyond the Metaphor: An Efficient Optimization Algorithm Based on Runge Kutta Method. Expert Systems with Applications, 115079.

Ahmed, A.E., Mohamed Abd, E., Diego, O., 2018. Image segmentation via multilevel thresholding using hybrid optimization algorithms. Journal of Electronic Imaging 27, 1-26.

Al-Betar, M.A., Awadallah, M.A., Krishan, M.M., 2020. A non-convex economic load dispatch problem with valve loading effect using a hybrid grey wolf optimizer. Neural Computing & Applications 32, 12127-12154.

Ali, M., Pant, M., 2011. Improving the performance of differential evolution algorithm using Cauchy mutation. Soft Computing 15, 991-1007.

Aljarah, I., Mafarja, M., Heidari, A.A., Faris, H., Mirjalili, S., 2019. Clustering analysis using a novel locality-informed grey wolf-inspired clustering approach. Knowledge and Information Systems.

Amirsadri, S., Mousavirad, S.J., Ebrahimpour-Komleh, H., 2018. A Levy flight-based grey wolf optimizer combined with back-propagation algorithm for neural network training. Neural Computing & Applications 30, 3707-3720.

Ba, A.F., Huang, H., Wang, M., Ye, X., Gu, Z., Chen, H., Cai, X., 2020. Levy-based antlion-inspired optimizers with orthogonal learning scheme. Engineering with Computers, 1-22.

Bhandari, A.K., 2020. A novel beta differential evolution algorithm-based fast multilevel thresholding for color image segmentation. Neural Computing and Applications 32, 4583-4613.

Bhandari, A.K., Rahul, K., 2019. A novel local contrast fusion-based fuzzy model for color image multilevel thresholding using grasshopper optimization. Applied Soft Computing 81, 105515.

Boubechal, I., Seghir, R., Benzid, R., 2019. A Generalized and Parallelized SSIM-Based Multilevel Thresholding Algorithm. Applied Artificial Intelligence 33, 1266-1289.

Buades, A., Coll, B., Morel, J., 2005. A non-local algorithm for image denoising, 2005 IEEE Computer Society Conference on Computer Vision and Pattern Recognition (CVPR'05), pp. 60-65 vol. 62.

Cai, J., Huang, Z., Liao, L., Luo, J., Liu, W.-X., 2021. APPM: Adaptive Parallel Processing Mechanism for Service Function Chains. IEEE Transactions on Network and Service Management 18, 1540-1555.

Cai, Z., Gu, J., Luo, J., Zhang, Q., Chen, H., Pan, Z., Li, Y., Li, C., 2019. Evolving an optimal kernel extreme learning machine by using an enhanced grey wolf optimization strategy. Expert Systems with Applications 138, 112814.

Chakraborty, R., Sushil, R., Garg, M.L., 2019. An Improved PSO-Based Multilevel Image Segmentation Technique Using Minimum Cross-Entropy Thresholding. Arabian Journal for Science and Engineering 44, 3005-3020.

Chantar, H., Mafarja, M., Alsawalqah, H., Heidari, A.A., Aljarah, I., Faris, H., 2020a. Feature selection using binary grey wolf optimizer with elite-based crossover for Arabic text classification. Neural Computing & Applications 32, 12201-12220.

Chantar, H., Mafarja, M., Alsawalqah, H., Heidari, A.A., Aljarah, I., Faris, H., 2020b. Feature selection using binary grey wolf optimizer with elite-based crossover for Arabic text classification. Neural Computing and Applications 32, 12201-12220.

Chen, H., Xu, Y., Wang, M., Zhao, X., 2019a. A balanced whale optimization algorithm for constrained

engineering design problems. Applied Mathematical Modelling 71, 45-59.
Chen, M.-R., Zeng, G.-Q., Lu, K.-D., Weng, J., 2019b. A two-layer nonlinear combination method for short-term wind speed prediction based on ELM, ENN, and LSTM. IEEE Internet of Things Journal 6, 6997-7010.
Chen, M., Zeng, G., Lu, K., Weng, J., 2019c. A Two-Layer Nonlinear Combination Method for Short-Term Wind Speed Prediction Based on ELM, ENN, and LSTM. IEEE Internet of Things Journal 6, 6997-7010.
Chen, S., Zhang, J., Meng, F., Wang, D., 2021. A Markov Chain Position Prediction Model Based on Multidimensional Correction. Complexity 2021.
Chen, W., Zhang, J., Lin, Y., Chen, N., Zhan, Z., Chung, H.S., Li, Y., Shi, Y., 2013. Particle Swarm Optimization With an Aging Leader and Challengers. IEEE Transactions on Evolutionary Computation 17, 241-258.
Chen, Z.-G., Zhan, Z.-H., Lin, Y., Gong, Y.-J., Gu, T.-L., Zhao, F., Yuan, H.-Q., Chen, X., Li, Q., Zhang, J., 2018. Multiobjective cloud workflow scheduling: A multiple populations ant colony system approach. IEEE transactions on cybernetics 49, 2912-2926.
Dappuri, B., Rao, M.P., Sikha, M.B., 2020. Non-blind RGB watermarking approach using SVD in translation invariant wavelet space with enhanced Grey-wolf optimizer. Multimedia Tools and Applications 79, 31103-31124.
Davahli, A., Shamsi, M., Abaei, G., 2020. Hybridizing genetic algorithm and grey wolf optimizer to advance an intelligent and lightweight intrusion detection system for IoT wireless networks. Journal of Ambient Intelligence and Humanized Computing 11, 5581-5609.
Deng, W., Liu, H., Xu, J., Zhao, H., Song, Y., 2020a. An Improved Quantum-Inspired Differential Evolution Algorithm for Deep Belief Network. IEEE Transactions on Instrumentation and Measurement 69, 7319-7327.
Deng, W., Liu, H., Xu, J., Zhao, H., Song, Y.J.I.T.o.I., Measurement, 2020b. An improved quantum-inspired differential evolution algorithm for deep belief network. IEEE Transactions on Instrumentation & Measurement, https://doi.org/10.1109/TIM.2020.2983233.
Deng, W., Xu, J., Song, Y., Zhao, H., 2020c. An effective improved co-evolution ant colony optimisation algorithm with multi-strategies and its application. International Journal of Bio-Inspired Computation 16, 158-170.
Deng, W., Xu, J., Zhao, H., Song, Y., 2020d. A Novel Gate Resource Allocation Method Using Improved PSO-Based QEA. IEEE Transactions on Intelligent Transportation Systems, http://doi.org/10.1109/TITS.2020.3025796
Deng, W., Xu, J., Zhao, H., Song, Y., 2020e. A Novel Gate Resource Allocation Method Using Improved PSO-Based QEA. IEEE Transactions on Intelligent Transportation Systems, 1-9.
Derrac, J., García, S., Molina, D., Herrera, F., 2011. A practical tutorial on the use of nonparametric statistical tests as a methodology for comparing evolutionary and swarm intelligence algorithms. Swarm and Evolutionary Computation 1, 3-18.
Dewangan, R.K., Shukla, A., Godfrey, W.W., 2019. Three dimensional path planning using Grey wolf optimizer for UAVs. Applied Intelligence 49, 2201-2217.
Dong, H., Dong, Z., 2020. Surrogate-assisted grey wolf optimization for high-dimensional, computationally expensive black-box problems. Swarm and Evolutionary Computation 57, 100713.
Dorigo, M., Blum, C., 2005. Ant colony optimization theory: A survey. Theoretical Computer Science 344, 243-278.
Fan, Q., Chen, Z., Li, Z., Xia, Z., Lin, Y., 2020. An efficient refracted salp swarm algorithm and its application in structural parameter identification. Engineering with Computers.

Fan, Q.F., Wang, T., Chen, Y., Zhang, Z.F., 2018. Design and Application of Interval Type-2 TSK Fuzzy Logic System Based on QPSO Algorithm. International Journal of Fuzzy Systems 20, 835-846.
Fan, Z., Ji, P.-p., Zhang, J., Segets, D., Chen, D.-R., Chen, S.-C., 2021. Wavelet neural network modeling for the retention efficiency of sub-15 nm nanoparticles in ultrafiltration under small particle to pore diameter ratio. Journal of Membrane Science, 119503.
Faris, H., Aljarah, I., Al-Betar, M.A., Mirjalili, S., 2018. Grey wolf optimizer: a review of recent variants and applications. Neural Computing & Applications 30, 413-435.
Gong, C., Hu, Y., Gao, J., Wang, Y., Yan, L., 2019. An improved delay-suppressed sliding-mode observer for sensorless vector-controlled PMSM. IEEE Transactions on Industrial Electronics 67, 5913-5923.
Guo, K., Hu, B., Ma, J., Ren, S., Tao, Z., Zhang, J., 2020. Toward anomaly behavior detection as an edge network service using a dual-task interactive guided neural network. IEEE Internet of Things Journal, DOI: 10.1109/JIOT.2020.3015987.
Gupta, S., Deep, K., 2019. A novel Random Walk Grey Wolf Optimizer. Swarm and Evolutionary Computation 44, 101-112.
Gupta, S., Deep, K., 2020. A memory-based Grey Wolf Optimizer for global optimization tasks. Applied Soft Computing 93, 106367.
Gupta, S., Deep, K., Heidari, A.A., Moayedi, H., Chen, H., 2019. Harmonized salp chain-built optimization. Engineering with Computers, 1-31.
Habba, M., Ameur, M., Jabrane, Y., 2018. A novel Gini index based evaluation criterion for image segmentation. Optik 168, 446-457.
He, Y., Dai, L., Zhang, H., 2020. Multi-Branch Deep Residual Learning for Clustering and Beamforming in User-Centric Network. IEEE Communications Letters 24, 2221-2225.
Heidari, A.A., Abbaspour, R.A., Chen, H., 2019a. Efficient boosted grey wolf optimizers for global search and kernel extreme learning machine training. Applied Soft Computing 81, 105521.
Heidari, A.A., Abbaspour, R.A., Chen, H., 2019b. Efficient boosted grey wolf optimizers for global search and kernel extreme learning machine training. Applied Soft Computing 81, 105521-105521.
Hu, B., Guo, K., Wang, X., Zhang, J., Zhou, D., 2021a. RRL-GAT: Graph Attention Network-driven Multi-Label Image Robust Representation Learning. IEEE Internet of Things Journal, DOI: 10.1109/JIOT.2021.3089180.
Hu, J., Chen, H., Heidari, A.A., Wang, M., Zhang, X., Chen, Y., Pan, Z., 2021b. Orthogonal learning covariance matrix for defects of grey wolf optimizer: Insights, balance, diversity, and feature selection. Knowledge-Based Systems 213, 106684.
Hu, L., Li, H., Cai, Z., Lin, F., Hong, G., Chen, H., Lu, Z., 2017. A new machine-learning method to prognosticate paraquat poisoned patients by combining coagulation, liver, and kidney indices. Plos One 12, e0186427.
Huang, H., Feng, X., Heidari, A.A., Xu, Y., Wang, M., Liang, G., Chen, H., Cai, X., 2020. Rationalized Sine Cosine Optimization With Efficient Searching Patterns. IEEE Access 8, 61471-61490.
Huang, H., Zhou, S., Jiang, J., Chen, H., Li, Y., Li, C., 2019. A new fruit fly optimization algorithm enhanced support vector machine for diagnosis of breast cancer based on high-level features. BMC bioinformatics 20, 1-14.
Huynh-Thu, Q., Ghanbari, M., 2008. Scope of validity of PSNR in image/video quality assessment. Electronics Letters 44, 800-801.
Ibrahim, R.A., Abd Elaziz, M., Lu, S., 2018. Chaotic opposition-based grey-wolf optimization algorithm based on differential evolution and disruption operator for global optimization. Expert Systems with

Applications 108, 1-27.
Jiang, N., Chen, J., Zhou, R.-G., Wu, C., Chen, H., Zheng, J., Wan, T., 2020a. PAN: Pipeline assisted neural networks model for data-to-text generation in social internet of things. Information Sciences 530, 167-179.
Jiang, N., Tian, F., Li, J., Yuan, X., Zheng, J., 2020b. MAN: mutual attention neural networks model for aspect-level sentiment classification in SIoT. IEEE Internet of Things Journal 7, 2901-2913.
Jiang, N., Xu, D., Zhou, J., Yan, H., Wan, T., Zheng, J., 2020c. Toward optimal participant decisions with voting-based incentive model for crowd sensing. Information Sciences 512, 1-17.
Jing, X., Wang, H., Huang, X., Chen, Z., Zhu, J., Wang, X., 2021. Digital image colorimetry detection of carbaryl in food samples based on liquid phase microextraction coupled with a microfluidic thread-based analytical device. Food Chemistry 337, 127971.
Kapur, J.N., Sahoo, P.K., Wong, A.K.C., 1985. A new method for gray-level picture thresholding using the entropy of the histogram. Computer Vision, Graphics, and Image Processing 29, 273-285.
Karaboga, D., Basturk, B., 2007. A powerful and efficient algorithm for numerical function optimization: artificial bee colony (ABC) algorithm. Journal of Global Optimization 39, 459-471.
Kennedy, J., Eberhart, R., 1995. Particle swarm optimization, Proceedings of ICNN'95 - International Conference on Neural Networks, pp. 1942-1948 vol.1944.
Khairuzzaman, A.K.M., Chaudhury, S., 2019. Masi entropy based multilevel thresholding for image segmentation. Multimedia Tools and Applications 78, 33573-33591.
Li, B.-H., Liu, Y., Zhang, A.-M., Wang, W.-H., Wan, S., 2020a. A Survey on Blocking Technology of Entity Resolution. Journal of Computer Science and Technology 35, 769-793.
Li, C., Hou, L., Sharma, B.Y., Li, H., Chen, C., Li, Y., Zhao, X., Huang, H., Cai, Z., Chen, H., 2018. Developing a new intelligent system for the diagnosis of tuberculous pleural effusion. Computer methods and programs in biomedicine 153, 211-225.
Li, H., Liu, J., Chen, L., Bai, J., 2019. Chaos-enhanced moth-flame optimization algorithm for global optimization. Journal of Systems Engineering and Electronics 30, 1144-1159.
Li, Q., Chen, H., Huang, H., Zhao, X., Cai, Z., Tong, C., Liu, W., Tian, X., 2017a. An enhanced grey wolf optimization based feature selection wrapped kernel extreme learning machine for medical diagnosis. Computational and mathematical methods in medicine 2017.
Li, Q., Chen, H., Huang, H., Zhao, X., Cai, Z., Tong, C., Liu, W., Tian, X., 2017b. An Enhanced Grey Wolf Optimization Based Feature Selection Wrapped Kernel Extreme Learning Machine for Medical Diagnosis. Computational and Mathematical Methods in Medicine 2017, 9512741.
Li, S., Chen, H., Wang, M., Heidari, A.A., Mirjalili, S., 2020b. Slime mould algorithm: A new method for stochastic optimization. Future Generation Computer Systems 111 300-323.
Liang, D., Zhan, Z.-H., Zhang, Y., Zhang, J., 2019. An efficient ant colony system approach for new energy vehicle dispatch problem. IEEE Transactions on Intelligent Transportation Systems 21, 4784-4797.
Liang, J.J., Qin, A.K., Suganthan, P.N., Baskar, S., 2006. Comprehensive learning particle swarm optimizer for global optimization of multimodal functions. IEEE Transactions on Evolutionary Computation 10, 281-295.
Liang, X., Cai, Z., Wang, M., Zhao, X., Chen, H., Li, C., 2020. Chaotic oppositional sine–cosine method for solving global optimization problems. Engineering with Computers, 1-17.
Lipare, A., Edla, D.R., Kuppili, V., 2019. Energy efficient load balancing approach for avoiding energy hole problem in WSN using Grey Wolf Optimizer with novel fitness function. Applied Soft Computing 84, 105706.

Liu, J., Yang, Z., Li, D., 2020. A multiple search strategies based grey wolf optimizer for solving multi-objective optimization problems. Expert Systems with Applications 145, 113134.
Liu, T., Hu, L., Ma, C., Wang, Z.-Y., Chen, H.-L., 2015. A fast approach for detection of erythemato-squamous diseases based on extreme learning machine with maximum relevance minimum redundancy feature selection. International Journal of Systems Science 46, 919-931.
Liu, X.-F., Zhan, Z.-H., Zhang, J., 2021. Resource-Aware Distributed Differential Evolution for Training Expensive Neural-Network-Based Controller in Power Electronic Circuit. IEEE Transactions on Neural Networks and Learning Systems, DOI: 10.1109/TNNLS.2021.3075205.
Long, W., Cai, S., Jiao, J., Tang, M., 2020a. An efficient and robust grey wolf optimizer algorithm for large-scale numerical optimization. Soft Computing 24, 997-1026.
Long, W., Cai, S., Jiao, J., Xu, M., Wu, T., 2020b. A new hybrid algorithm based on grey wolf optimizer and cuckoo search for parameter extraction of solar photovoltaic models. Energy Conversion and Management 203, 112243.
Lu, C., Gao, L., Li, X., Hu, C., Yan, X., Gong, W., 2020. Chaotic-based grey wolf optimizer for numerical and engineering optimization problems. Memetic Computing 12, 371-398.
Lu, C., Gao, L., Pan, Q., Li, X., Zheng, J., 2019. A multi-objective cellular grey wolf optimizer for hybrid flowshop scheduling problem considering noise pollution. Applied Soft Computing 75, 728-749.
Lu, C., Gao, L., Yi, J., 2018. Grey Wolf Optimizer with Cellular Topological Structure. Expert Systems with Applications 107, 89-114.
Luo, J., Chen, H., zhang, Q., Xu, Y., Huang, H., Zhao, X., 2018. An improved grasshopper optimization algorithm with application to financial stress prediction. Applied Mathematical Modelling 64, 654-668.
Luo, J., Li, J., Jiao, L., Cai, J., 2020a. On the Effective Parallelization and Near-Optimal Deployment of Service Function Chains. IEEE Transactions on Parallel and Distributed Systems 32, 1238-1255.
Luo, J., Li, M., Liu, X., Tian, W., Zhong, S., Shi, K., 2020b. Stabilization analysis for fuzzy systems with a switched sampled-data control. Journal of the Franklin Institute 357, 39-58.
Luo, K., Zhao, Q., 2019. A binary grey wolf optimizer for the multidimensional knapsack problem. Applied Soft Computing 83, 105645.
Ma, X., Mei, X., Wu, W., Wu, X., Zeng, B., 2019. A novel fractional time delayed grey model with Grey Wolf Optimizer and its applications in forecasting the natural gas and coal consumption in Chongqing China. Energy 178, 487-507.
Meng, F., Pang, A., Dong, X., Han, C., Sha, X., 2018. $H\infty$ optimal performance design of an unstable plant under bode integral constraint. Complexity 2018.
Mi, C., Huang, Y., Fu, C., Zhang, Z., Postolache, O., 2021. Vision-Based Measurement: Actualities and Developing Trends in Automated Container Terminals. IEEE Instrumentation & Measurement Magazine 24, 65-76.
Miao, Z., Yuan, X., Zhou, F., Qiu, X., Song, Y., Chen, K., 2020. Grey wolf optimizer with an enhanced hierarchy and its application to the wireless sensor network coverage optimization problem. Applied Soft Computing 96, 106602.
Mirjalili, S., Aljarah, I., Mafarja, M., Heidari, A.A., Faris, H., 2020. Grey Wolf Optimizer: Theory, Literature Review, and Application in Computational Fluid Dynamics Problems, in: Mirjalili, S., Song Dong, J., Lewis, A. (Eds.), Nature-Inspired Optimizers: Theories, Literature Reviews and Applications. Springer International Publishing, Cham, pp. 87-105.
Mirjalili, S., Dong, J.S., Lewis, A., 2019. Nature-inspired optimizers: theories, literature reviews and applications. Springer.

Mirjalili, S., Mirjalili, S.M., Lewis, A., 2014. Grey wolf optimizer. Advances in engineering software 69, 46-61.

Mittal, H., Saraswat, M., 2018. An optimum multi-level image thresholding segmentation using non-local means 2D histogram and exponential Kbest gravitational search algorithm. Engineering Applications of Artificial Intelligence 71, 226-235.

Morales-Castaeda, B., Zaldívar, D., Cuevas, E., Fausto, F., Rodríguez, A., 2020. A better balance in metaheuristic algorithms: Does it exist? Swarm Evolutionary Computation 54, 100671.

Naidu, M.S.R., Rajesh Kumar, P., Chiranjeevi, K., 2018. Shannon and Fuzzy entropy based evolutionary image thresholding for image segmentation. Alexandria Engineering Journal 57, 1643-1655.

Niu, P., Niu, S., Chang, L., 2019a. The defect of the Grey Wolf optimization algorithm and its verification method. Knowledge-Based Systems 171, 37-43.

Niu, P., Niu, S., Liu, N., Chang, L., 2019b. The defect of the Grey Wolf optimization algorithm and its verification method. Knowledge-Based Systems 171, 37-43.

Oliva, D., Nag, S., Elaziz, M.A., Sarkar, U., Hinojosa, S., 2019. Multilevel thresholding by fuzzy type II sets using evolutionary algorithms. Swarm and Evolutionary Computation 51, 100591.

Pang, J., Zhou, H., Tsai, Y.-C., Chou, F.-D., 2018. A scatter simulated annealing algorithm for the bi-objective scheduling problem for the wet station of semiconductor manufacturing. Computers & Industrial Engineering 123, 54-66.

Pare, S., Bhandari, A.K., Kumar, A., Singh, G.K., 2018. A new technique for multilevel color image thresholding based on modified fuzzy entropy and Levy flight firefly algorithm. Computers & Electrical Engineering 70, 476-495.

Pathak, Y., Arya, K.V., Tiwari, S., 2019. Feature selection for image steganalysis using levy flight-based grey wolf optimization. Multimedia Tools and Applications 78, 1473-1494.

Pei, H., Yang, B., Liu, J., Chang, K., 2020. Active Surveillance via Group Sparse Bayesian Learning. IEEE Transactions on Pattern Analysis and Machine Intelligence, DOI: 10.1109/TPAMI.2020.3023092.

Qiu, S., Wang, Z., Zhao, H., Hu, H., 2016. Using distributed wearable sensors to measure and evaluate human lower limb motions. IEEE Transactions on Instrumentation and Measurement 65, 939-950.

Qiu, S., Wang, Z., Zhao, H., Qin, K., Li, Z., Hu, H., 2018. Inertial/magnetic sensors based pedestrian dead reckoning by means of multi-sensor fusion. Information Fusion 39, 108-119.

Qu, C., Gai, W., Zhang, J., Zhong, M., 2020. A novel hybrid grey wolf optimizer algorithm for unmanned aerial vehicle (UAV) path planning. Knowledge-Based Systems 194, 105530.

Qu, C., Zeng, Z., Dai, J., Yi, Z., He, W., 2018. A Modified Sine-Cosine Algorithm Based on Neighborhood Search and Greedy Levy Mutation. Computational Intelligence and Neuroscience 2018, 4231647.

Rahkar Farshi, T., Demirci, R., Feizi-Derakhshi, M.-R., 2018. Image Clustering with Optimization Algorithms and Color Space. Entropy 20.

Rajput, S.S., Bohat, V.K., Arya, K.V., 2019. Grey wolf optimization algorithm for facial image super-resolution. Applied Intelligence 49, 1324-1338.

Saxena, A., Kumar, R., Das, S., 2019. beta-Chaotic map enabled Grey Wolf Optimizer. Applied Soft Computing 75, 84-105.

Saxena, A., Soni, B.P., Kumar, R., Gupta, V., 2018. Intelligent Grey Wolf Optimizer - Development and application for strategic bidding in uniform price spot energy market. Applied Soft Computing 69, 1-13.

Shen, L., Chen, H., Yu, Z., Kang, W., Zhang, B., Li, H., Yang, B., Liu, D., 2016. Evolving support vector machines using fruit fly optimization for medical data classification. Knowledge-Based Systems 96, 61-75.

Storn, R., Price, K., 1997. Differential Evolution – A Simple and Efficient Heuristic for global Optimization over Continuous Spaces. Journal of Global Optimization 11, 341-359.

Sun, G., Cong, Y., Wang, Q., Zhong, B., Fu, Y., 2020. Representative task self-selection for flexible clustered lifelong learning. IEEE Transactions on Neural Networks and Learning Systems.

Sundaramurthy, S., Jayavel, P., 2020. A hybrid Grey Wolf Optimization and Particle Swarm Optimization with C4.5 approach for prediction of Rheumatoid Arthritis. Applied Soft Computing 94, 106500.

Tang, H., Xu, Y., Lin, A., Heidari, A.A., Wang, M., Chen, H., Luo, Y., Li, C., 2020a. Predicting Green Consumption Behaviors of Students Using Efficient Firefly Grey Wolf-Assisted K-Nearest Neighbor Classifiers. IEEE Access 8, 35546-35562.

Tang, H., Xu, Y., Lin, A., Heidari, A.A., Wang, M., Chen, H., Luo, Y., Li, C.J.I.A., 2020b. Predicting Green Consumption Behaviors of Students Using Efficient Firefly Grey Wolf-Assisted K-Nearest Neighbor Classifiers. 8, 35546-35562.

Teng, Z.-j., Lv, J.-l., Guo, L.-w., 2019. An improved hybrid grey wolf optimization algorithm. Soft Computing 23, 6617-6631.

Tubishat, M., Abushariah, M.A.M., Idris, N., Aljarah, I., 2019. Improved whale optimization algorithm for feature selection in Arabic sentiment analysis. Applied Intelligence 49, 1688-1707.

Upadhyay, P., Chhabra, J.K., 2020. Kapur's entropy based optimal multilevel image segmentation using Crow Search Algorithm. Applied Soft Computing 97, 105522.

Villalón, C.L.C., Stützle, T., Dorigo, M., 2020. Grey Wolf, Firefly and Bat Algorithms: Three Widespread Algorithms that Do Not Contain Any Novelty, International Conference on Swarm Intelligence. Springer, pp. 121-133.

W, D., JJ, X., YJ, S., HM, Z., 2020. An Effective Improved Co-evolution Ant Colony Optimization Algorithm with Multi-Strategies and Its Application. International Journal of Bio-Inspired Computation, 16(13): 158–170.

Wang, B., Zhang, B., Liu, X., Zou, F., 2020a. Novel infrared image enhancement optimization algorithm combined with DFOCS. Optik 224, 165476.

Wang, M., Chen, H., 2020. Chaotic multi-swarm whale optimizer boosted support vector machine for medical diagnosis. Applied Soft Computing 88, 105946.

Wang, M., Chen, H., Li, H., Cai, Z., Zhao, X., Tong, C., Li, J., Xu, X., 2017a. Grey wolf optimization evolving kernel extreme learning machine: Application to bankruptcy prediction. Engineering Applications of Artificial Intelligence 63, 54-68.

Wang, M., Chen, H., Yang, B., Zhao, X., Hu, L., Cai, Z., Huang, H., Tong, C., 2017b. Toward an optimal kernel extreme learning machine using a chaotic moth-flame optimization strategy with applications in medical diagnoses. Neurocomputing 267, 69-84.

Wang, P., Wang, L., Leung, H., Zhang, G., 2020b. Super-Resolution Mapping Based on Spatial–Spectral Correlation for Spectral Imagery. IEEE Transactions on Geoscience and Remote Sensing 59, 2256-2268.

Wang, T., Liu, W., Zhao, J., Guo, X., Terzija, V., 2020c. A rough set-based bio-inspired fault diagnosis method for electrical substations. International Journal of Electrical Power & Energy Systems 119, 105961.

Wang, W.-c., Xu, L., Chau, K.-w., Xu, D.-m., 2020d. Yin-Yang firefly algorithm based on dimensionally Cauchy mutation. Expert Systems with Applications 150, 113216.

Wang, X.-F., Gao, P., Liu, Y.-F., Li, H.-F., Lu, F., 2020e. Predicting Thermophilic Proteins by Machine Learning. Current Bioinformatics 15, 493-502.

Wang, X., Zhao, H., Han, T., Zhou, H., Li, C., 2019a. A grey wolf optimizer using Gaussian estimation of

distribution and its application in the multi-UAV multi-target urban tracking problem. Applied Soft Computing 78, 240-260.
Wang, Y., Zhang, G., Zhang, X., 2019b. Multilevel Image Thresholding Using Tsallis Entropy and Cooperative Pigeon-inspired Optimization Bionic Algorithm. Journal of Bionic Engineering 16, 954-964.
Wang, Z.-J., Zhan, Z.-H., Yu, W.-J., Lin, Y., Zhang, J., Gu, T.-L., Zhang, J., 2019c. Dynamic group learning distributed particle swarm optimization for large-scale optimization and its application in cloud workflow scheduling. IEEE transactions on cybernetics 50, 2715-2729.
Wei, Y., Ni, N., Liu, D., Chen, H., Wang, M., Li, Q., Cui, X., Ye, H., 2017. An Improved Grey Wolf Optimization Strategy Enhanced SVM and Its Application in Predicting the Second Major. Mathematical Problems in Engineering 2017, 9316713.
Weng, L., He, Y., Peng, J., Zheng, J., Li, X., 2021. Deep cascading network architecture for robust automatic modulation classification. Neurocomputing 455, 308-324.
Xu, L., Jia, H., Lang, C., Peng, X., Sun, K., 2019a. A Novel Method for Multilevel Color Image Segmentation Based on Dragonfly Algorithm and Differential Evolution. IEEE Access 7, 19502-19538.
Xu, Y., Chen, H., Heidari, A.A., Luo, J., Zhang, Q., Zhao, X., Li, C., 2019b. An Efficient Chaotic Mutative Moth-flame-inspired Optimizer for Global Optimization Tasks. Expert Systems with Applications 129, 135-155.
Xu, Y., Chen, H., Luo, J., Zhang, Q., Jiao, S., Zhang, X., 2019c. Enhanced Moth-flame optimizer with mutation strategy for global optimization. Information Sciences 492, 181-203.
Yang, X.-S., 2010. Firefly algorithm, stochastic test functions and design optimization. International Journal of Bio-Inspired Computation 2(2), 78-84.
Yang, X.S., Deb, S., 2010. Engineering Optimisation by Cuckoo Search. International Journal of Mathematical Modelling & Numerical Optimisation 1, 330-343.
Yang, Y., Chen, H., Heidari, A.A., Gandomi, A.H., 2021a. Hunger games search: Visions, conception, implementation, deep analysis, perspectives, and towards performance shifts. Expert Systems with Applications 177, 114864.
Yang, Y., Chen, H., Heidari, A.A., Gandomi, A.H., 2021b. Hunger Games Search: Visions, Conception, Implementation, Deep Analysis, Perspectives, and Towards Performance Shifts. Expert Systems with Applications, 114864.
Yu, C., Chen, M., Cheng, K., Zhao, X., Ma, C., Kuang, F., Chen, H., 2021. SGOA: annealing-behaved grasshopper optimizer for global tasks. Engineering with Computers, 10.1007/s00366-00020-01234-00361.
Yu, H., Zhao, N., Wang, P., Chen, H., Li, C., 2020. Chaos-enhanced synchronized bat optimizer. Applied Mathematical Modelling 77, 1201-1215.
Zeng, G.-Q., Chen, J., Dai, Y.-X., Li, L.-M., Zheng, C.-W., Chen, M.-R.J.N., 2015. Design of fractional order PID controller for automatic regulator voltage system based on multi-objective extremal optimization. Neurocomputing 160, 173-184.
Zeng, G.-Q., Lu, K.-D., Dai, Y.-X., Zhang, Z.-J., Chen, M.-R., Zheng, C.-W., Wu, D., Peng, W.-W.J.N., 2014. Binary-coded extremal optimization for the design of PID controllers. Neurocomputing 138, 180-188.
Zeng, G.-q., Lu, Y.-z., Mao, W.-J., 2011a. Modified extremal optimization for the hard maximum satisfiability problem. Journal of Zhejiang University SCIENCE C 12, 589-596.
Zeng, G.-q., Lu, Y.-z., Mao, W.-J.J.J.o.Z.U.S.C., 2011b. Modified extremal optimization for the hard maximum satisfiability problem. Journal of Zhejiang University SCIENCE C 12, 589-596.
Zeng, G.-Q., Xie, X.-Q., Chen, M.-R., Weng, J., 2019. Adaptive population extremal optimization-based

PID neural network for multivariable nonlinear control systems. Swarm and Evolutionary Computation 44, 320-334.
Zeng, G., Lu, Y., Dai, Y., Wu, Z., Mao, W., Zhang, Z., Zheng, C.J.I.J.I.C.I.C., 2012. Backbone guided extremal optimization for the hard maximum satisfiability problem. International Journal of Innovative Computing Information and Control 8, 8355-8366.
Zhan, Z.-H., Liu, X.-F., Zhang, H., Yu, Z., Weng, J., Li, Y., Gu, T., Zhang, J., 2016. Cloudde: A heterogeneous differential evolution algorithm and its distributed cloud version. IEEE Transactions on Parallel and Distributed Systems 28, 704-716.
Zhang, H., Cai, Z., Ye, X., Wang, M., Kuang, F., Chen, H., Li, C., Li, Y., 2020a. A multi-strategy enhanced salp swarm algorithm for global optimization. Engineering with Computers, 1-27.
Zhang, L., Zhang, L., Mou, X., Zhang, D., 2011. FSIM: A Feature Similarity Index for Image Quality Assessment. IEEE Transactions on Image Processing 20, 2378-2386.
Zhang, X., Kang, Q., Cheng, J., Wang, X., 2018. A novel hybrid algorithm based on Biogeography-Based Optimization and Grey Wolf Optimizer. Applied Soft Computing 67, 197-214.
Zhang, X., Xu, Y., Yu, C., Heidari, A.A., Li, S., Chen, H., Li, C., 2020b. Gaussian mutational chaotic fruit fly-built optimization and feature selection. Expert Systems with Applications 141, 112976.
Zhang, Y., Liu, R., Heidari, A.A., Wang, X., Chen, Y., Wang, M., Chen, H., 2020c. Towards augmented kernel extreme learning models for bankruptcy prediction: Algorithmic behavior and comprehensive analysis. Neurocomputing, https://doi.org/10.1016/j.neucom.2020.1010.1038.
Zhang, Y., Liu, R., Wang, X., Chen, H., Li, C., 2020d. Boosted binary Harris hawks optimizer and feature selection. Engineering with Computers, 1-30.
Zhao, C., Zhong, S., Zhang, X., Zhong, Q., Shi, K., 2020a. Novel results on nonfragile sampled - data exponential synchronization for delayed complex dynamical networks. International Journal of Robust and Nonlinear Control 30, 4022-4042.
Zhao, D., Liu, L., Yu, F., Asghar Heidari, A., Wang, M., Oliva, D., Muhammad, K., Chen, H., 2020b. Ant Colony Optimization with Horizontal and Vertical Crossover Search: Fundamental Visions for Multi-threshold Image Segmentation. Expert Systems with Applications, 114122 (https://doi.org/114110.111016/j.eswa.112020.114122).
Zhao, D., Liu, L., Yu, F., Heidari, A.A., Wang, M., Liang, G., Muhammad, K., Chen, H., 2020c. Chaotic random spare ant colony optimization for multi-threshold image segmentation of 2D Kapur entropy. Knowledge-Based Systems, 106510 (https://doi.org/106510.101016/j.knosys.102020.106510).
Zhao, D., Liu, L., Yu, F., Heidari, A.A., Wang, M., Oliva, D., Muhammad, K., Chen, H., 2021. Ant colony optimization with horizontal and vertical crossover search: Fundamental visions for multi-threshold image segmentation. Expert Systems with Applications 167, 114122.
Zhao, H., Liu, H., Xu, J., Deng, W., 2020d. Performance Prediction Using High-Order Differential Mathematical Morphology Gradient Spectrum Entropy and Extreme Learning Machine. IEEE Transactions on Instrumentation and Measurement 69, 4165-4172.
Zhao, H., Liu, H., Xu, J., Deng, W.J.I.T.o.i., measurement, 2019a. Performance prediction using high-order differential mathematical morphology gradient spectrum entropy and extreme learning machine. IEEE Transactions on Instrumentation & Measurement, https://doi.org/10.1109/TIM.2019.2948414.
Zhao, X., Li, D., Yang, B., Chen, H., Yang, X., Yu, C., Liu, S., 2015. A two-stage feature selection method with its application. Computers & Electrical Engineering 47, 114-125.
Zhao, X., Li, D., Yang, B., Ma, C., Zhu, Y., Chen, H., 2014. Feature selection based on improved ant colony optimization for online detection of foreign fiber in cotton. Applied Soft Computing 24, 585-596.

Zhao, X., Zhang, X., Cai, Z., Tian, X., Wang, X., Huang, Y., Chen, H., Hu, L., 2019b. Chaos enhanced grey wolf optimization wrapped ELM for diagnosis of paraquat-poisoned patients. Computational Biology and Chemistry 78, 481-490.

Zhong, Z., Xiao, G., Wang, S., Wei, L., Zhang, X., 2022. PESA-Net: Permutation-Equivariant Split Attention Network for correspondence learning. Information Fusion 77, 81-89.

Zhou, H., Pang, J., Chen, P.-K., Chou, F.-D., 2018. A modified particle swarm optimization algorithm for a batch-processing machine scheduling problem with arbitrary release times and non-identical job sizes. Computers & Industrial Engineering 123, 67-81.

Zhou, S.-Z., Zhan, Z.-H., Chen, Z.-G., Kwong, S., Zhang, J., 2020. A multi-objective ant colony system algorithm for airline crew rostering problem with fairness and satisfaction. IEEE Transactions on Intelligent Transportation Systems, DOI: 10.1109/TITS.2020.2994779.

Zhou, W., Bovik, A.C., Sheikh, H.R., Simoncelli, E.P., 2004. Image quality assessment: from error visibility to structural similarity. IEEE Transactions on Image Processing 13, 600-612.

Zhou, W., Guo, Q., Lei, J., Yu, L., Hwang, J.-N., 2021. IRFR-Net: Interactive Recursive Feature-reshaping Network for Detecting Salient Objects in RGB-D Images. IEEE Transactions on Neural Networks and Learning Systems.

Zhu, A., Xu, C., Li, Z., Wu, J., Liu, Z., 2015. Hybridizing grey wolf optimization with differential evolution for global optimization and test scheduling for 3D stacked SoC. Journal of Systems Engineering and Electronics 26, 317-328.

Zhu, X., Guo, K., Fang, H., Chen, L., Ren, S., Hu, B., 2021a. Cross View Capture for Stereo Image Super-Resolution. IEEE Transactions on Multimedia, DOI: 10.1109/TMM.2021.3092571.

Zhu, X., Guo, K., Ren, S., Hu, B., Hu, M., Fang, H., 2021b. Lightweight Image Super-Resolution with Expectation-Maximization Attention Mechanism. IEEE Transactions on Circuits and Systems for Video Technology, DOI: 10.1109/TCSVT.2021.3078436.